1986ApJ...311..526H

THE ASTROPHYSICAL JOURNAL, 311:526–547, 1986 December 15
© 1986. The American Astronomical Society. All rights reserved. Printed in U.S.A.

GALAXY COLLISIONS AND MERGERS: THE GENESIS OF VERY POWERFUL RADIO SOURCES?

T. M. HECKMAN,[1,2] ERIC P. SMITH,[2] AND STEFI A. BAUM[2,3]
Astronomy Program, University of Maryland

W. J. M. VAN BREUGEL[2]
Radio Astronomy Laboratory, University of California, Berkeley

G. K. MILEY[2,4] AND G. D. ILLINGWORTH[2]
Space Telescope Science Institute

G. D. BOTHUN[2]
Department of Astronomy, Caltech

AND

B. BALICK[2]
Department of Astronomy, University of Washington
Received 1986 February; accepted 1986 June 2

ABSTRACT

We discuss a program of deep optical broad- and narrow-band imaging of 43 radio galaxies, supplemented by optical long-slit spectroscopy and VLA radio mapping. Our principal result is that between one-fourth and one-third of very powerful (log $P_{408\,\mathrm{MHz}} \gtrsim 25.5$ W Hz^{-1} for $H_0 = 75$ km s^{-1} Mpc^{-1}) radio galaxies are strongly peculiar in *optical* morphology at relatively high levels of surface brightness (μ_V brighter than 25 mag arcsec^{-2}). This fraction is much greater than for less powerful radio galaxies and for radio-quiet ellipticals. Thus, in contrast to conventional wisdom, very powerful radio galaxies are *not* always normal ellipticals.

The morphological peculiarities take the form of tails, fans, bridges, dust features, shells, etc. They are continuum-emitting and/or line-emitting structures and usually bear no simple morphological relationship to the radio source. We conclude that they probably arise from the collision or merger of galaxy pairs, at least one member of which is a disk galaxy. This conclusion is also supported by evidence for recent or current star formation in some of the morphologically peculiar galaxies, and by the relatively isolated location of many of the galaxies.

Within the class of very powerful radio galaxies we find that those with peculiar *optical* morphologies have stronger optical emission lines, are less luminous optically, inhabit regions of lower average galaxy density, and are *less* likely to exhibit an edge-darkened radio morphology ("Fanaroff-Riley class I," "3C 31-Type"). We also confirm the relationships between optical line emission, radio morphology, and local galaxy density previously discussed by others.

We are led to propose two idealized classes of radio galaxies. Class A galaxies have strong optical emission lines and edge-brightened radio morphologies ("Fanaroff-Riley class II," "Cygnus A-type"). They also inhabit regions of lower average galaxy density and frequently have peculiar optical morphologies. These may be radio sources fueled by collisions or mergers involving at least one gas-rich system. Class B galaxies have weak or no optical emission lines, edge-darkened radio morphologies, inhabit regions of very high local galaxy density, and are morphologically normal giant elliptical or cD galaxies. These radio sources may be powered by the stored rotational energy of a central black hole or by accretion of either an intracluster medium or of the galaxy's own gaseous atmosphere. The implications of this picture for our understanding of the unity of the various classes of active galaxies and quasars and for the investigation of galaxy evolution at high redshifts are briefly discussed.

Subject headings: galaxies: clustering — galaxies: structure — radio sources: galaxies

I. INTRODUCTION

One of the most promising clues to the origin of nuclear activity has been the discovery that many types of active galaxies are located in denser regions of the universe and/or are more likely to be interacting than are quiescent galaxies (see review by Balick and Heckman 1982 and more recent papers by, e.g., Yee and Green 1984; Dahari 1984; Hutchings, Crampton, and Campbell 1984; Heckman, Carty, and Bothun 1985; Keel *et al.* 1985). This suggests that gravitational interactions between galaxies may in some way trigger nuclear activity—an idea first suggested by Baade and Minkowski (1954) and explored theoretically by Toomre and Toomre (1972; hereafter TT).

An encounter between two galaxies which is intense enough

[1] Alfred P. Sloan Foundation Fellow and Visiting Faculty Member, Department of Physics and Astronomy, Johns Hopkins University.

[2] Visiting observers at the Kitt Peak National Observatory and Cerro Tololo Inter-American Observatory of the NOAO, operated by AURA, Inc., under contract to the NSF.

[3] Also the National Radio Astronomy Observatory.

[4] Affiliated with the Astrophysics Division, Space Department of the European Space Agency. On leave from Leiden Observatory.

© American Astronomical Society • Provided by the NASA Astrophysics Data System

1986ApJ...311..526H

TABLE 1

OBSERVATIONAL MATERIAL

Observatory (1)	Telescope (2)	Instrument (3)	Field Size (4)	Pixel Size (5)	Resolution (6)	Wavelength (7)	Exposure Time (minutes) (8)	Dates (9)	Purpose (10)	References (11)
KPNO	4.0 m	Prime focus CCD (Fairchild)	1′.9 × 1′.4	0″.59 × 0″.35	1″	R	15	1982 Jan	Optical imaging	1
KPNO	4.0 m	Prime focus CCD (TI)	4′.0 × 4′.0	0″.60	1″	V, R, Hα	10–20	1985 Dec 1986 Apr	Optical imaging	2
KPNO	4.0 m	Video camera	1′.25 × 1′.25	0″.29	1″	6100–6300 Å	13	1983 Aug, Dec	Optical imaging	3
KPNO	4.0 m	Cryogenic camera	4′.0 × 3400 Å	0″.83 × 4.3 Å	2″ × 15 Å	4500–7900 Å	30	1980 May, 1982 Apr	Optical spectroscopy	1
KPNO	4.0 m	High gain video spectrometer	2′.8 × 700 Å	1″.3 × 1.3 Å	2″ × 4 Å	4900–5600 Å	various	1980 May, 1982 Apr	Optical spectroscopy	3
KPNO	2.1 m	Video camera	1′.9 × 1′.9	0″.45	1″.5	V	13	1978 Nov	Optical imaging	3
KPNO	0.9 m	CCD direct (RCA)	4′.7 × 6′.8	0″.8	2″	R	20	1983 Aug	Optical imaging	4
CTIO	4.0 m	Prime focus CCD (RCA)	3′.2 × 5′.1	0″.6	1″.5	V	30	1983 Oct 1985 Jun	Optical imaging	2
Lick	3.0 m	CCD	2′.2 × 2′.2 2′.2 × 2200 Å	0″.7 0″.7 × 2.7Å	1″ 2″ × 7Å	R 5800–8000 Å	various	1985 Jan 1985 Jun	Optical imaging and spectroscopy	5
NRAO	VLA	Continuum receiver	3′.4 × 3′.4	0″.4	1″.2	$\lambda = 6$ cm	20	various	Radio imaging	1, 3

REFERENCES.—(1) van Breugel *et al.* 1985*a*. (2) Smith *et al.* 1986. (3) Heckman *et al.* 1982. (4) Heckman, Carty, and Bothun 1985. (5) van Breugel *et al.* 1985*b*.

© American Astronomical Society • Provided by the NASA Astrophysics Data System

1986ApJ...311..526H

to result in substantial mass transfer and/or a significant rearrangement of the internal dynamics of the galaxies (as envisaged by TT in their "stoking the furnace" scenario) can have morphologically spectacular consequences when at least one of the participants has a dynamically "cold" component (e.g., a disk). Such morphological features as "bridges," "tails," and "shells" (TT; Quinn 1984) can be readily understood in this context. Suggestively, an abnormally large fraction of Seyfert galaxies and low-redshift quasar "host" galaxies do exhibit morphological peculiarities (see above references).

The situation regarding galaxy interactions and the galaxian environment of radio galaxies is complex. It now appears that moderately powerful radio galaxies ($P_{408\,\mathrm{MHz}} \approx 10^{23.5}$–$10^{25.5}$ W Hz^{-1} for $H_0 = 75$ km s^{-1}, $q_0 = 0$, as used throughout this paper) are located in regions of abnormally high galaxy density (e.g., Longair and Seldner 1978; Heckman, Carty, and Bothun 1985). However, few of these radio galaxies are known to exhibit strongly peculiar optical morphologies—most appear to be rather normal, luminous ($M_B \lesssim -21$) elliptical galaxies. At higher levels of radio power, the situation is less clear. Very little is known about the optical morphology or local environment of these radio galaxies because (owing to their low space densities) they are generally located at substantial redshifts ($z > 0.05$). For some very powerful radio galaxies at $z \gtrsim 1$, there is evidence for enhanced star formation (Lilly and Longair 1984; Eisenhardt and Lebofsky 1985) and for strong, spatially resolved emission-line nebulae whose structure suggests a tidal origin (Spinrad and Djorgovski 1984*a*, *b*). Such nebulae also seem to be commonly associated with radio-loud quasars (e.g., Boroson, Persson, and Oke 1985; Stockton 1984).

In the present paper we will discuss a large body of deep optical imaging data and a smaller amount of optical spectroscopic data concerning the parent galaxies of very powerful radio sources (log $P_{408} \gtrsim 10^{25.5}$ W Hz^{-1}). The data clearly establish that (contrary to astronomical folklore) the parents of very powerful radio sources are not all necessarily normal luminous elliptical galaxies. Indeed, we will show that $\sim 30\%$ instead exhibit disturbed optical morphologies. These results implicate galaxy interactions in the genesis of powerful radio sources.

We will describe our observations and sample selection in § II, discuss individual morphologically peculiar galaxies in § III, explore the general properties of our sample and their interpretation in § IV, and summarize our conclusions and their implications in § V.

II. OBSERVATIONS AND SAMPLE SELECTION

The various telescope and detector combinations used in this investigation are listed in Table 1, together with the relevant instrumental parameters. Standard observation, calibration, and reduction procedures were followed for all the observations and have been described elsewhere as noted in Table 1 (see, e.g., Heckman *et al.* 1982; Heckman, van Breugel, and Miley 1984; van Breugel, Miley, and Heckman 1984; van Breugel *et al.* 1985*a*). We will discuss the results of our VLA observations elsewhere in detail.

The radio galaxies observed, and the observations made of them are summarized in Table 2. Twenty-three of the 43 radio galaxies were observed because they are part of a complete radio-selected sample of radio sources which we are investigating using the VLA and diverse optical facilities. This sample consists of all radio sources stronger than 8.5 Jy located between declinations of $-30°$ and $+20°$. We refer to these objects henceforth as our "complete" sample, and denote them with an asterisk in Table 2. This sample was observed without prior knowledge of the galaxy optical morphology, and should constitute an unbiased and representative sample of very powerful radio galaxies. The other 20 objects are not part of any well-defined sample, and were originally observed by us as parts of several different observing programs. In some cases, the peculiar optical morphologies of these latter galaxies were known to us prior to our observations.

III. INDIVIDUAL PECULIAR GALAXIES

We discuss below the 19 galaxies in Table 2 which exhibited significant departures from an elliptical symmetry in their optical morphology at levels of surface brightness higher than $\mu_V = 25V$ mag arcsec^{-2}.

a) 3C 33

Several types of morphological peculiarities can be seen in our image of 3C 33 (Figs. 1, 2 [Pl. 10]). (1) There is a strong radial change in the isophotal ellipticity and major axis position angle (see Simkin and Michel 1985) between $r \approx 3''$ (3.5 kpc) and $r \approx 14''$ (16 kpc). (2) A curving tail-like feature with a surface brightness of $\mu_V \approx 23.5$–24.0 mag arcsec^{-2} can be traced from $10''$ (~ 12 kpc) east to $15''$ (~ 17 kpc) SSE of the nucleus. (3) Faint ($\mu_V \approx 25.5$–26.0 mag arcsec^{-2}) and rather diffuse emission extends outward $\sim 40''$–$50''$ (47–58 kpc) mainly to the north from the main body of the galaxy. These various peculiar structures have also been reported by Simkin and Michel (1985), who also find a more morphologically complex (spiral-like) feature in the $r - i$ color map they have constructed.

Long-slit spectroscopy of 3C 33 (Simkin 1979; Heckman *et al.* 1985) and our own narrow-band imaging imply that the above morphological features are continuum-emitting structures. The spectra also reveal a rapidly rotating region of emission-line gas $\sim 12''$ (14 kpc) in diameter, with a rotation axis in P.A. $\approx 20°$ (close to the radio ejection axis). This axis is skewed relative to the principal galaxy photometric axes, and probably also relative to the stellar rotation axis (Heckman *et al.* 1985). This represents evidence for an extrinsic origin for the gas, but 3C 33 is rather isolated at present. Despite these morphological peculiarities, the photometry of Sandage (1972) yields a normal (red) color for this radio galaxy.

b) PKS 0349−278

This radio galaxy has been investigated recently by Danziger *et al.* (1984, hereafter D84). Our new optical and radio data are complementary to those presented by D84, and corroborate the scenario they have proposed. Figures 3*a* and 3*b* (Plates 11–12) are deep narrow-band ([O III] λ5007) and broad-band (V) images. The tail-like structure is produced by emission-line gas. D84 found that the objects $22'' = 26$ kpc east and $17'' = 20$ kpc NE of the parent galaxy are companion galaxies (the latter galaxy lies along the radio axis, at least in projection). The kinematics of the ionized gas have been interpreted by D84 as a combination of rotation and outflow which is dynamically related to an interaction between the parent galaxy and its eastern neighbor. The morphology of the ionized gas (a bridge joining the companion and the parent galaxy, and an oppositely directed tail extending at least $17'' = 20$ kpc to the west), is consistent with this idea.

© American Astronomical Society • Provided by the NASA Astrophysics Data System

1986ApJ...311..526H

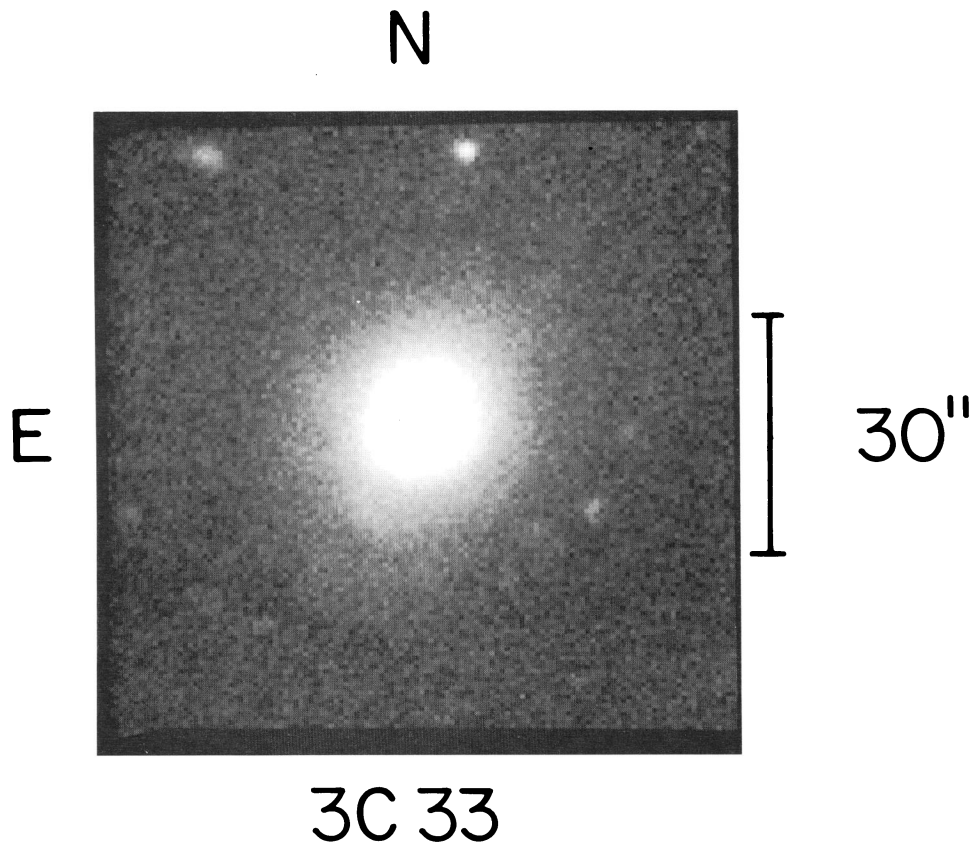

FIG. 1.—Inner SE tail of 3C 33 in V-band image

HECKMAN *et al.* (*see* page 528)

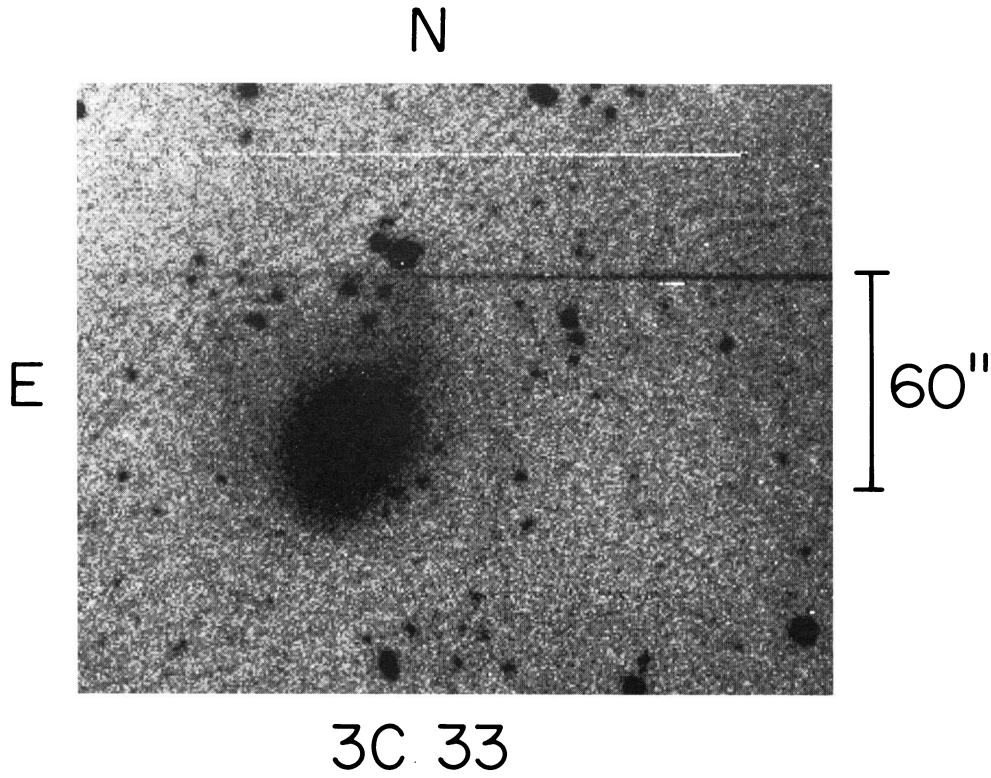

FIG. 2.—Outer N and NE fan of 3C 33 in V-band image

HECKMAN *et al.* (*see* page 528)

© American Astronomical Society • Provided by the NASA Astrophysics Data System

1986ApJ...311..526H

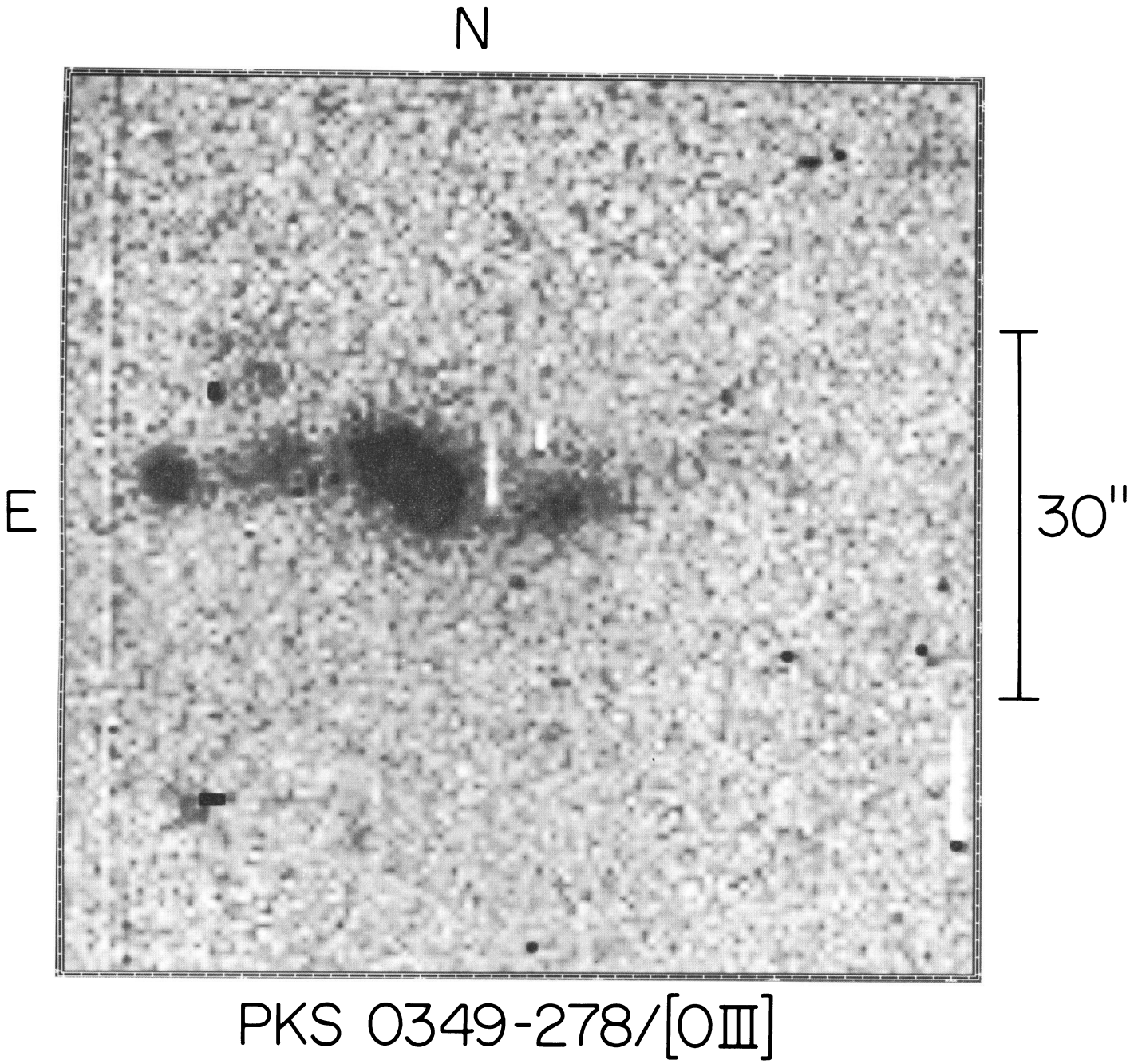

FIG. 3*a*

FIG. 3.—(*a*) Image of PKS 0349 − 278 taken with a narrow-band ($\Delta\lambda \sim 50$ Å) filter centered on the redshifted [O III] λ5007 line. (*b*) Broad-band (V) image of PKS 0349 − 278.

HECKMAN *et al.* (*see* page 528)

© American Astronomical Society • Provided by the NASA Astrophysics Data System

1986ApJ...311..526H

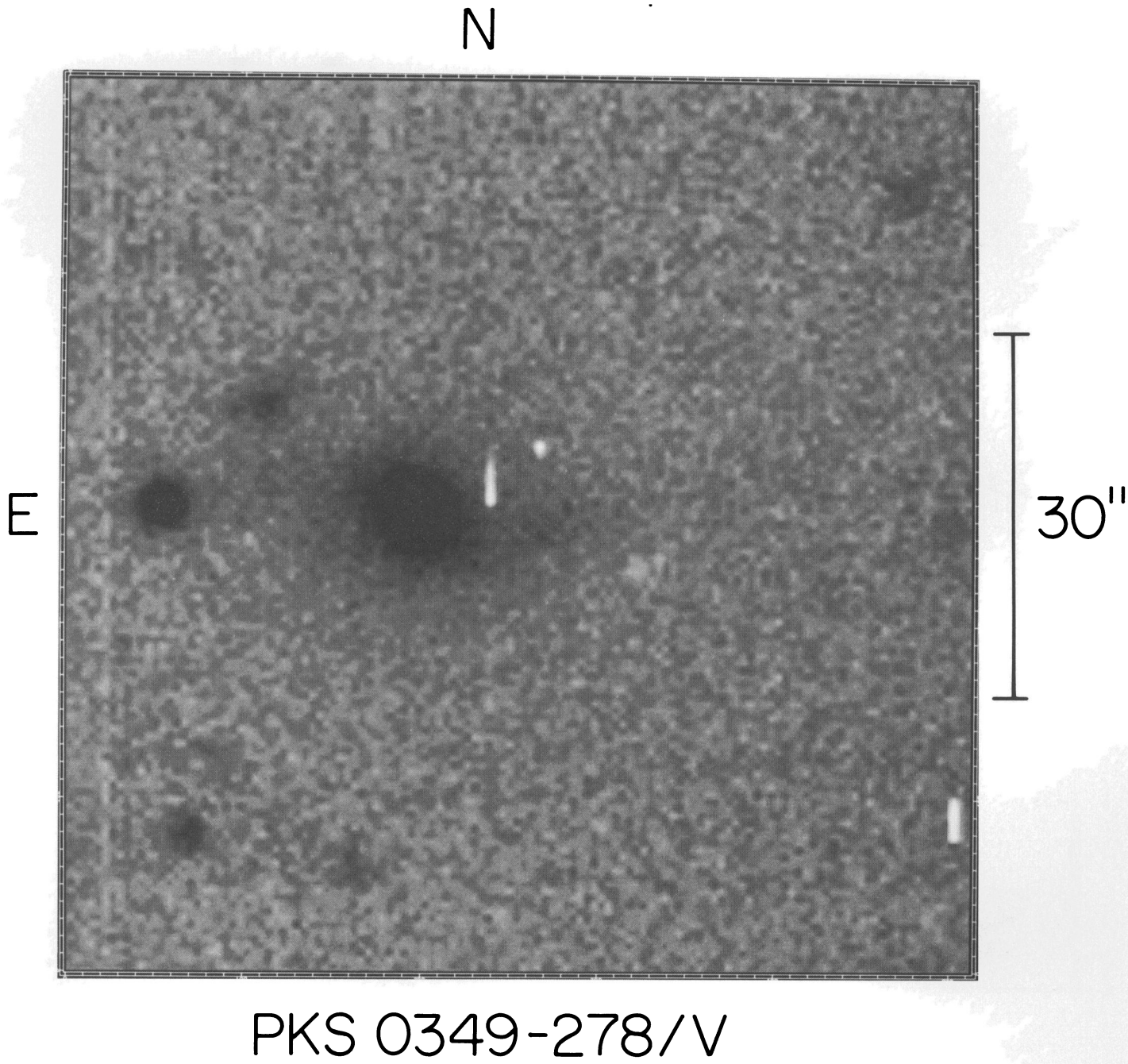

FIG. 3*b*

HECKMAN *et al.* (*see* page 528)

© American Astronomical Society • Provided by the NASA Astrophysics Data System

1986ApJ...311..526H

TABLE 2

SAMPLE AND OBSERVATIONS

αδ (1)	Name (2)	z (3)	V (4)	S_{408} (5)	Observations (6)	Slit Position Angles (7)
0035−024*	3C 17	0.220	18.0	13.0	1, 2, 3	122
0106+130*	3C 33	0.060	15.2	29.6	1, 2, 3, 4, 7	19, 67, 110, 114
0137+012	PKS	0.260	17.2	2.8	1, 8	26
0213−132*	3C 62	~0.1	~16	14.2	1, 3	...
0218−021*	3C 63	0.175	17.5	10.3	1, 2, 3, 4	34
0349−278*	PKS	0.066	16.8	11.2	1, 2, 3, 4	56
0430+052	3C 120	0.033	14.1	6	3, 5, 6, 7	43, 123
0736+017	PKS	0.191	16.7	3	1	...
0836+299	4C 29.30	0.065	15.7	1.6	2, 3, 4, 6, 7, 8	4, 85, 95
0915−118*	3C 218	0.055	14.0	109.6	1, 2, 3, 4, 9	1, 120, 144
0945+076*	3C 227	0.086	16.3	19.4	1, 3, 4, 8	91
1137+180	NGC 3801	0.011	12.3	2.5	2, 3, 4, 5, 7, 9	26, 120, 124
1319+428	3C 285	0.079	16.0	5.7	4, 8	80, 125
1345+125*	4C 12.50	0.122	16.1	9.1	1, 3, 4, 8	90
1350+316	3C 293	0.045	14.4	11.5	3, 4, 5, 7, 9	60, 65, 150
1358−113	PKS	0.025	13.3	4.2	1	...
1420+198*	3C 300	0.270	~18	9.6	1, 3	...
1448+638	3C 305	0.042	13.7	9.6	3, 4, 5, 7, 9	57, 90, 100, 150, 165
1502+262	3C 310	0.054	15.2	23.4	3, 5, 7, 9	63, 153
1514+072*	3C 317	0.035	13.2	23.2	1, 3, 4, 6, 9	...
1529+242*	3C 321	0.096	~16	11.0	1, 4, 8	134
1559+021*	3C 327	0.104	15.9	27.5	1, 3, 4, 8	100, 122
1602+178	NGC 6047	0.032	14.0	2.1	1	...
1641+173*	3C 346	0.161	17.2	9.1	1, 2, 3, 4, 5, 8	74, 123, 124
1648+051*	3C 348	0.154	16.8	141.7	1, 3, 4, 8	121
1717−009*	3C 353	0.030	15.4	114.5	1, 3, 4, 8	...
1934−638	PKS	0.182	18.0	7	1	...
1949+023*	3C 403	0.059	15.3	13.6	1, 2, 3, 4, 9	77, 167
2045+068*	3C 424	0.127	18.4	9.0	1, 3	...
2058−282*	PKS	0.038	14.1	13.9	1, 3, 8	133
2104−256S*	PKS	0.038	13.7	~11	1, 3	...
2104−256N*	PKS	0.036	13.0	~11	1, 3	...
2121+248	3C 433	0.102	16.2	32.8	1, 3, 5	...
2135−147*	PKS	0.200	15.4	11.6	1	...
2141+175	OX 169	0.213	15.6	0.4	1	...
2141+279	3C 436	0.215	18.2	11.3	1	...
2211−173*	3C 444	0.153	16.5	33.3	1, 3	...
2221−023*	3C 445	0.056	15.7	14.5	1, 2, 3, 5, 8	172, 45
2247+140	PKS	0.237	16.5	3.7	1, 3	...
2300−189	PKS	0.129	16.7	2.0	1, 2	131, 167
2314+038*	3C 459	0.220	17.5	13.0	1, 2, 3	4, 94
2328+167	MC3	0.284	18.2	0.4	1	...
2355−082	PKS	0.211	16.8	0.3	1	...

Col. (1).—IAU designation. Asterisk denotes member of complete sample (see text).

Col. (2).—Common name.

Col. (3).—Redshift from sources compiled by Spinard *et al.* 1985, Kühr *et al.* 1979, Burbidge and Crowne 1979, and Hewitt and Burbidge 1980, except for 3C 62, for which the redshift is only an estimate based on V.

Col. (4).—Total V magnitude from our images, from Sandage 1972, or from references cited by Spinrad *et al.* 1985.

Col. (5).—Radio flux density at 408 MHz in janskys, taken from Kühr *et al.* 1979, Burbidge and Crowne 1979, or Dixon 1970. In a few cases, the value for S_{408} was extrapolated from higher frequency data.

Col. (6).—Observations conducted according to the following key (see Table 1 for details): (1) CTIO, 4 m, CCD (images). (2) KPNO, 4 m, cryogenic camera (spectra). (3) NRAO, VLA (radio maps). (4) KPNO, 4 m, CCD (images). (5) KPNO, 4 m, Video Camera (images). (6) KPNO, 2.1 m, Video Camera (images). (7) KPNO, 4 m, HGVS (spectra). (8) Lick, 3 m, CCD (images and spectra). (9) KPNO, 0.9 m, CCD (images).

c) 3C 120

We have previously published [O III] narrow-band images (Heckman and Balick 1979) and VLA radio maps (Balick, Heckman, and Crane 1982) of this enigmatic radio galaxy. The kinematics of the complex emission-line nebulosity have been discussed by Baldwin *et al.* (1980). Here we present (Fig. 4 [Pl. 13]) a V-band frame obtained with the KPNO 2.1 m and Video Camera showing the pure continuum-emitting structure of 3C 120. To produce this image we have subtracted from the V-band image a narrow band image of the [O III] λ5007 line-emitting material scaled by a factor of ~1.4 to account for emission lines in the V-band pass (primarily [O III] λ5007 and λ4959 and Hβ). At faint levels, 3C 120 exhibits a rather smooth, oval morphology ~45″ × 30″ (~30 × 20 kpc) in size, with a major axis in P.A. ≈ 115°. Note that the complex filamentary structure seen in Arp's (1975) beautiful broad-band image is produced by emission-line gas—not starlight. Closer to the nucleus (~10″–12″ ≈ 7 kpc) are bright ($\mu_V \approx 22.5$ mag arcsec^{-2}) continuum-emitting tails or knots in P.A.s ≈ 135° and 315°. These latter features do not bear any obvious morphological relationship to the radio source (see Bridle and Perley 1984). Baldwin *et al.* (1980) have in fact detected stellar

© American Astronomical Society • Provided by the NASA Astrophysics Data System

1986ApJ...311..526H

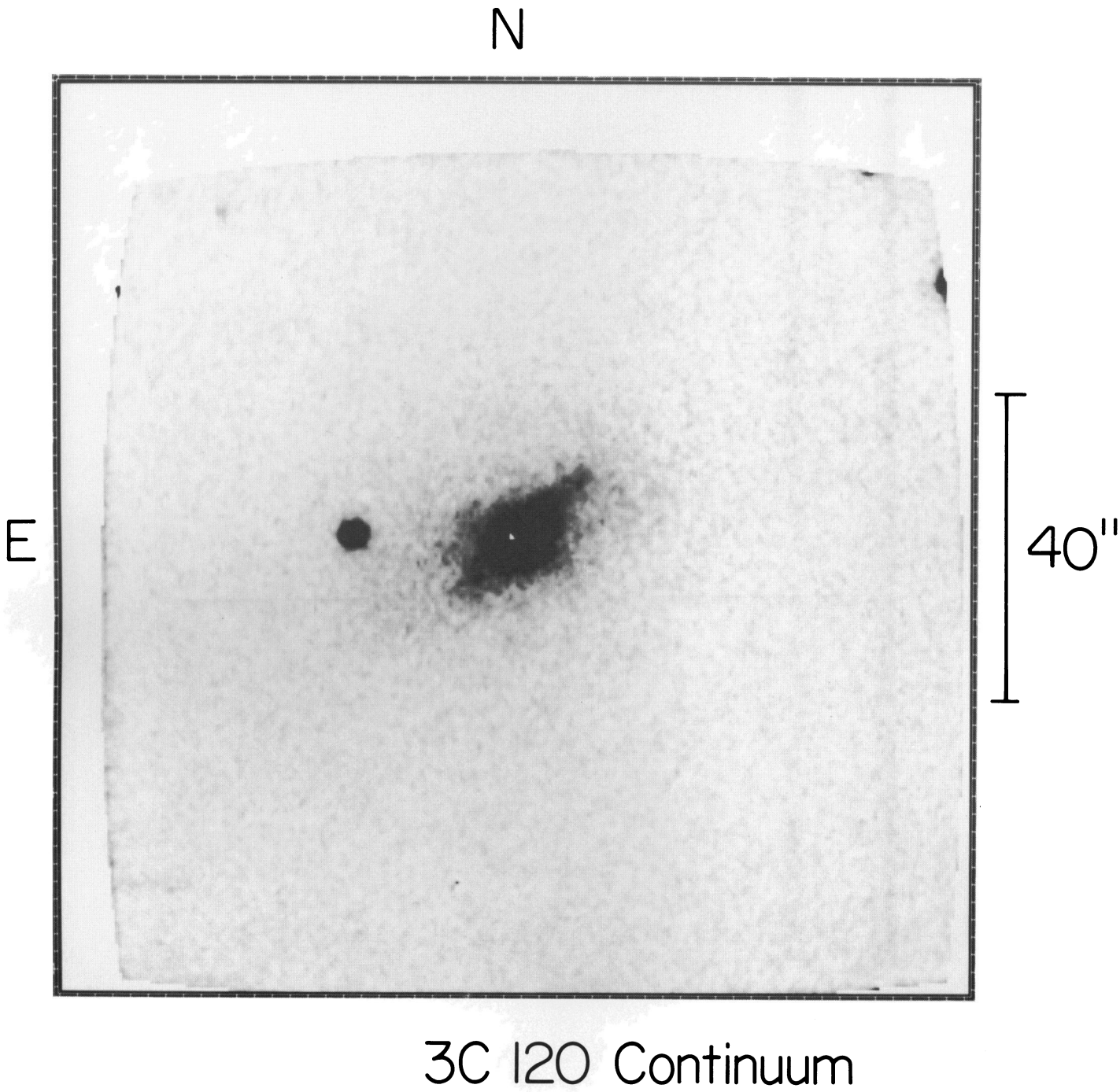

FIG. 4.—V-band image of 3C 120 with the contribution of line-emitting gas subtracted (see text)

HECKMAN *et al.* (*see* page 529)

© American Astronomical Society • Provided by the NASA Astrophysics Data System

1986ApJ...311..526H

absorption-lines from the "fuzz" $\sim 5''$ (3.3 kpc) east of the nucleus, and so it is likely that the knots/tails are composed of stars. We note that 3C 120 appears to be rather isolated on the sky, and is a moderately strong far-infrared source ($\sim 4 \times 10^{10}$ $L_\odot$, see footnote to Table 3).

d) 4C 29.30

We have discussed our detailed radio and optical observations of this radio source elsewhere (van Breugel *et al.* 1986). Here we emphasize the peculiar properties of the parent galaxy of 4C 29.30:

1. Shell-like structures with surface brightnesses ranging from $\sim 10\%$–100% of the sky are found $\sim 20''$–$30''$ (25–36 kpc) to the west and east of the galaxy (Fig. 5*a* [Pl. 14]), approximately transverse to the radio axis.

2. A compact blue object (secondary nucleus?) is seen $\sim 4''$ (5 kpc) east of the nucleus of the parent galaxy (Fig. 5*b* [Pl. 15]).

3. The radio galaxy nucleus is apparently encircled by a small ($\sim 4'' = 5$ kpc) dust lane (Fig. 5*b*) along whose minor axis the radio source emerges (see Kotanyi and Ekers 1979).

4. 4C 29.30 is in a region of low galaxy density.

5. 4C 29.30 has also been detected as a strong ($\sim 6 \times 10^{10}$ $L_\odot$) far-infrared source by *IRAS* (Table 3).

e) 3C 227

This classic N galaxy (Fig. 6*a*, Fig. 6*b* [Pl. 16]) consists of a bright nucleus and a complex of knots and tails which our narrow-band Hα image reveals to be mostly emission-line gas. Knotty, tail-like structure can be seen with $\mu_V \approx 24.5$ mag arcsec^{-2} curving out to $\sim 10''$–$11''$ (~ 15 kpc) SE of the nucleus. Another knot with $V \approx 20$ mag is located $\sim 12''$ (17 kpc) WNW of the nucleus. This knot emits strongly in the continuum and could be a companion galaxy. At fainter levels ($\mu_V \approx 25.5$–26) two long patchy tails are visible: a straight one stretching $35''$–$40''$ (~ 55 kpc) to the SW, and a curved one

TABLE 3

OPTICAL MORPHOLOGY

Name (1)	Type (2)	Components (3)	μ_V (4)	Spectrum (5)	Participants (6)
3C 33*	DE4	F, T, TI	23.5–26.0	C	ED
PKS 0349−278*	E	B, T		E	ED or EE
3C 120	N	2T, IR	22–23	C, E	DD
4C 29.30	S0	S, D, IR	22–25	C, E	ED
3C 227*	N	T, F, CE	24.5–25.5	E	DD
NGC 3801	E	2F, D, TI, T	20–25	C, E	ED or DD
3C 285	E	2F, YS	24	C, E	ED
4C 12.50*	S0	D, 2T, IR	22–25.5	C	DD
3C 293	D6	B, T, D, IR	21–24.5	C, E	ED or DD
3C 305	Sa	2T, D, YS, IR	21–25	C, E	DD
3C 321	DB	T, F, CE, IR	22–25.5	C, E	ED
3C 327*	D	S, IR	23.5–24.5	C	ED
NGC 6047	E	TI	22–25	C	EE
PKS 1934−638	Gal.	2F, CE, YS	23–24.5	?	DD or ED
OX 169	Q	2T, F	23.5–26.0	C	DD
3C 445*	N	T, F?, IR	23–26	E	ED
PKS 2247+140	Q	T, F	24.5–26.0	?	ED
PKS 2300−189	N	2T, CE, S?	24.5–26.5	C, E	ED or DD
3C 459*	N	2F, YS, IR	24–25	C	ED or DD

Col. (1).—Name. Asterisk denotes member of complete sample.

Col. (2).—Published morphological type (Burbidge and Crowne 1979; Hewitt and Burbidge 1980; Spinrad *et al.* 1985).

Col. (3).—Morphological/spectroscopic components present, according to the following key (see text for details):

B: Bridge from radio galaxy to companion.

CE: Radio galaxy and companion immersed in a common envelope.

D: Dust lanes or patches present.

F, 2F: One or two fans present.

IR: Powerful ($> 10^{10}$ $L_\odot$) far-IR ($\lambda \sim 60$ μm) source. Infrared luminosities are calculated from 60 μm fluxes from either the *IRAS* point source catalog or from pointed observations of a sample of radio galaxies. The 60 μm "luminosities" are taken to be νP_ν, where ν is the frequency corresponding to 60 μm in the galaxy rest frame and P_ν is the monochromatic power at 60 μm.

S: Shells present.

T, 2T: One or two tails present.

TI: Strongly twisted isophotes.

YS: Spectroscopic or photometric evidence for young stellar population (relatively strong Balmer absorption lines or spatially extended blue region, respectively).

Col. (4).—Level of V-band surface brightness (as measured in the Earth's frame) of the observed morphological peculiarities (see text for details). Units are magnitudes per square arcsec.

Col. (5).—Nature of the optical spectrum of the morphologically peculiar material, where "C" denotes continuum-emitting (presumably starlight) and "E" denotes emission-line gas. See text for details concerning individual objects.

Col. (6).—*Guess* as to the nature of the galaxian participants in the interaction, based on the available clues in cols. (3) and (5). Here "E" and "D" denote elliptical and disk galaxies, respectively. We stress the uncertainty involved.

© American Astronomical Society • Provided by the NASA Astrophysics Data System

1986ApJ...311..526H

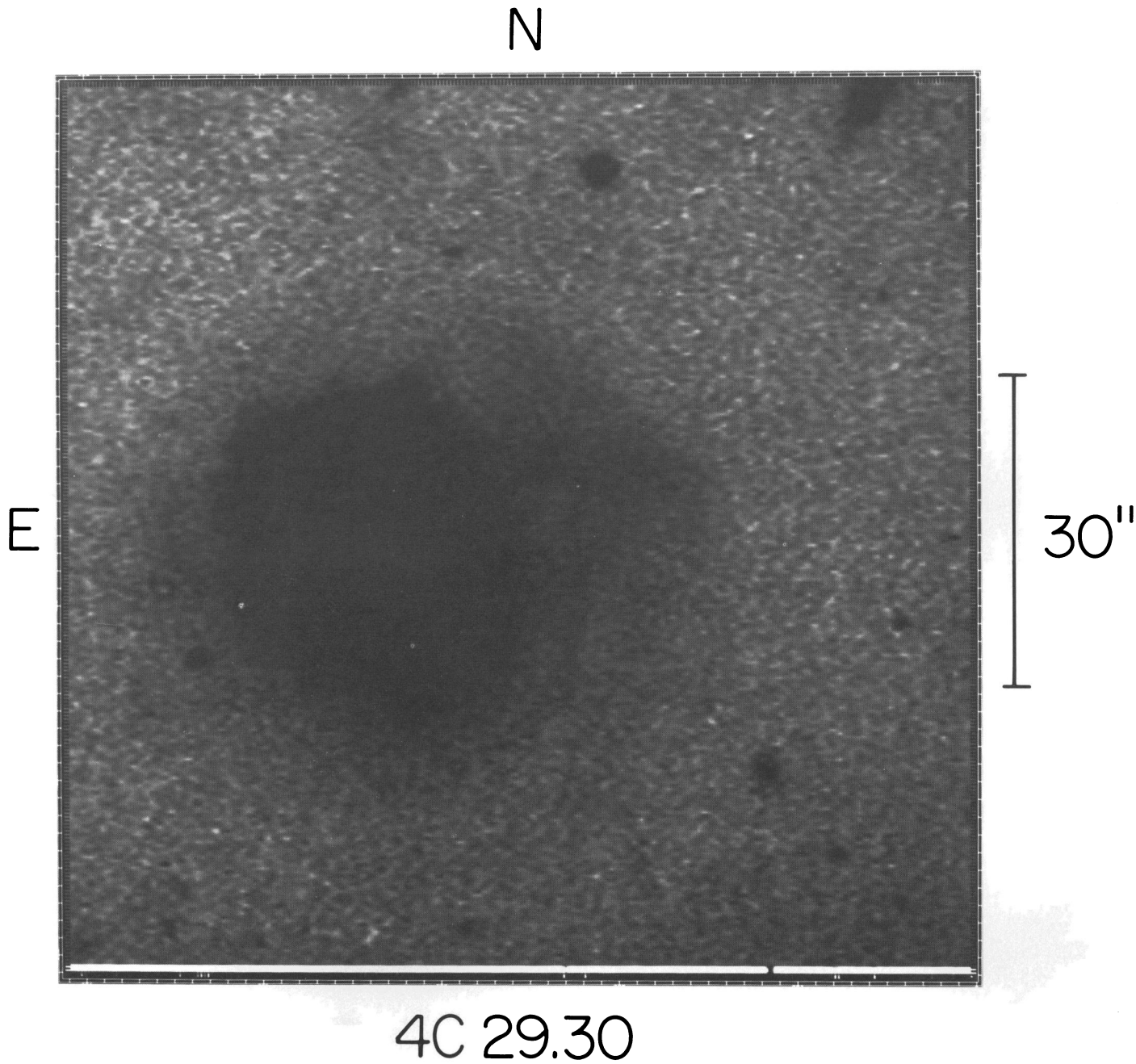

FIG. 5*a*

FIG. 5.—(*a*) *R*-band image of 4C 29.30 showing shell or fanlike structure to the west and east. (*b*) *R*-band image displayed to show small dust lane to SW of nucleus and possible secondary nucleus to the east.

HECKMAN *et al.* (*see* page 530)

© American Astronomical Society • Provided by the NASA Astrophysics Data System

1986ApJ...311..526H

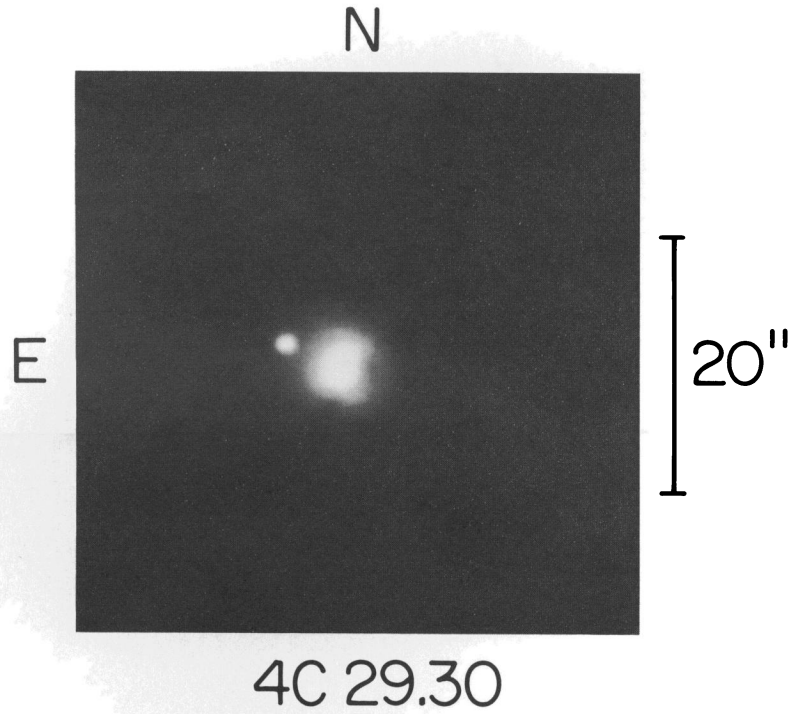

FIG. 5*b*

HECKMAN *et al.* (*see* page 530)

© American Astronomical Society • Provided by the NASA Astrophysics Data System

1986ApJ...311..526H

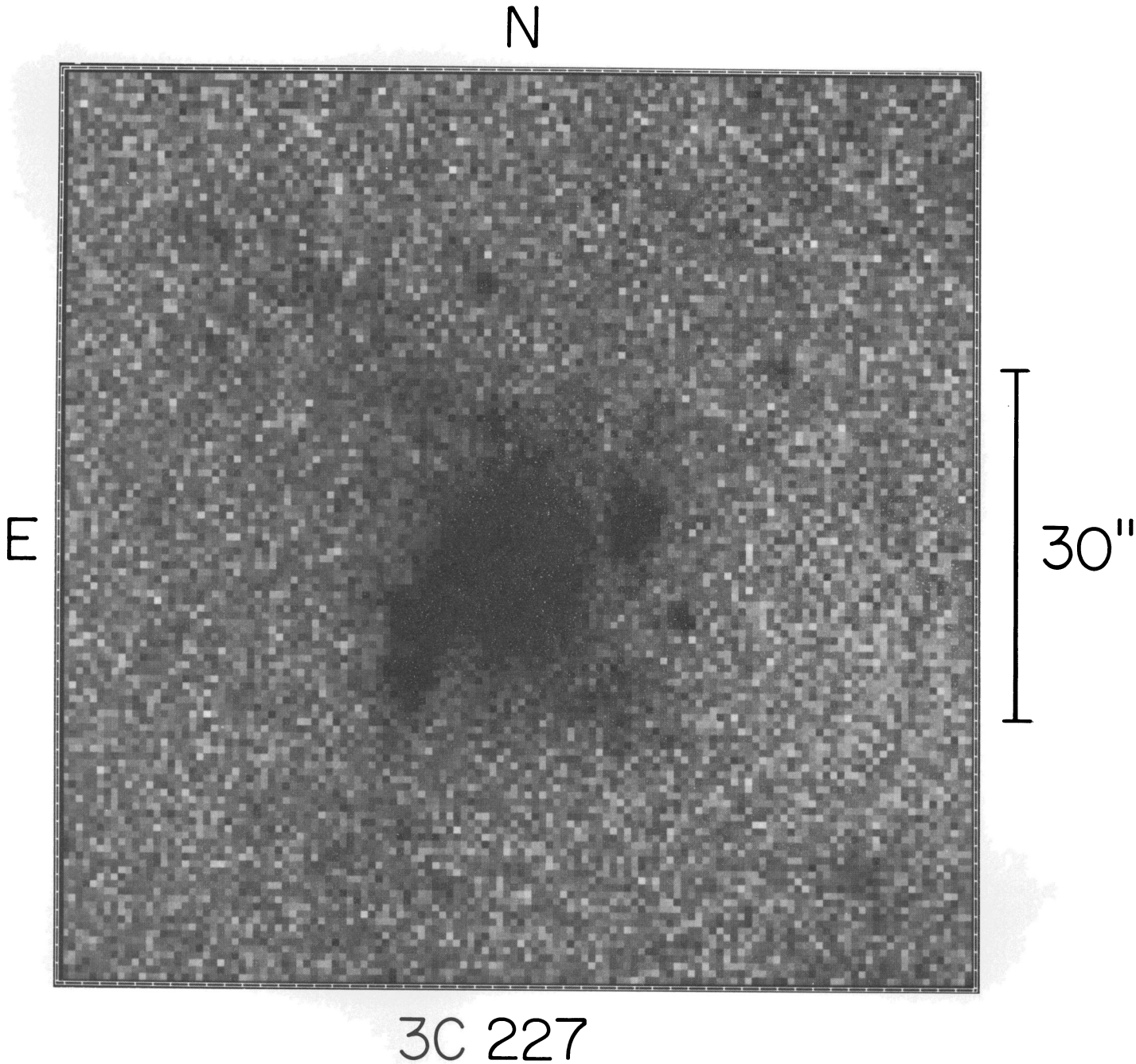

FIG. 6*b*.—Gray-scale representation of 3C 227 *V*-band image showing the SE tail

HECKMAN *et al.* (*see* page 530)

© American Astronomical Society • Provided by the NASA Astrophysics Data System

1986ApJ...311..526H

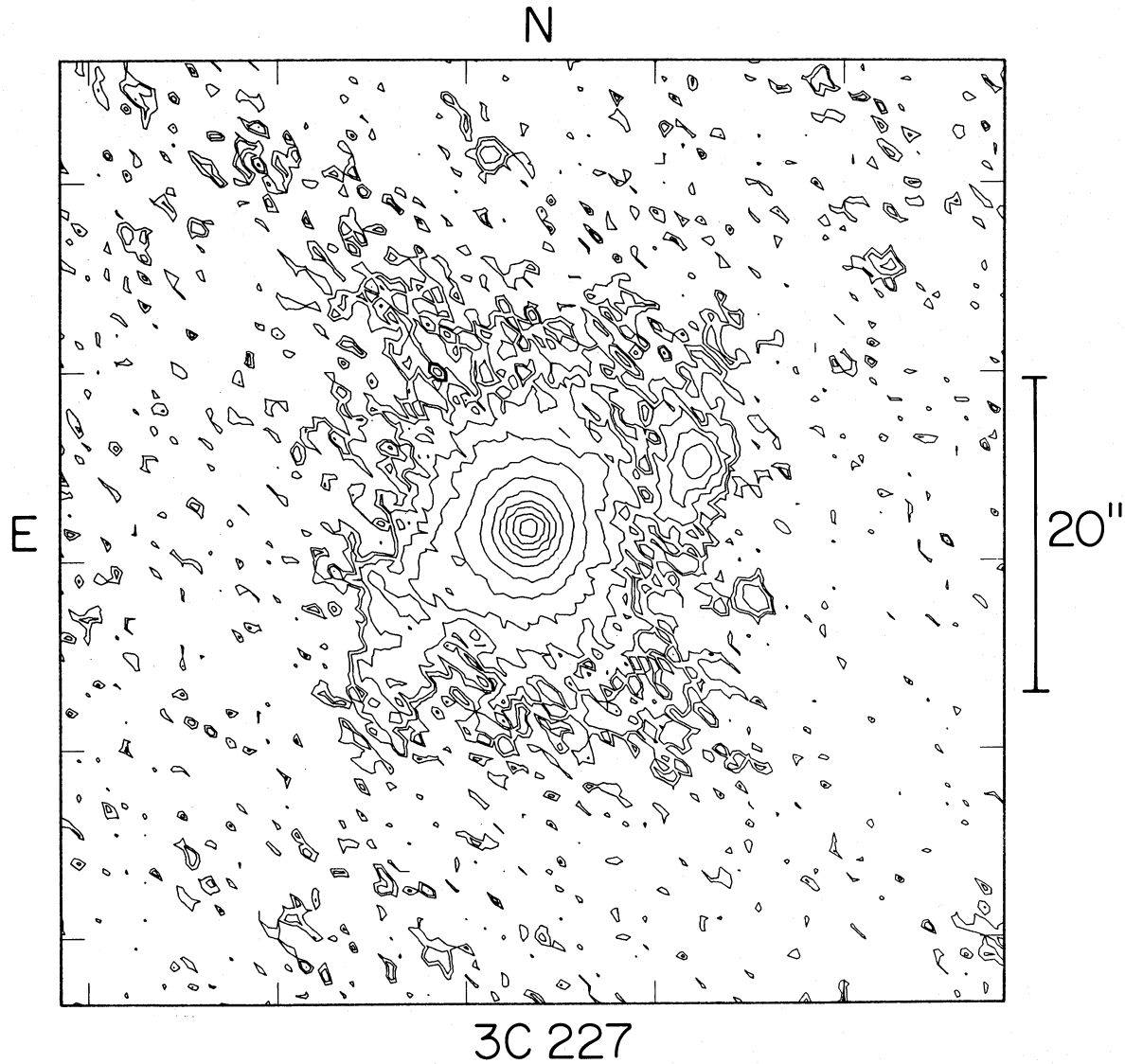

FIG. 6*a*.—Contour plot of 3C 227 *V*-band image. Contour levels are at 10, 20, 40, 80, etc., units above the sky, where 25 mag arcsec^{-2} is equal to 26 units. The peculiar structure is produced by redshifted emission in the lines of Hβ and [O III] λ5007, 4959 (see text).

which proceeds out to the NE and ends about 30″ to the east of the nucleus. The double tail system has an overall length of $\sim 1'$ ($\sim$85 kpc).

f) *NGC 3801 (4C 17.52)*

We have previously discussed the unusual H I properties and the kinematics of the stars and gas in this remarkable radio galaxy (Heckman *et al.* 1983; Heckman *et al.* 1985). Here we emphasize the peculiar optical morphology of the galaxy. As seen in Figure 7*a* (Plate 17), the main elliptical body of the galaxy is crossed by two main dust features: an S-shaped dust lane lying along the galaxy minor axis, and a patchy dust lane along the eastern half of the major axis. Many other fainter and more complex dust features are also present, especially in the western half of the galaxy. At fainter levels ($\mu_V \approx$ 23–24 mag arcsec^{-2}) the galaxy envelope is distorted into an open S-shape (Fig. 7*b* [Pl. 18]). At still fainter levels, a box-shaped halo and a short tail extending out to $\sim 1'.2$ ($\sim$16 kpc) to the ESE of the galaxy nucleus can be discerned.

g) *3C 285*

A photographic image of this peculiar radio galaxy has also been published by Saslaw, Tyson, and Crane (1978). The radio galaxy (Fig. 8 [Pl. 19]) has an ellipsoidal main body $-14'' \times 8''$ (19 × 10 kpc) and a distorted S-shaped envelope $\sim 35'' \times 17''$ (48 × 24 kpc) in size with a surface brightness of $\mu_V \approx 24$ mag arcsec^{-2}. The orientation of the envelope is roughly orthogonal to the E-W radio axis, but is aligned with the location of an apparent companion galaxy $\sim 40''$ (55 kpc) NNW of the radio galaxy. Our narrow-band Hα image shows that the S-shaped extensions are continuum-emitting structures. Sandage (1972) found 3C 285 to be unusually blue for a luminous elliptical galaxy (by $\Delta(B-V) \approx 0.2$ mag).

h) *4C 12.50 (PKS 1345+125)*

The spectacularly distorted morphology of this radio galaxy is evident in Figure 9*a* and Figure 9*b* (Plate 20). A double nucleus with a separation of $\sim 1''.5$ (2.9 kpc) is imbedded in a

© American Astronomical Society • Provided by the NASA Astrophysics Data System

1986ApJ...311..526H

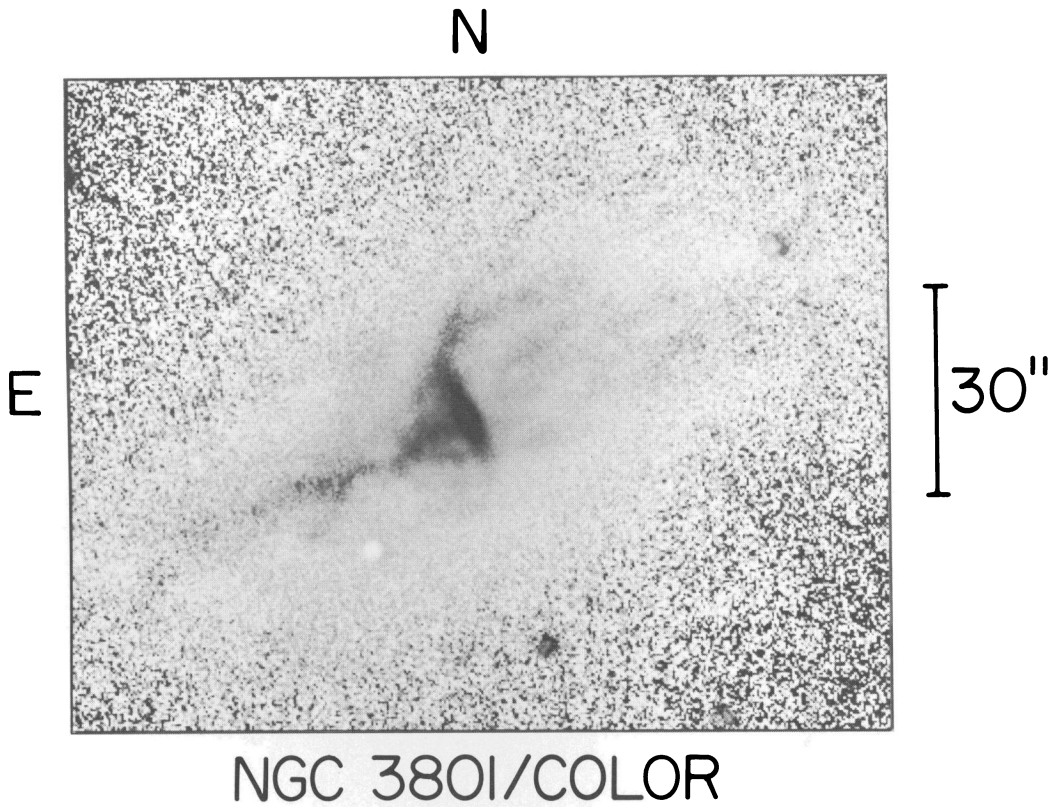

FIG. 7*a*

FIG. 7.—(*a*) Color map of the interior of NGC 3801 (*B*/*R*). Darker regions are redder. (*b*) Faint outer structure of NGC 3801 in a deep *R*-band frame.

HECKMAN *et al.* (*see* page 531)

© American Astronomical Society • Provided by the NASA Astrophysics Data System

1986ApJ...311..526H

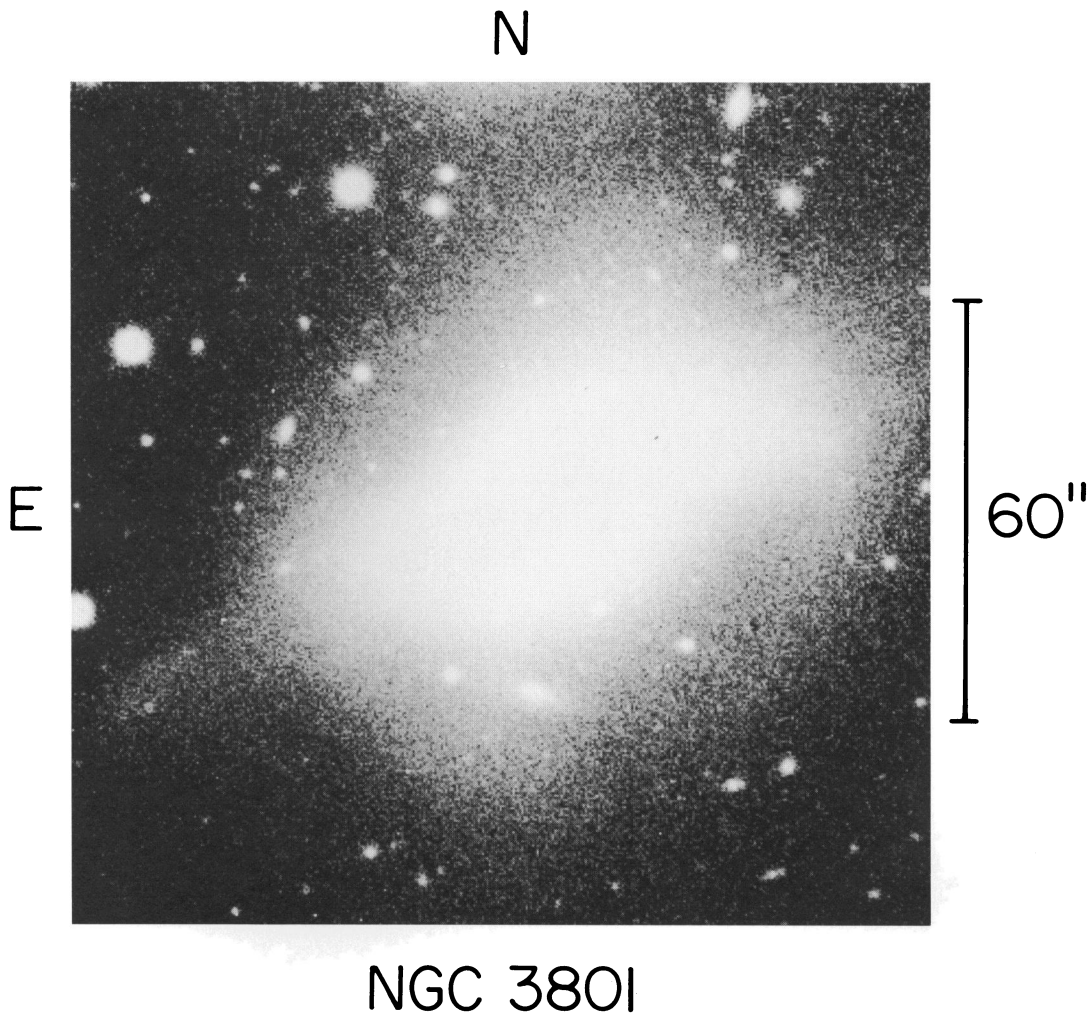

FIG. 7*b*

HECKMAN *et al.* (*see* page 531)

© American Astronomical Society • Provided by the NASA Astrophysics Data System

1986ApJ...311..526H

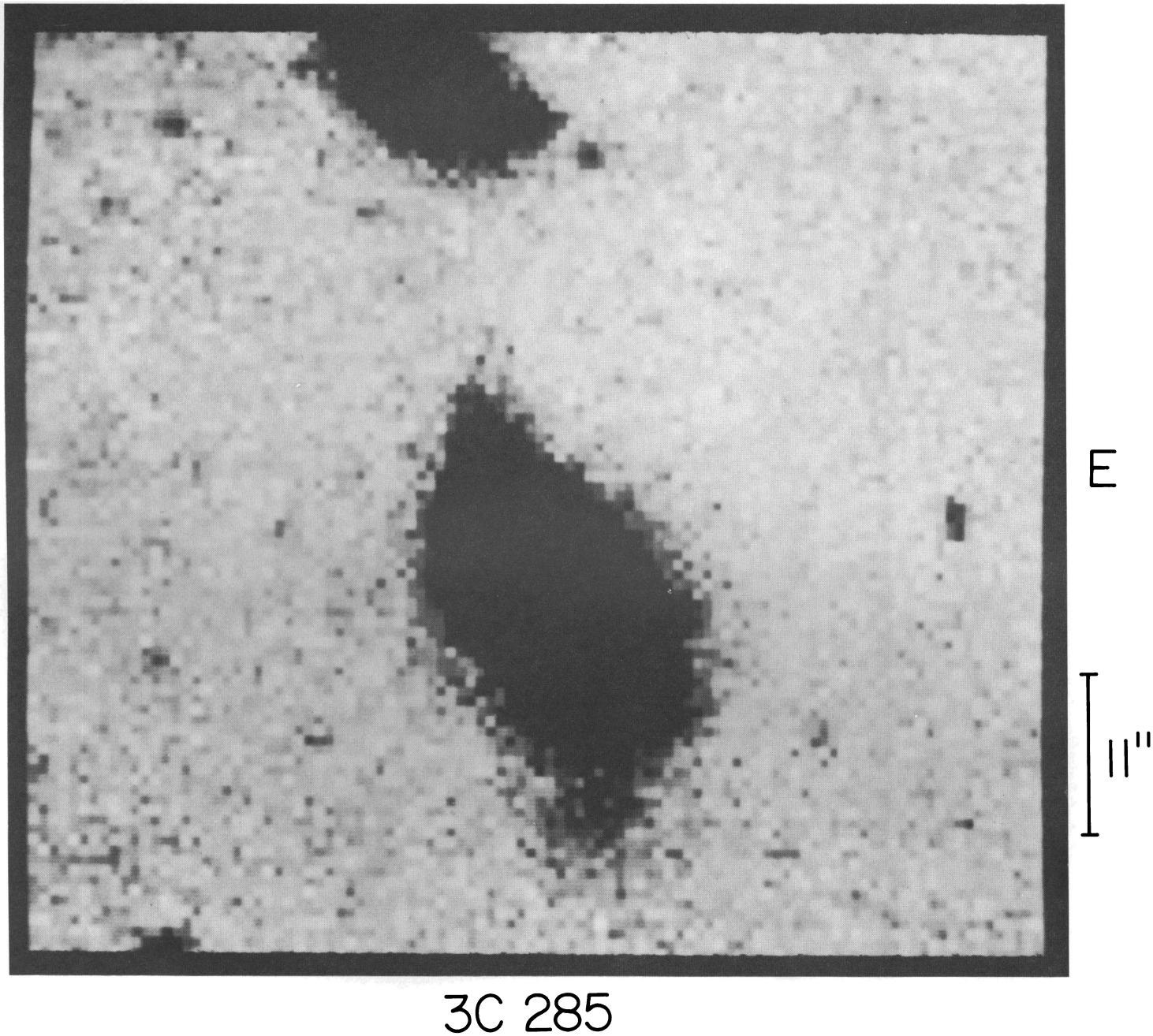

FIG. 8.—*R*-band frame of 3C 285, showing its S-shaped outer envelope. Note orientation flipped from usual sense.

HECKMAN *et al.* (*see* page 531)

© American Astronomical Society • Provided by the NASA Astrophysics Data System

1986ApJ...311..526H

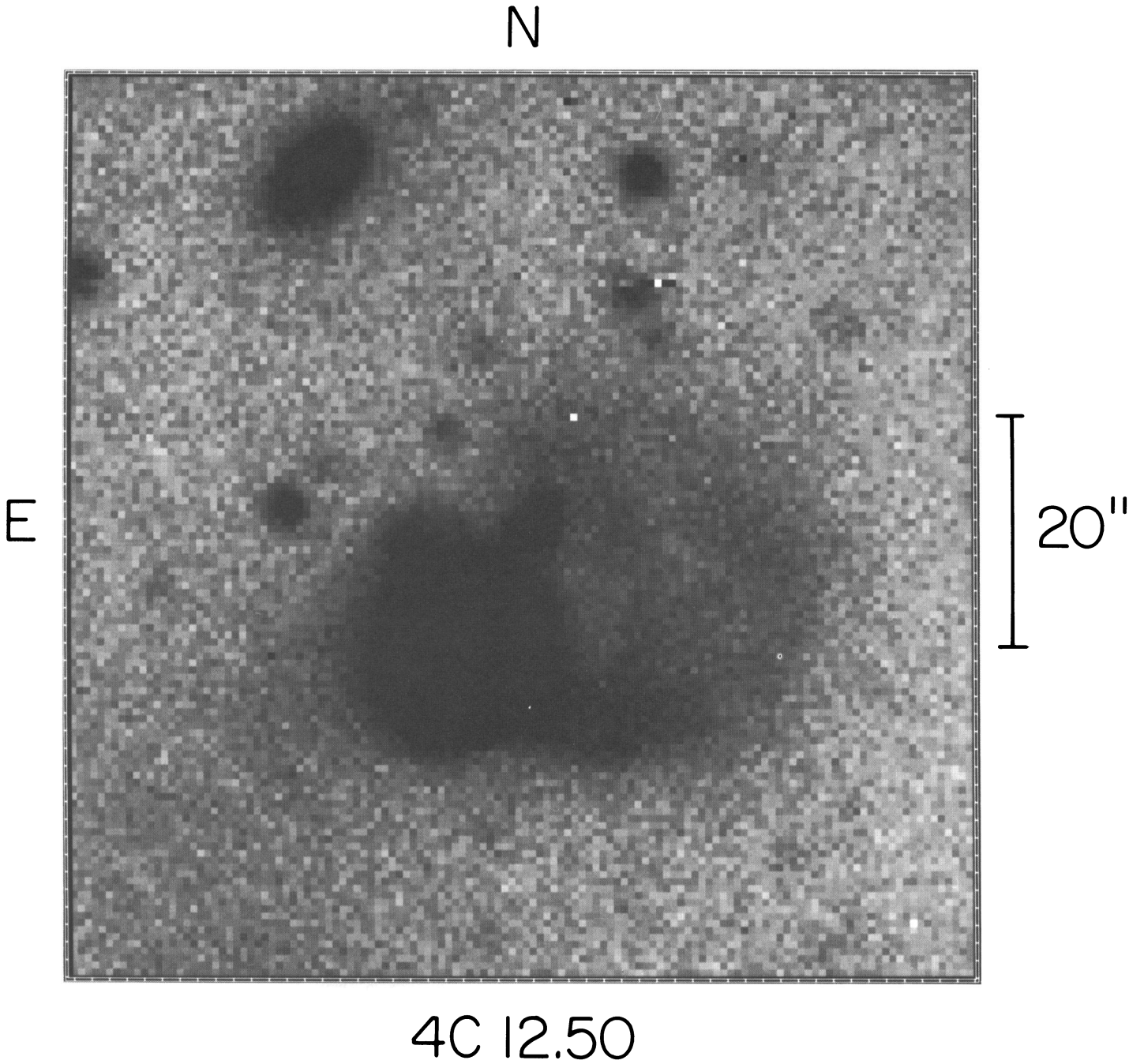

FIG. 9*b*.—Gray-scale representation of *V*-band image of 4C 12.50 showing twin west tails

HECKMAN *et al.* (*see* page 531)

© American Astronomical Society • Provided by the NASA Astrophysics Data System

1986ApJ...311..526H

main body ($\sim 15'' = 29$ kpc across) which is rather asymmetric and peculiarly pear-shaped at high level of surface-brightness ($\mu_V \approx 22$ mag arcsec^{-2}). Dust may be responsible for the former. A double-braided and strongly curved tail or fan with $\mu_V \approx 25$–25.5 unwinds in a counterclockwise fashion from the SW side of the main body to its termination $\sim 25''$ (= 48 kpc) to the NW of the nucleus. Our long-slit spectrum in P.A. = 90° crosses the twin-tails to the west, and indicates that they are continuum-emitting material. This is also confirmed by our narrow-band (Hα plus [N II] λ6584) image.

The radio galaxy is close to a group of about 15 faint ($V \approx 20.5$–22.0 mag) nebulous objects, which may be intrinsically faint objects ($M_V \approx -16.8$ to -18.3) associated with the radio galaxy. Several of these objects can be seen in or near the distorted halo of the radio galaxy. The radio galaxy may then be the dominant member of a group of galaxies. This galaxy has recently been discussed in more detail by Gilmore and Shaw (1986).

IRAS detected 4C 12.50 as a very powerful far-IR source whose properties rival those of Arp 220 (Soifer *et al.* 1984): $L_{IR} \approx 8 \times 10^{11}\ L_\odot$; $L_{IR}/L_{opt} \approx 20$ (Table 3).

i) 3C 293

We have discussed radio and optical imaging and optical spectroscopy of this galaxy in van Breugel *et al.* (1984). Our new result, which is presented here, is a deeper image (Fig. 10 [Pl. 21]) covering a wider field. This image shows that the primary galaxy (the parent of 3C 293) and a companion galaxy $\sim 37'' = 32$ kpc away (see van Breugel *et al.* 1984) are joined by a bridge ($\mu_V \approx 23$–23.5 mag arcsec^{-2}) of optical emission and that a fan or tail ($\mu_V \approx 24.5$) of optical emission extends some 60″–70″ (50–60 kpc) beyond the companion. The primary galaxy is also peculiar in having a copious interstellar medium which is observed as dust and ionized gas (see images published by van Breugel *et al.* 1984) and as strong H I absorption (Baan and Haschick 1981; 1984). Sandage (1972) calculates $B-V = 0.81$ in the rest frame of 3C 293 ≈ 0.1–0.2 mag bluer than a luminous elliptical (despite the probably substan-

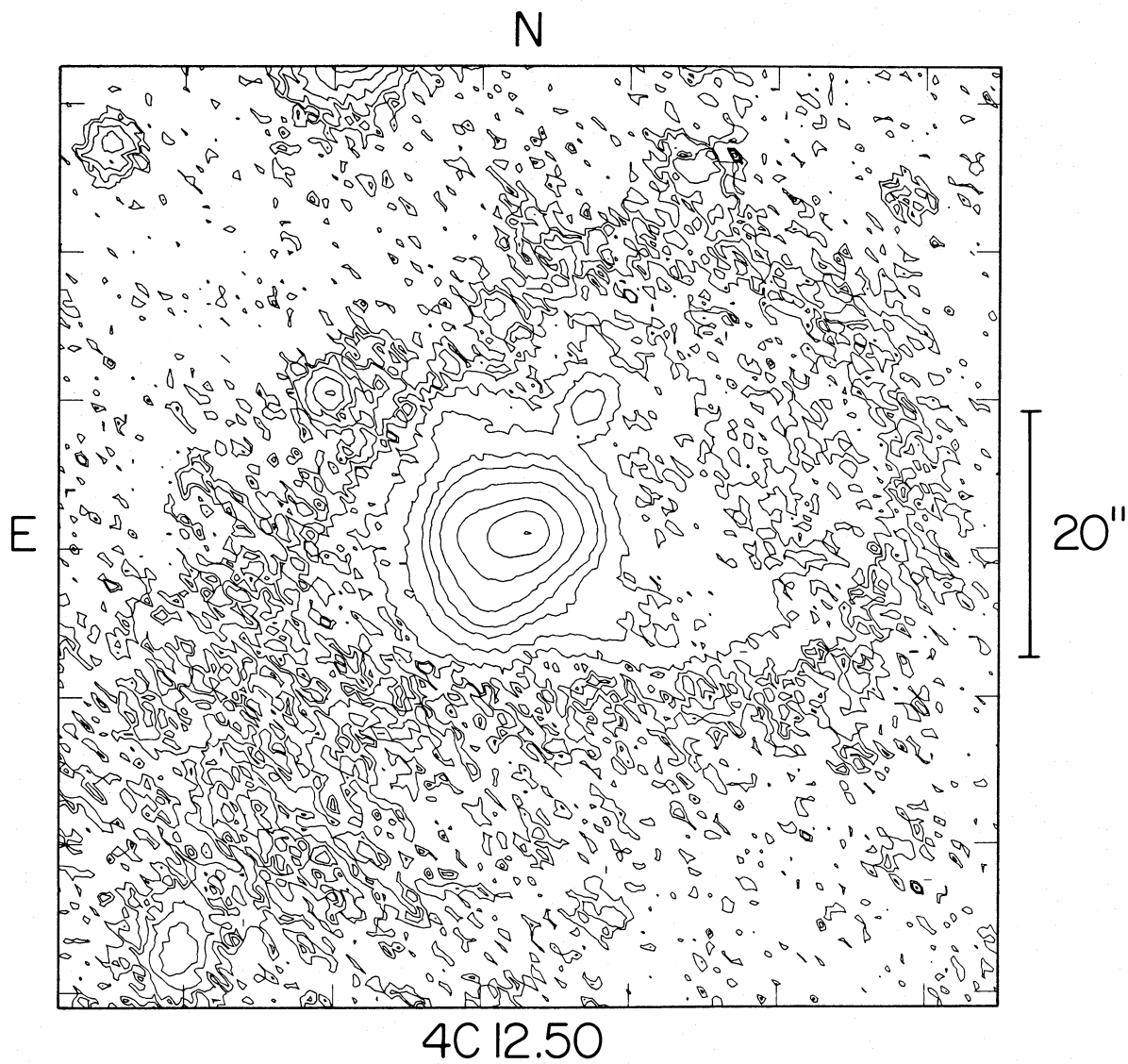

FIG. 9*a*.—Contour plot of the V-band image of 4C 12.50 = PKS 1345+125. Contour levels are 10, 20, 40, 80, etc., units above the sky, where 25 mag arcsec^{-2} is equal to 44 units.

© American Astronomical Society • Provided by the NASA Astrophysics Data System

1986ApJ...311..526H

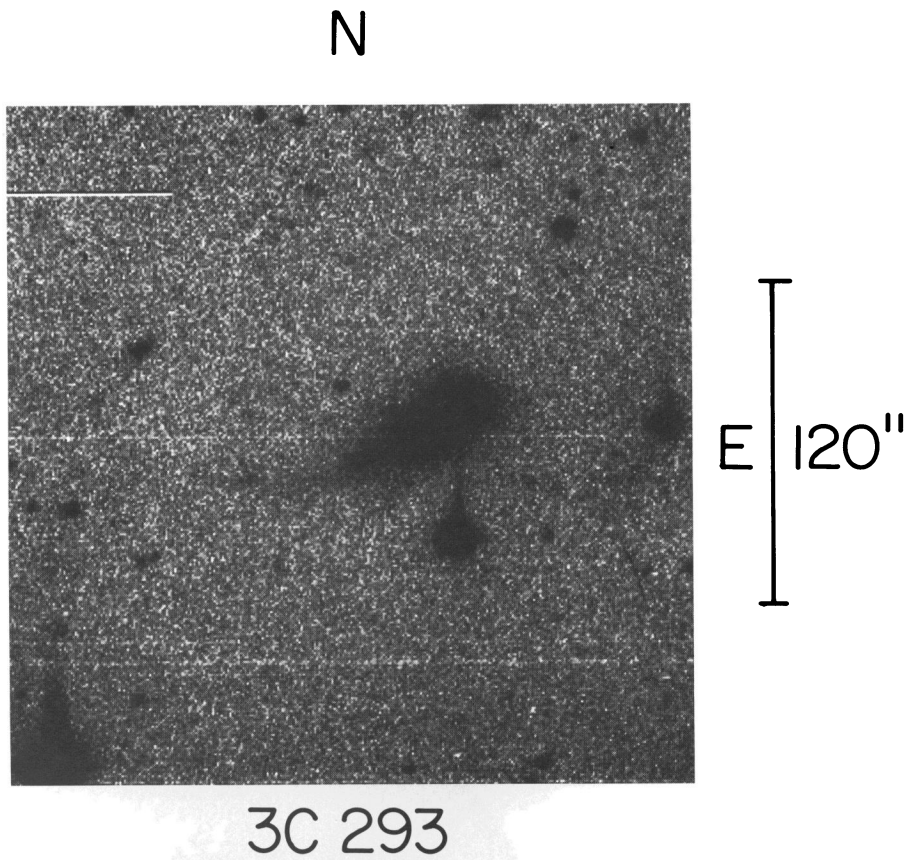

FIG. 10.—*R*-band CCD image of 3C 293 showing its bridge-tail system and companion galaxy. Note orientation flipped from usual sense.

HECKMAN *et al.* (*see* page 532)

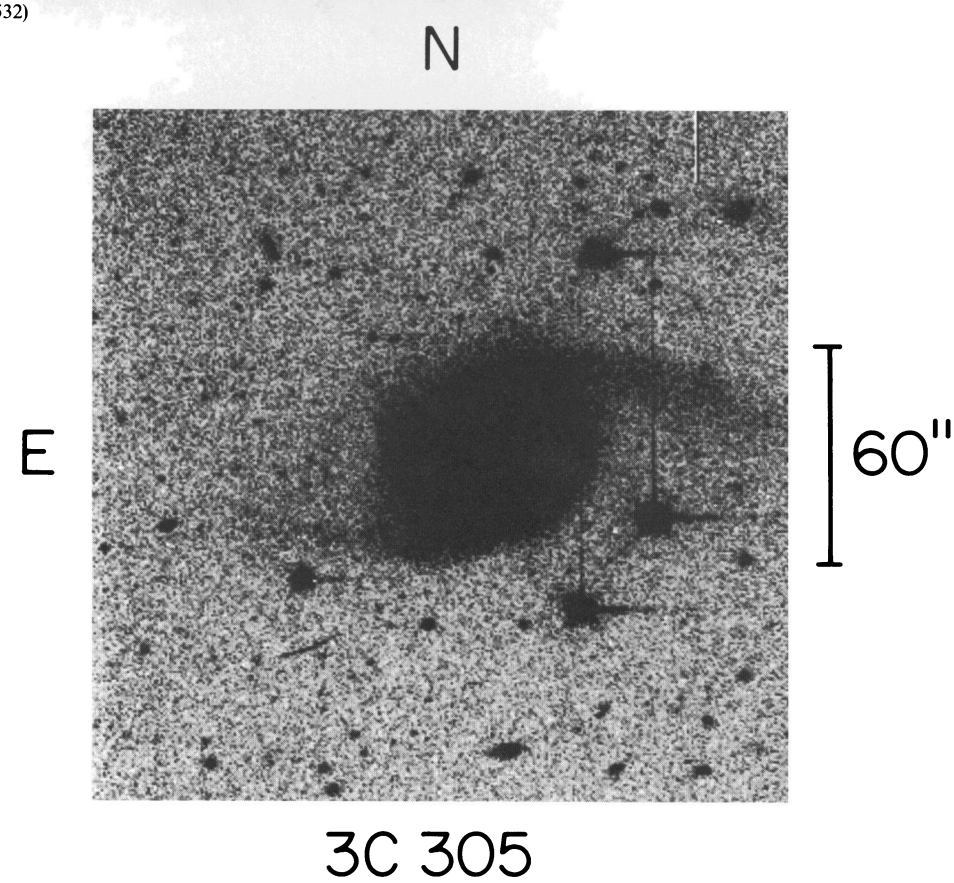

FIG. 11.—*B*-band CCD image of 3C 305 showing its long-tail system

HECKMAN *et al.* (*see* page 532)

© American Astronomical Society • Provided by the NASA Astrophysics Data System

1986ApJ...311..526H

tial internal reddening produced by the observed dust). 3C 293 has also been detected by *IRAS* and has $L_{IR} \approx 10^{10}\ L_{\odot}$ (Table 3). Apart from the presence of a close companion, 3C 293 is isolated.

j) 3C 305

We have previously published the results of detailed optical and radio observations of this galaxy (Heckman *et al.* 1982) but have recently obtained a CCD image which is much deeper and which also covers a much wider field than the Vidicon image published therein. This image (Fig. 11 [Pl. 21]) shows two "tails" with $\mu_V \approx 25$ mag arcsec^{-2}, each preceeding out to distances of $\sim 75'' \approx 60$ kpc from the nucleus SE and NW of the main elliptical body of the parent galaxy. The galaxy isophotal major axis also rotates from P.A. $\approx 70°$ in the inner $\sim 20''$ to P.A. $\approx 130°$ at $r \approx 30''$. Other properties of 3C 305 are also of considerable interest:

1. Within the main body of the galaxy, the stellar velocity dispersion (~ 180 km s^{-1}) is too high for a stellar disk (see Heckman *et al.* 1985).

2. The galaxy occurs in a sparse environment, and there are no close companion galaxies whose recent passage would have provoked the observed morphological disturbance.

3. The spectroscopy reported in Heckman *et al.* (1982) and the photometry of Sandage (1972) both imply that 3C 305 has an unusually hot and blue stellar population for a giant elliptical galaxy (i.e., relatively strong Balmer absorption lines). *IRAS* pointed observations of 3C 305 yield $L_{IR} \approx 10^{10}\ L_{\odot}$ (Table 3).

4. The galaxy contains a substantial cool ($T \leq 10^4$ K) interstellar medium, observed in the form of a large ($\sim 3 \times 13$ kpc) region of emission-line gas and a complex network of prominent dust lanes and patches (see images in Heckman *et al.* 1982, 1985; Sandage 1966). These latter distort the optical morphology at high levels of surface brightness ($\mu_V \approx 21$).

5. The *stellar* dynamics of 3C 305 are peculiar (Heckman *et al.* 1985) relative to normal ellipticals of similar absolute magnitude ($M_B = -21.7$ and $M_V = -22.4$ for $H_0 = 75$ km s^{-1} Mpc^{-1}): 3C 305 exhibits rapid rotation of 140 km s^{-1} (it lies near the line populated by rotationally supported oblate spher-

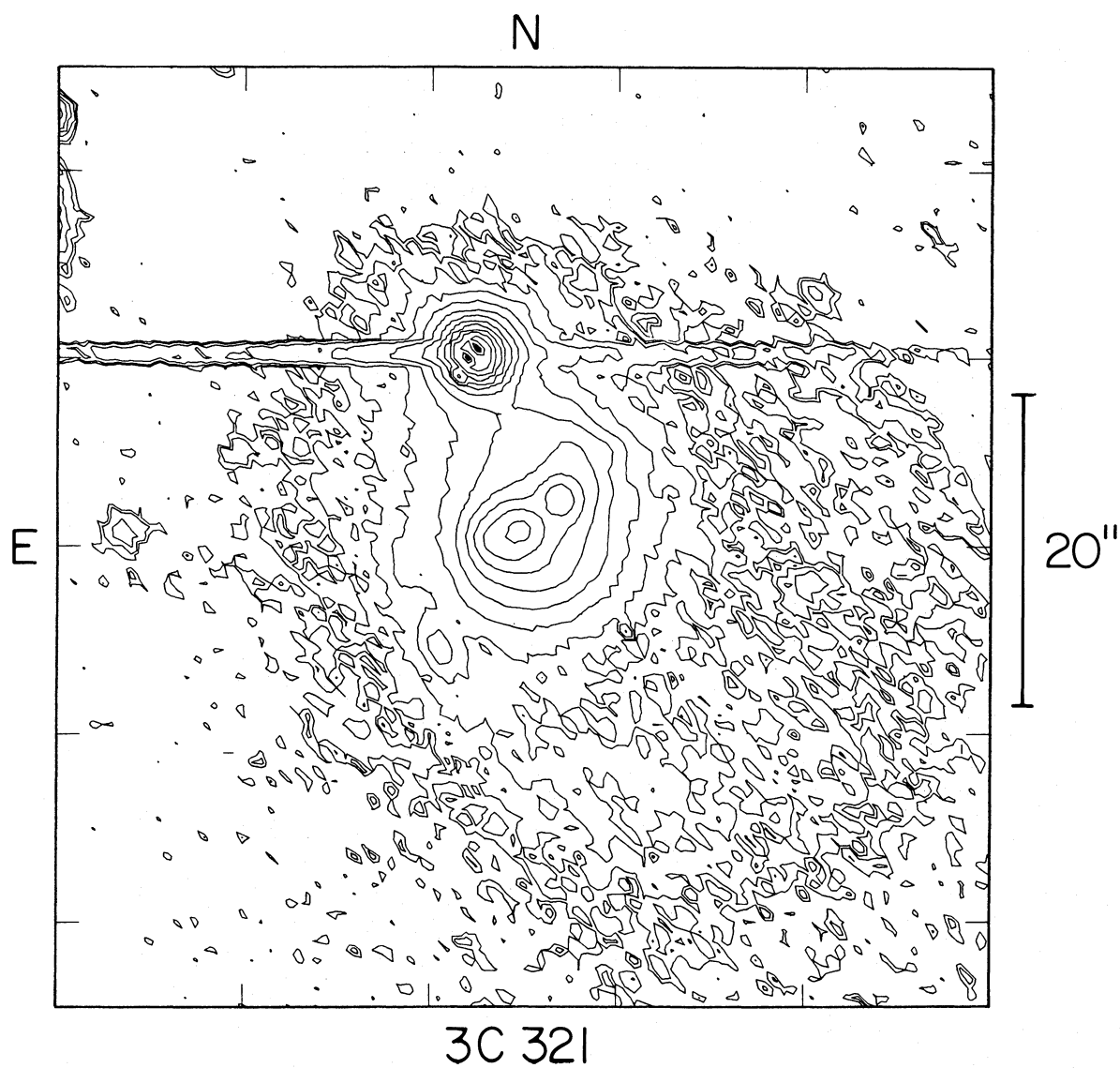

FIG. 12*a*.—Contour plot of *V*-band image of 3C 321. Contour levels are at 10, 20, 40, 80, etc., units above the sky (sky level is 1140 units).

© American Astronomical Society • Provided by the NASA Astrophysics Data System

1986ApJ...311..526H

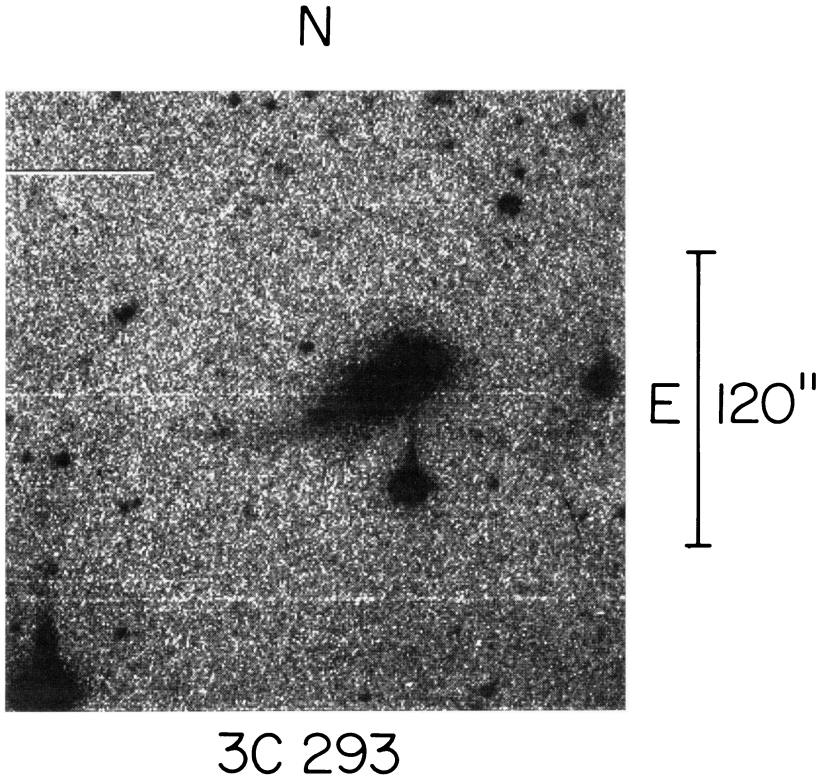

FIG. 10.—*R*-band CCD image of 3C 293 showing its bridge-tail system and companion galaxy. Note orientation flipped from usual sense.

HECKMAN *et al.* (*see* page 532)

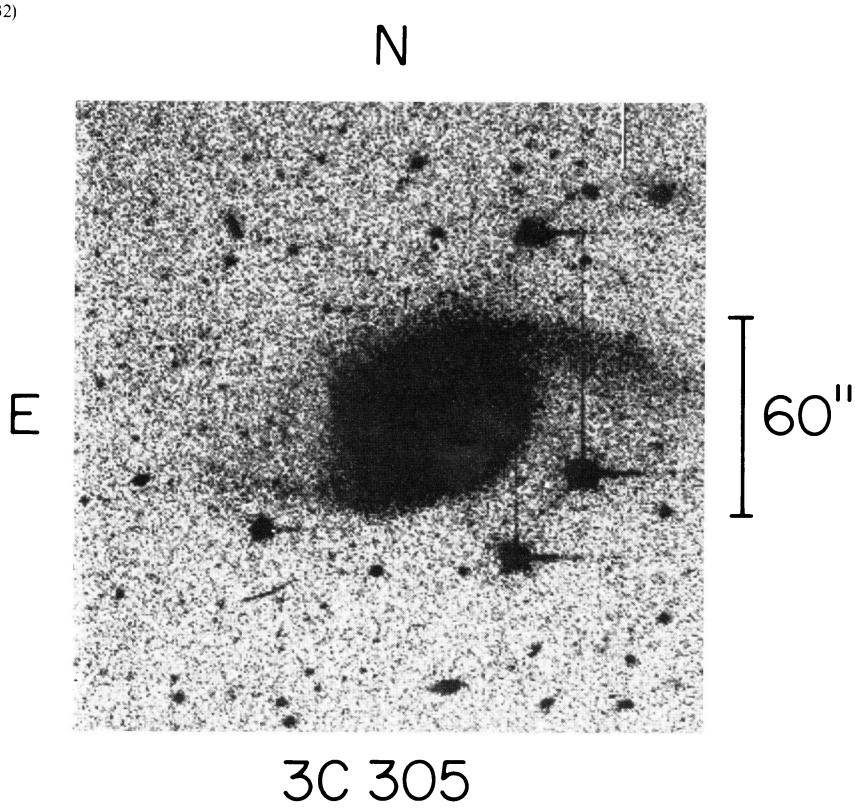

FIG. 11.—*B*-band CCD image of 3C 305 showing its long-tail system

HECKMAN *et al.* (*see* page 533)

© American Astronomical Society • Provided by the NASA Astrophysics Data System

1986ApJ...311..526H

oids in the [v_{rot}/σ, elliptically]-plane) and has a low central velocity dispersion ($\sigma = 180$ km s^{-1} vs. an expected σ of ~ 300 km s^{-1}) based on its M_B and the relation between M_B and σ found by Davies *et al.* (1983) for normal ellipticals.

k) 3C 321

This peculiar radio galaxy (Fig. 12*a*, Fig. 12*b* [Pl. 22]) consists of two nuclei embedded in a complex, asymmetric envelope $\sim 49'' \times 40''$ ($\sim 80 \times 65$ kpc) in size. The nuclei lie roughly along the NW/SE radio source axis, with the SE nucleus being the brighter and the NW nucleus ($\sim 3'' = 5$ kpc away) being ~ 0.5–1.0 mag fainter. The knot $\sim 9''$ to the SE of the bright nucleus is an emission-line feature. An emission-line tail curves out $\sim 6''$ (10 kpc) to the north from the NW nucleus, and a fan or broad tail (continuum plus emission lines) can be seen stretching $\sim 25''$ (41 kpc) to the SW. The straight but knotty shell some 25–30″ (~ 45 kpc) to the WNW is also an emission-line structure. A faint spiral galaxy $\sim 37''$ (61 kpc) to the NE is the only other galaxy seen within $\sim 2'$ (200 kpc) of 3C 321. Finally, the *IRAS* detection of 3C 321 at $\lambda = 60$ μm implies a substantial far-IR luminosity of $\sim 2 \times 10^{11}$ $L_\odot$ (Table 3).

l) 3C 327

In addition to the main ellipsoidal body of the galaxy $35'' \times 25''$ (55×39 kpc) in extent, peculiar fanlike structure (spatially unresolved shells?) can also be discerned (Figs. 13*a*, 13*b* [Pls. 23–24]) out to a distance of $\sim 16''$ (28 kpc) on the SE side. This feature has $\mu_V \approx 23.5$–24.5 mag arcsec^{-2}. The fan does not lie along the radio axis (P.A. = 100°). Our long-slit spectroscopy (P.A. = 122°–100°) and narrow-band imaging reveal that this feature is continuum emitting.

The red color of 3C 327 (Sandage 1972) might imply a normal (old) stellar population for 3C 327. However, 3C 327 has been detected at $\lambda = 60$ μm by *IRAS* with an implied luminosity of $\sim 2 \times 10^{11}$ $L_\odot$ (Table 3).

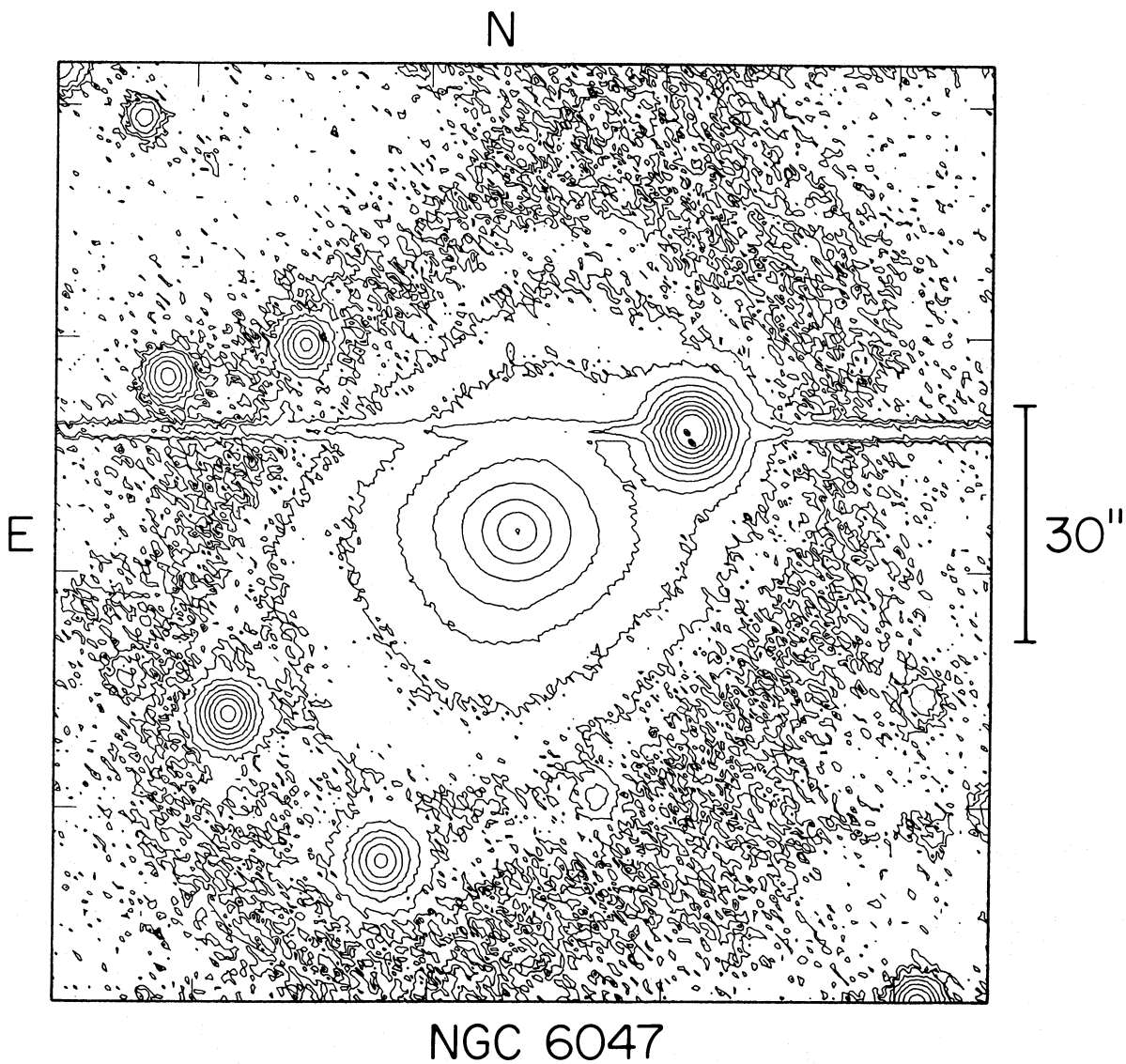

FIG. 14.—Contour plot of V-band image of NGC 6047 (4C 17.60). Contour levels are at 10, 20, 40, 80, etc., units above the sky, where 25 mag arcsec^{-2} is equal to 22 units.

© American Astronomical Society • Provided by the NASA Astrophysics Data System

1986ApJ...311..526H

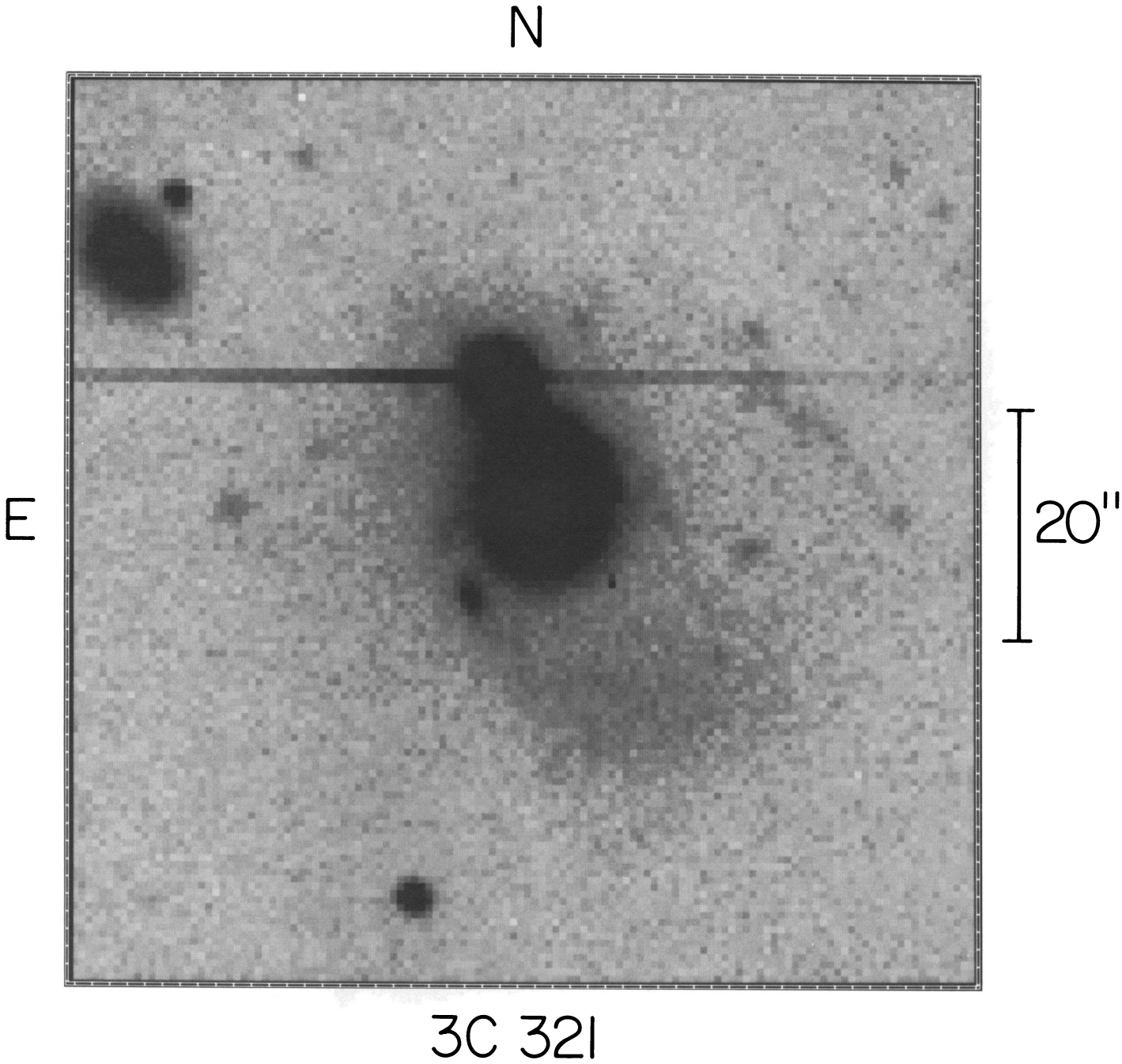

FIG. 12*b*.—Gray-scale representation of 3C 321 *V*-band image showing the fan or tail emanating from the SE companion galaxy. Except for this fan, the other peculiar structures are produced by redshifted emission in the lines of Hβ and [O III] $\lambda\lambda$5007, 4959 (see text).

HECKMAN *et al.* (*see* page 534)

© American Astronomical Society • Provided by the NASA Astrophysics Data System

1986ApJ...311..526H

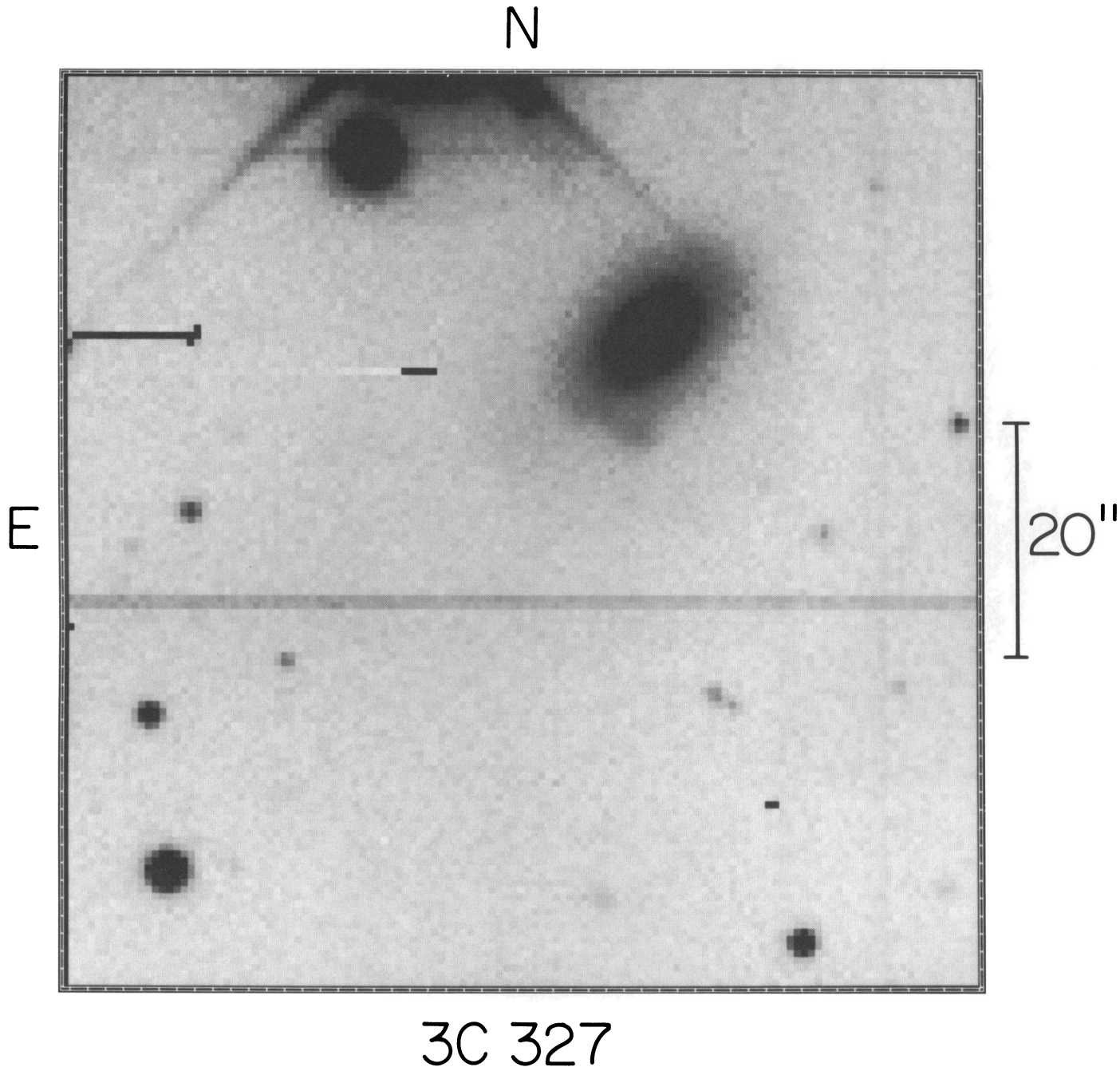

FIG. 13*a*

FIG. 13.—(*a*) *V*-band image of 3C 327 showing the inner shell or fanlike structure to the SE. (*b*) Image of 3C 327 displayed to show the faint outer fan or shell to the SE.

HECKMAN *et al.* (*see* page 534)

© American Astronomical Society • Provided by the NASA Astrophysics Data System

1986ApJ...311..526H

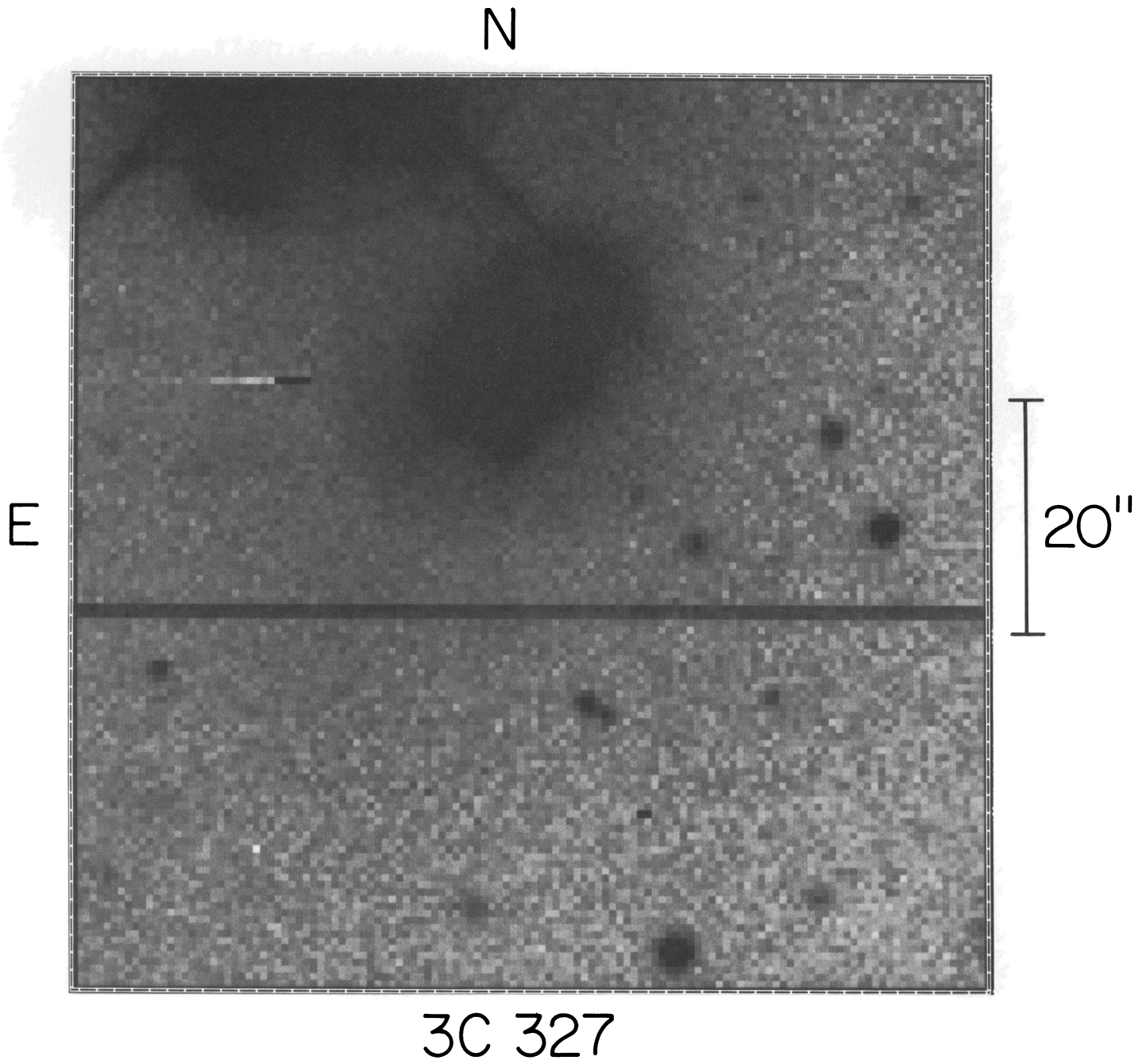

FIG. 13*b*

HECKMAN *et al.* (*see* page 534)

© American Astronomical Society • Provided by the NASA Astrophysics Data System

1986ApJ...311..526H

m) NGC 6047 (4C 17.60)

In contrast to most of the examples of morphologically peculiar radio galaxies discussed in this section, NGC 6047 does not exhibit any tails or fans. Instead, its peculiarities (Fig. 14) are a rapid and strong rotation in the isophotal major axis between $r = 14''$ and $21''$ (8 and 12 kpc), and the boxy shape of the isophotes at radii $r > 7''$ (4 kpc) corresponding to levels of surface brightness $\mu_V \geq 22$ mag arcsec^{-2}. A bright ($V \approx 14$ mag), peculiar spiral galaxy is located ~ 60 kpc north of NGC 6047. However, there is no morphological evidence that NGC 6047 is interacting with this system at present. This galaxy is near the center of the Hercules cluster (Abell 2151). Lauer (1985) has found boxy isophotes in three of 42 elliptical galaxies for which he has detailed CCD surface photometry. The isophotes in his galaxies deviate from ellipses at the $\sim 1\%$ level, while the deviations in NGC 6047 are much larger.

n) PKS 1934−638

We have obtained deep B and V band images of the parent galaxy of this highly powerful compact (~ 120 pc) radio source. As seen in Figure 15, the galaxy apparently consists of two knots (nuclei?) separated by $\sim 3''$–$4''$ (~ 10 kpc), the eastern one of which is the brighter (by ~ 1 mag). Fans or tail-like features with $\mu_V \approx 23$–23.5 mag arcsec^{-2} stretch $\sim 4''$–$5''$ (~ 12 kpc) SW of the east knot and north of the west knot, and are embedded in an amorphous, irregular envelope $\sim 15'' \times 13''$ (41×36 kpc) in size. Several other faint ($V \approx 22.0$ mag), nebulous objects are seen in the vicinity of the radio galaxy.

Penston and Fosbury (1978) have studied this galaxy, and suggested that it does *not* have two nuclei, but is instead analogous to Centaurus A and Cygnus A, consisting of an ellipsoidal main body bisected by a dust lane (but see Thompson 1984 regarding Cygnus A). Our B and V imaging data imply that the integrated $B-V$ color is 1.25, ~ 0.20 mag bluer than a normal elliptical at $z = 0.18$. The region considered to be the dust lane by Penston and Fosbury has the same color. We therefore interpret the optical morphology as indicative of two distinct (close companion) galaxies, although the presence of dust can not be ruled out.

o) OX 169 (PKS 2141+175)

Hutchings, Crampton, and Campbell (1984) and Gehren *et al.* (1984) have previously reported the optical "jet" associated

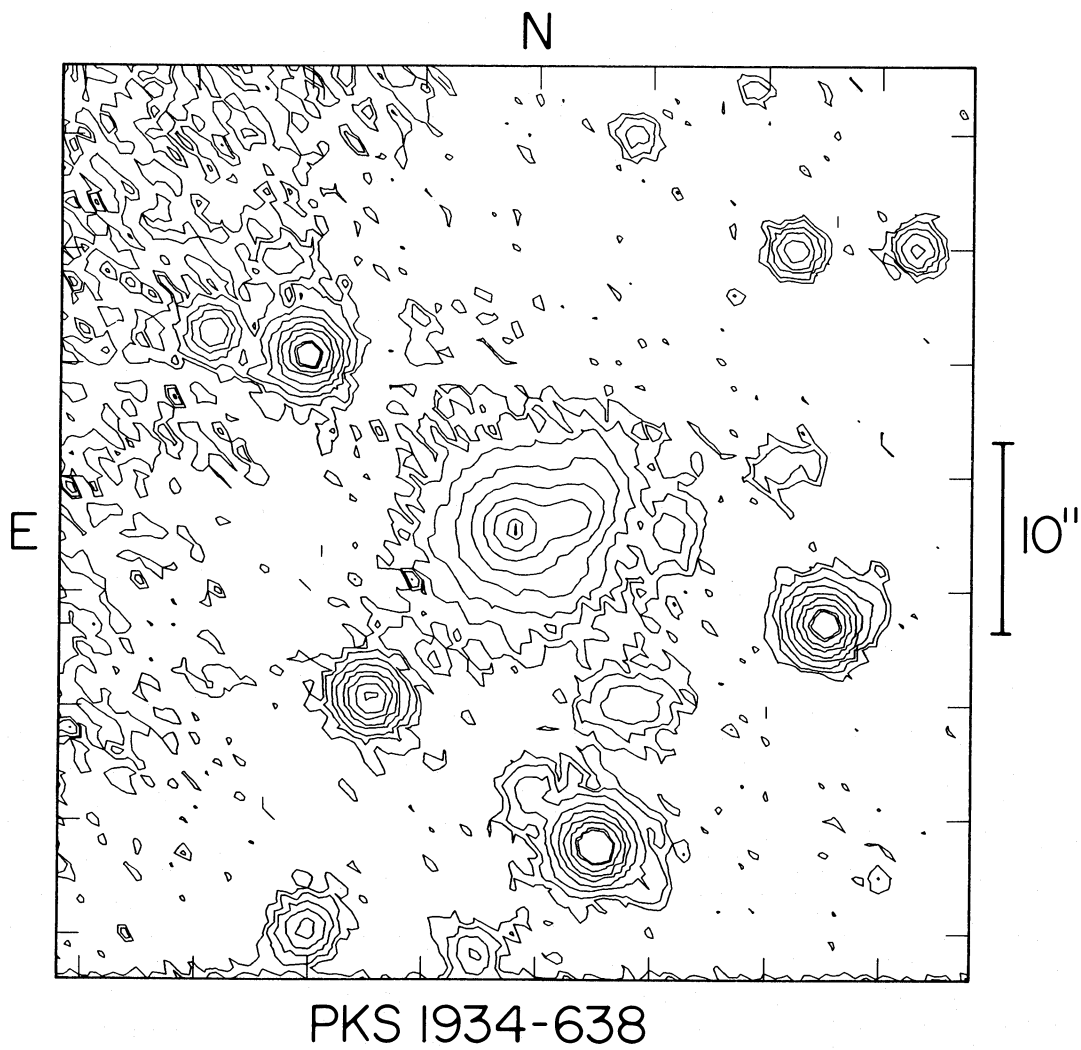

FIG. 15.—Contour plot of V-band image of PKS 1934−638. Contour levels are at 10, 20, 40, 80, etc., units above the sky, where 25 mag arcsec^{-2} is equal to 25 units.

© American Astronomical Society • Provided by the NASA Astrophysics Data System

1986ApJ...311..526H

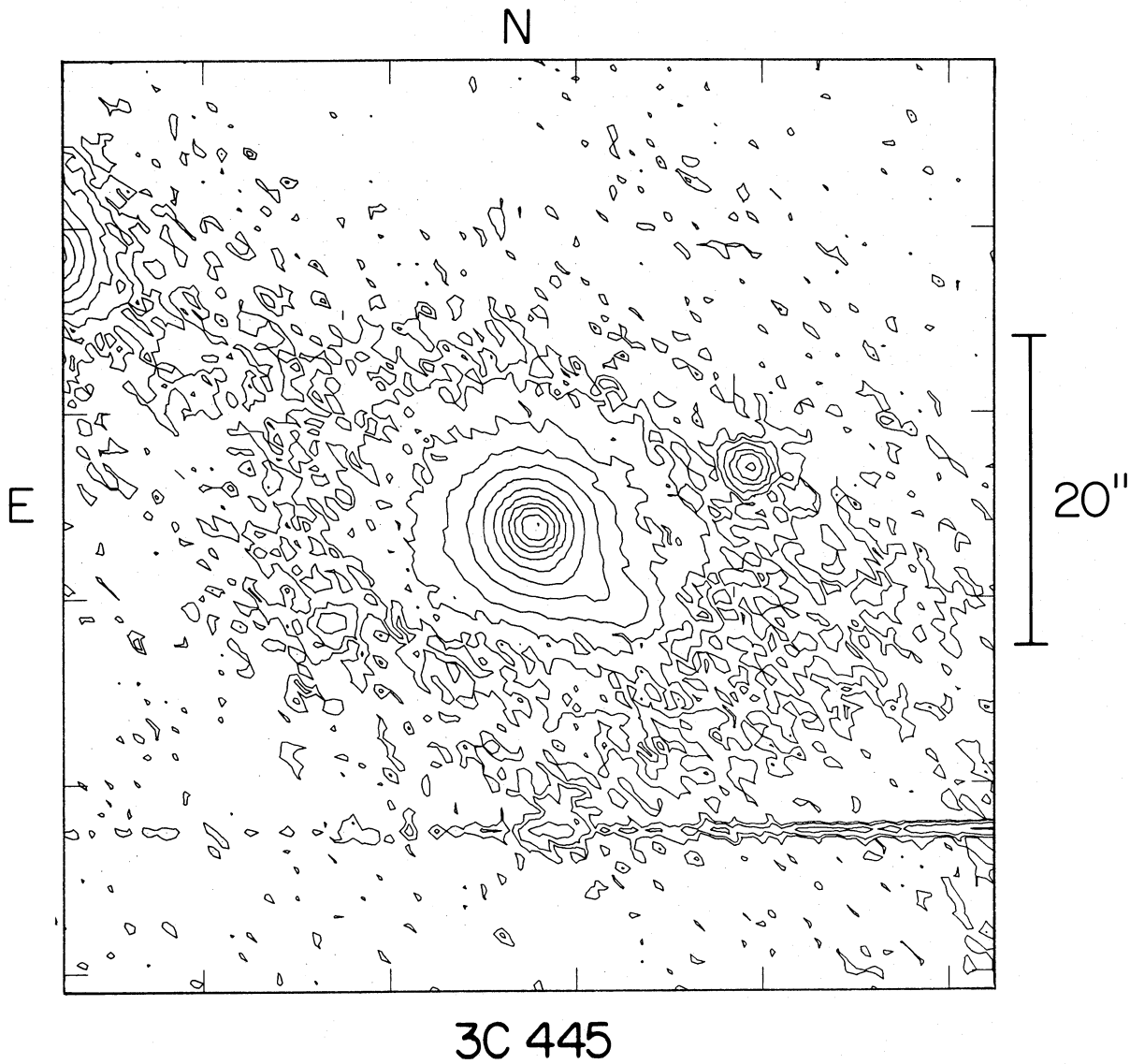

FIG. 17*a*.—Contour plot of V-band image of 3C 445. Contour levels are at 10, 20, 40, 80, etc., units above the sky, where 25 mag arcsec^{-2} is equal to 22 units.

with this radio-compact quasar. Our deep 4 m CCD frame (Fig. 16 [Pl. 25]) reveals that the faint optical fuzz surrounding the quasar has a complex appearance, consisting of a long, linear feature with $\mu_V \approx 23.5$–25.5 mag arcsec^{-2} (tail) extending $\sim 12''$ (~ 40 kpc) to the ESE (the "jet"), a more stubby, but similarly bright countertail extending $\sim 9''$ (~ 30 kpc) to the WNW, and a fainter ($\mu_V \approx 26$) fanlike region extending $\sim 8''$ (27 kpc) to the SW. The overall size of the optical system (~ 70 kpc) is larger than a normal disk galaxy.

Boroson and Oke (1984) have published long-slit CCD data on OX 169 taken in position angles passing through the tail and countertail. They detect no [O III] $\lambda 5007$ and Hβ emission there, so we are seeing continuum-emitting material in our V-band image.

The radio source OX 169 is compact ($< 1''$ in size), so the tails are not likely to be nonthermal (synchrotron-emitting) material. A galaxy with $V \approx 19.8$ mag located 115 kpc west of OX 169 is the only galaxy brighter than $V \approx 22$ mag within ~ 150 kpc of the quasar (note Smith *et al.* 1986 find that the host galaxy underlying OX 169 has $V \approx 18.2$ mag or $M_B \approx -21.5$). A contour plot of our CCD image of OX 169 can be found in Smith *et al.* (1986).

p) 3C 445

The parent of this powerful large-scale (~ 560 kpc) double radio source is a well-known N galaxy. Our optical image (Fig. 17*a*, Fig. 17*b* [Pl. 26]) reveals that a bright ($\mu_V \approx 23$–24 mag arcsec^{-2}) tail extends out from the galaxy center for $\sim 10''$ (10 kpc) in P.A. $\approx -130°$ ($\sim 53°$ off from the P.A. $= 177°$ of the radio source). Long-slit spectroscopy of the tail implies that it is a strong source of emission lines. At larger radii (~ 10–20 kpc) to the SW, a faint ($\mu_V \approx 25.5$–26.0) fan may also be present. An apparent companion galaxy with $V \approx 17.6$ mag is seen ~ 37 kpc away to the NE, but no luminous connection to 3C 445 with $\mu_V < 26.0$ mag arcsec^{-2} is evident. 3C 445 has been detected by *IRAS*, and has $L_{\rm IR} \approx 2 \times 10^{10}\ L_\odot$ (Table 3).

q) PKS 2247+140

The host galaxy of this low-redshift radio-loud quasar ($z = 0.237$) consists of an oval nebulosity $\sim 18'' \times 12''$

© American Astronomical Society • Provided by the NASA Astrophysics Data System

1986ApJ...311..526H

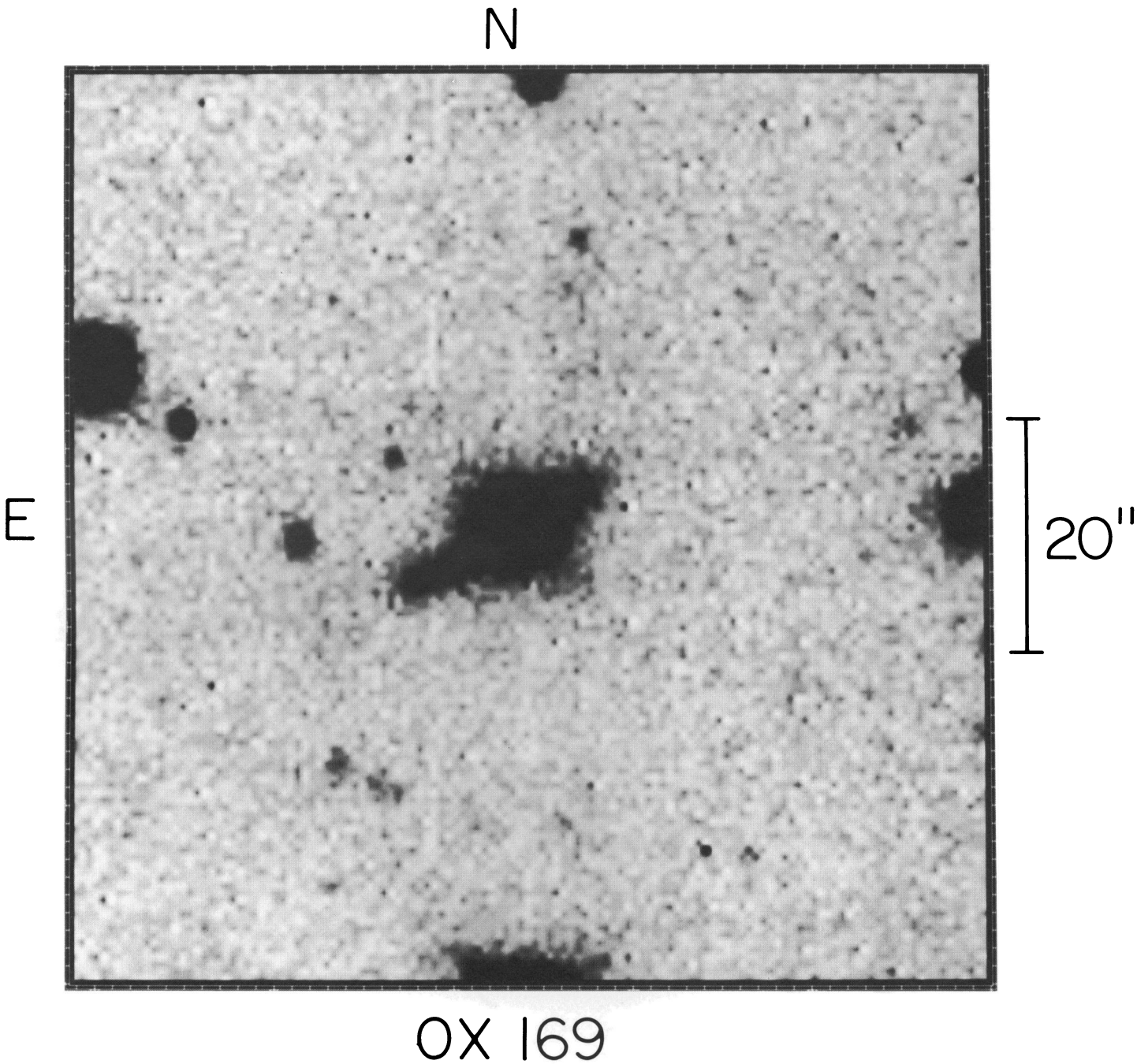

FIG. 16.—V-band image of OX 169 (PKS 2141 + 175) showing the two bright tails (SE and NW)

HECKMAN *et al.* (*see* page 536)

© American Astronomical Society • Provided by the NASA Astrophysics Data System

1986ApJ...311..526H

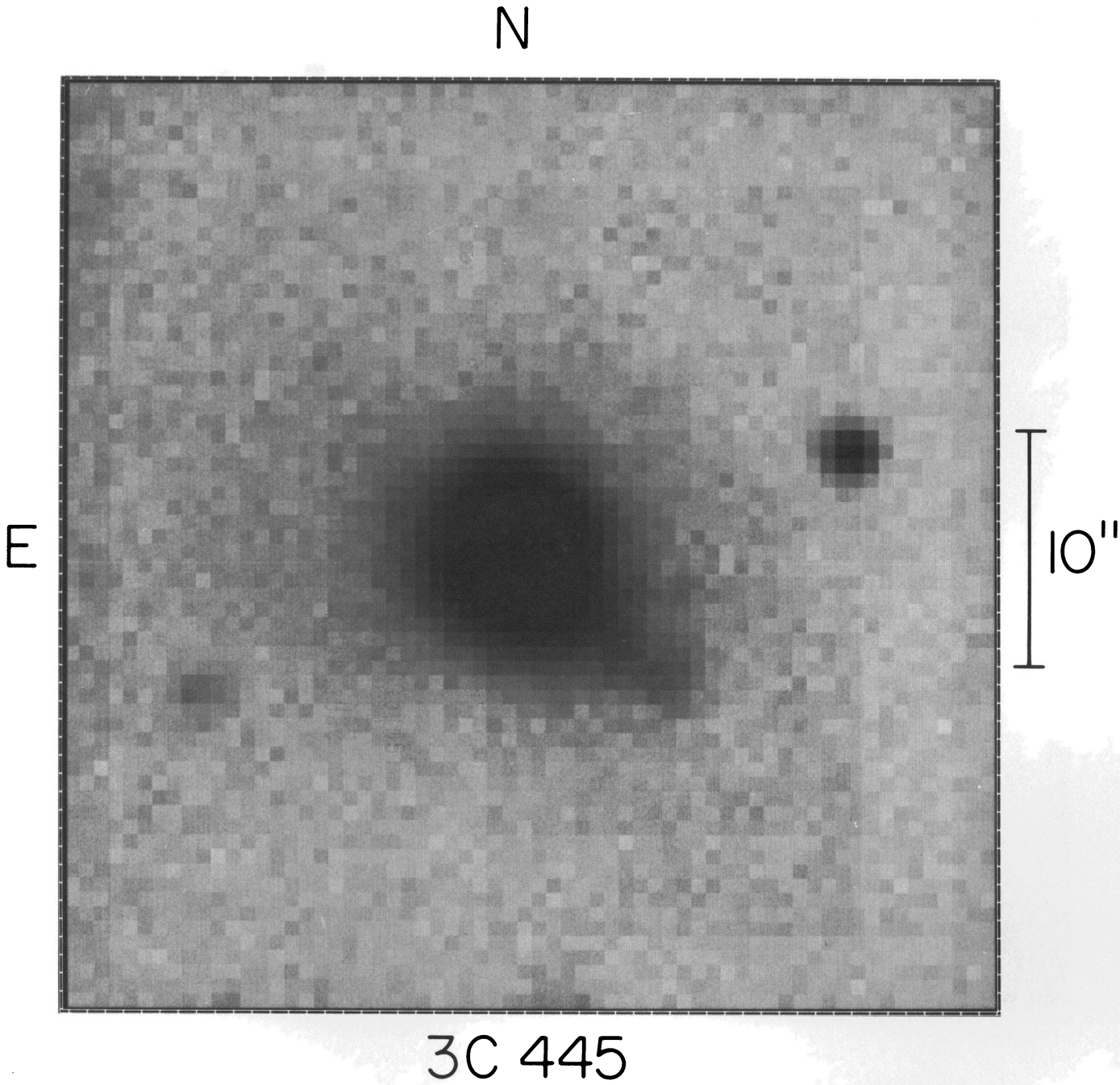

FIG. 17*b*.—Gray-scale representation of *V*-band image of 3C 445 showing inner tail (a strong source of line emission, see text)

HECKMAN *et al.* (*see* page 536)

© American Astronomical Society • Provided by the NASA Astrophysics Data System

1986ApJ...311..526H

(= 68 × 45 kpc) in size within which is found a fan or tail-like appendage on the SE side of the nucleus with $\mu_V \approx 24.5$ mag arcsec^{-2} (Fig. 18 [Pl. 27]). A region of faint ($\mu_V \approx 26$ mag arcsec^{-2}) nebulosity extends asymmetrically out to $\sim 22'' = 83$ kpc to the NW of the galaxy. The radio source is a member of the kiloparsec scale steep-spectrum compact class (size ~ 1.2 kpc as measured by van Breugel, Miley, and Heckman 1984). A contour plot of our CCD image of PKS 2247+140 can be found in Smith *et al.* (1986).

r) PKS 2300−189

This radio-loud low-redshift ($z = 0.129$) quasar/N galaxy (Hunstead *et al.* 1984) is one of the most spectacular objects in our sample. Our deep CCD image (Fig. 19*a*, Fig. 19*b* [Pl. 28]) and cyrogenic camera spectra reveal the following:

1. Within the main ellipsoidal envelope ($\sim 20'' \times 25'' = 44 \times 56$ kpc) are found two galaxy nuclei separated by $6'' \approx 13$ kpc: the SE of these is the quasar/N-galaxy nucleus, while the NW exhibits only a stellar absorption-line spectrum (see Hunstead *et al.* 1984). The envelope shows distortions at a level $\mu_V \approx 24.5$ mag arcsec^{-2} to the NE and SW of the fainter nucleus.

2. After subtraction of the "quasar" light, the radio galaxy has $V \approx 17.1$ mag, $M_B \approx -20.6$ (Smith *et al.* 1986).

3. Protruding from the main body of the galaxy is a long, straight tail with $\mu_V \approx 26$ mag arcsec^{-2} which extends $\sim 40''$ (~ 90 kpc) to the SE of the quasar. The tail also appears resolved in the transverse direction ($\sim 5'' = 10$ kpc). There are other faint ($\mu_V \approx 26$ mag arcsec^{-2}) shells or filaments surrounding the envelope of the main body as well, and possibly a very faint ($\mu_V \approx 26.5$) countertail extending $\sim 66''$ (~ 150 kpc) to the NW. None of these features are morphologically related to the radio jet, which emerges in P.A. $\approx 17°$ (Hunstead *et al.* 1984), almost perpendicular to the orientation of the SE tail. Our spectra

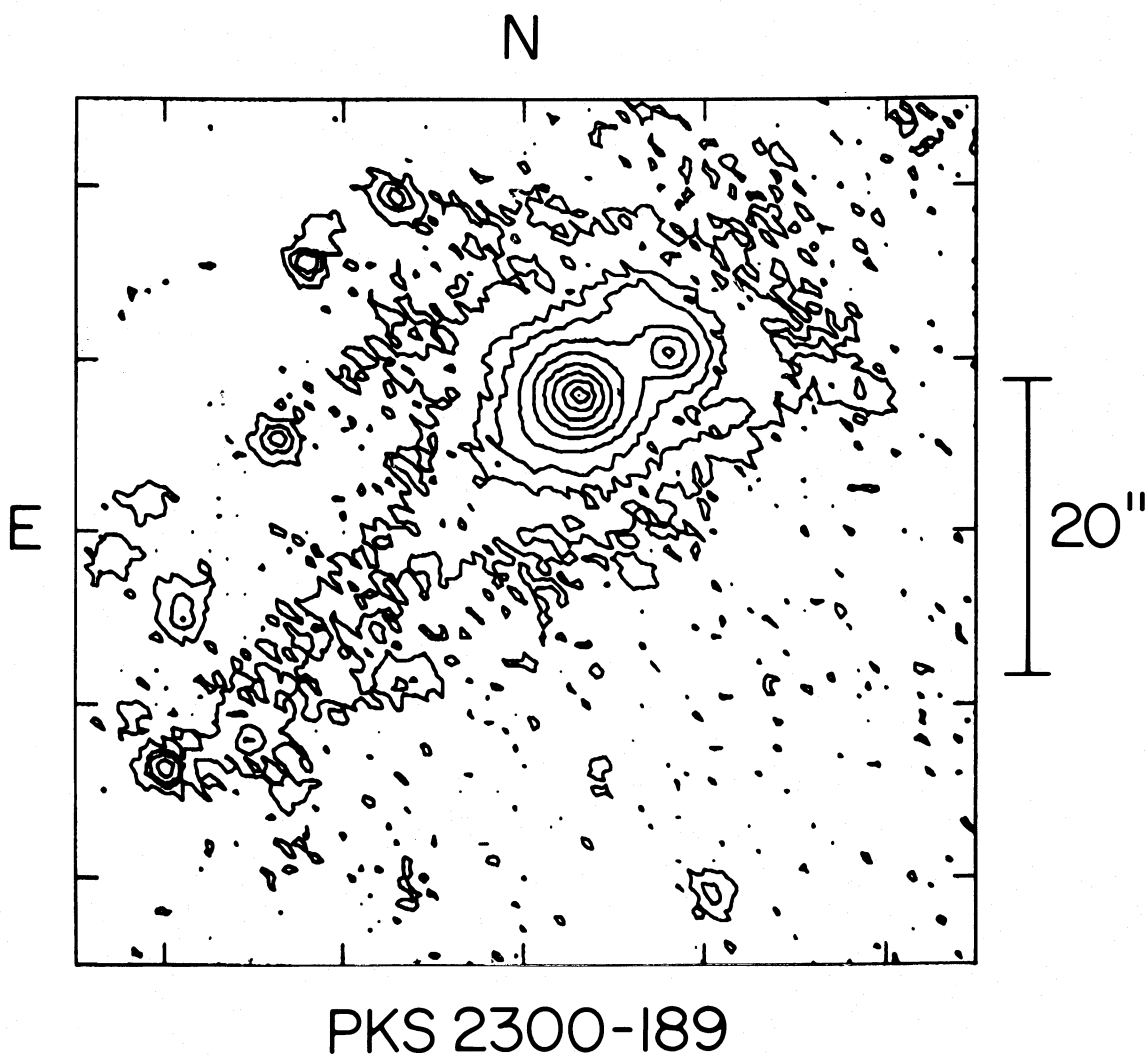

FIG. 19*a*.—Contour plot of *V*-band image of PKS 2300−189. Contour levels are at 20, 60, 100, 200, 400, 800, etc., above sky, where 24 mag arcsec^{-2} is equal to 53 units.

© American Astronomical Society • Provided by the NASA Astrophysics Data System

1986ApJ...311..526H

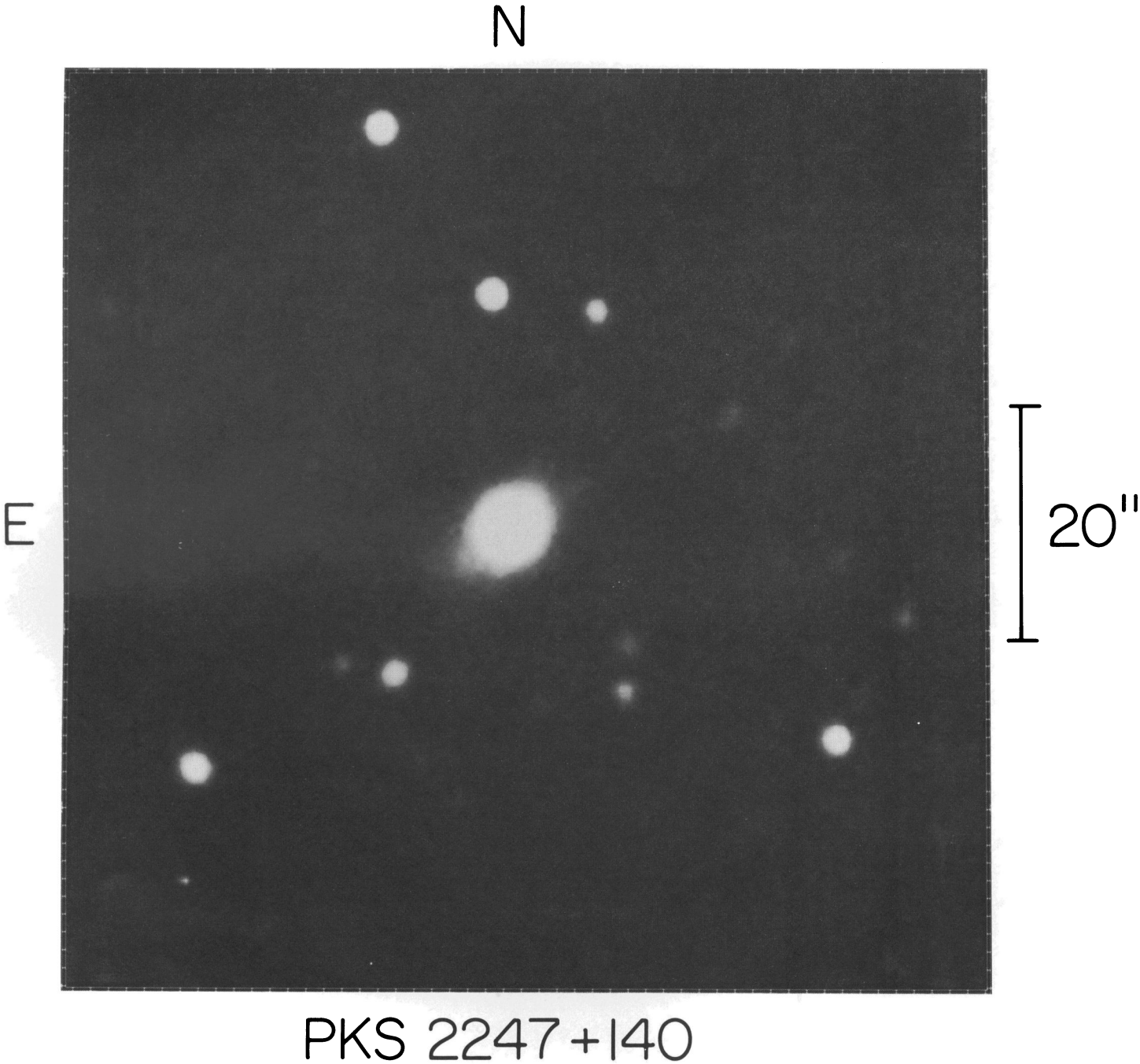

FIG. 18.—V-band image of PKS 2247+140 showing the curving SE tail or fan

HECKMAN *et al.* (*see* page 537)

© American Astronomical Society • Provided by the NASA Astrophysics Data System

1986ApJ...311..526H

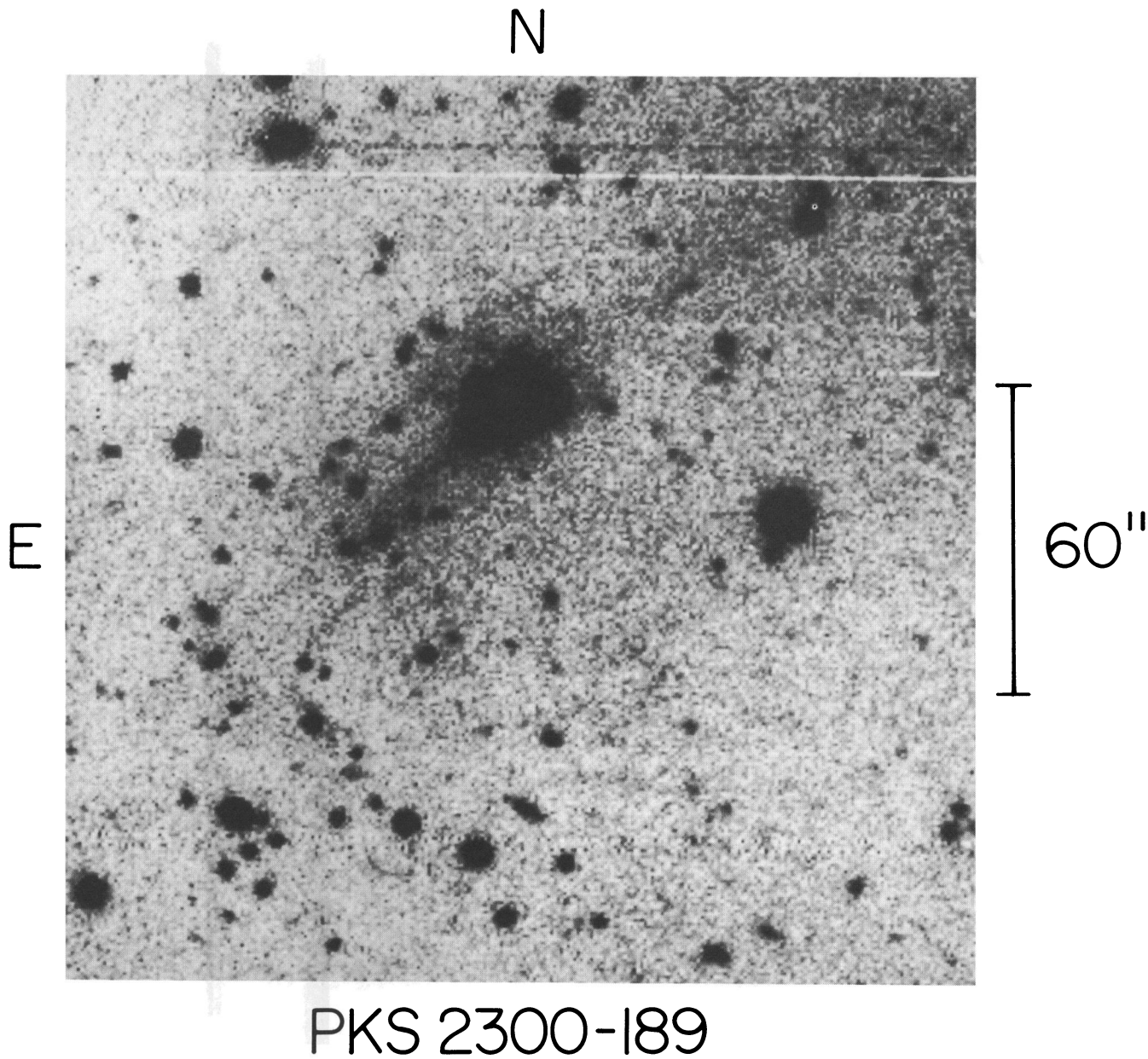

FIG. 19*b*.—Gray-scale representation of *V*-band image of PKS 2300 − 189 showing SE tail

HECKMAN *et al.* (*see* page 537)

© American Astronomical Society • Provided by the NASA Astrophysics Data System

1986ApJ...311..526H

show that the SE tail emits only in the continuum (no emission lines were detected). We conclude that it is made of stars rather than nonthermal plasma or hot gas.

4. As in many of the cases discussed earlier, PKS 2300−189 appears to reside in a moderately sparse environment. The only other galaxy in our CCD frame (projected size $\sim 650 \times 375$ kpc at the distance of PKS 2300−189) comparable in brightness to the host galaxy itself is a spiral with $V \approx 17.4$ located $\sim 100''$ (~ 220 kpc) to the west. Other galaxies in our frame have $V \gtrsim 19.3$ mag ($M_B \gtrsim -18$ if associated with the quasar/N galaxy).

5. There is a region of spatially extended ($\sim 8'' = 18$ kpc) optical emission-line gas present which is centered on the quasar/N galaxy nucleus. Our spectra in P.A. = 167° show velocities which increase from south to north by ~ 130 km s^{-1}. A small ($< 3''$) knot of emission-line gas is also seen $\sim 21''$ (~ 47 kpc) north of the quasar. This knot is redshifted by ~ 230 km s^{-1} relative to the quasar. A more detailed investigation of the emission-line nebulosity should prove interesting.

s) 2314+038 = 3C 459

This very powerful radio galaxy at $z \approx 0.22$ has been the subject of a detailed radio investigation by Ulvestad (1985). The radio source is small (~ 29 kpc total extent) and highly asymmetric (the east lobe is only 4.1 kpc from the nucleus and is strongly Faraday depolarized by ionized gas associated with it). The parent galaxy is unusual in showing strong stellar Balmer absorption lines in its spectrum (Miller 1981), is ~ 0.7 mag bluer than a normal elliptical at $z \approx 0.2$ (Sandage 1972), and is a very luminous ($\sim 8 \times 10^{11}$ $L_\odot$) far-infrared source (Table 3).

Our new imaging data (Fig. 20 [Pl. 29]) show that the host galaxy is definitely not a normal elliptical. In particular, a fanlike protrusion ($\mu_v \approx 24.5$ mag arcsec^{-2}) can be traced out to $\sim 8''$ (26 kpc) to the east of the galaxy, and a similar, but more "knotty" feature is seen to the south. No other galaxies brighter than $V = 22$ mag are found within 150 kpc of 3C 459 (3C 459 itself has $V = 17.5$). We have also obtained long-slit spectroscopic data along and perpendicular to the radio source axis and passing through the east and south fans. The gas is fairly compact; the fans are therefore continuum-emitting structures.

IV. GENERAL RESULTS AND DISCUSSION

a) Introduction

Our imaging survey was directed primarily at very powerful (defined as log $P_{408} > 25.5$ W Hz^{-1}) radio galaxies. Thus, the results discussed in § III imply that many such radio galaxies are not normal ellipticals (contrary to the conventional wisdom). Several important questions follow from this conclusion, and will be addressed below:

1. Do the origins of these peculiarities lie in the collisions/mergers of galaxies?
2. If so, what type of galaxies are involved in the interactions?
3. What fraction of very powerful radio galaxies have peculiar optical morphologies, and how does this fraction compare to that for lower power radio galaxies and radio-quiet elliptical galaxies?
4. How do the radio galaxies with peculiar optical morphologies differ in their other properties from the radio galaxies of similar radio power, but with normal optical morphologies?
5. Aside from direct collisions/mergers, how does the local ($\lesssim$few hundred kpc) clustering environment affect the radio galaxy and its activity?
6. What are the implications of our results for our understanding of radio galaxies and their evolution?

b) The Nature and Origin of the Optical Morphological Peculiarities

To address this important issue, the morphological properties of the various peculiar features must be considered, of course. The stellar populations, dynamical states, and clustering environments of the radio galaxies will also provide valuable clues.

i) *Optical Morphological Features*

In column (3) of Table 3 we summarize these features. By "tails" (T), we mean narrow (≥ 3:1 ratio of length-to-width) curvilinear features with a roughly radial orientation. In some cases, the galaxies exhibit only one tail (1T), while in others *two* tails are seen (2T). "Fans" (F) are similar to tails, but are stubbier (length-to-width ratio < 3). By "bridges" (B), we refer to features joining the radio galaxy to an apparent companion galaxy (unlike fans or tails, which lead nowhere). Shells (S) are curving filamentary structures which have a primarily tangential rather than radial orientation with respect to the galaxy center. Finally, dust features (D) are clearly seen in several objects, sometimes with complex morphologies. We emphasize that these morphological features are generally seen at relatively *high levels of surface brightness* ($\mu_V \approx 21$–25 mag arcsec^{-2}; see col. [4] of Table 3).

In some cases we have spectroscopic and/or narrow-band imaging observations which demonstrate that the various morphological features (T, F, B, S) are continuum-emitting material (C) or emission-line material (E). This information is summarized in column (5) of Table 3 and is important in establishing the nature of the disturbed features. Pure emission-line structures may arise either through gravitational (tidal) interactions or explosive nuclear phenomena. Continuum-emitting structures are more likely to be of tidal origin if we can determine that the emission is starlight (but see Williams and Christiansen 1985). We believe this to be true for our sample, since none of the features listed in Table 3 bears any simple morphological relation to the radio source.

How are we to account for the diverse array of tails, fans, dust lanes and patches, bridges, and shells? Toomre and Toomre (1972, hereafter TT), Toomre (1977), Quinn (1984), and others have shown how interactions (or mergers) between ellipticals and spirals or spirals and spirals can produce a rich array of such features. We can summarize these results as follows.

1. As discussed by TT, the production of a long narrow feature (tail) requires the presence in at least one of the galaxies of a dynamically cold component (a disk). Moreover, to produce a well-defined tail, the galaxy encounter should be in the proper sense and the viewing angle should be optimal (tails are really rather sheetlike and will appear brighter and more well-defined when viewed close to edge-on).
2. Production of two well-defined long tails requires that both of the interacting galaxies possessed substantial disks prior to the encounter (e.g., Toomre 1977). Again, not all encounters between two disk galaxies will necessarily produce two well-defined tails (encounter sense, viewing angle, and galaxy mass ratio are important factors).

© American Astronomical Society • Provided by the NASA Astrophysics Data System

1986ApJ...311..526H

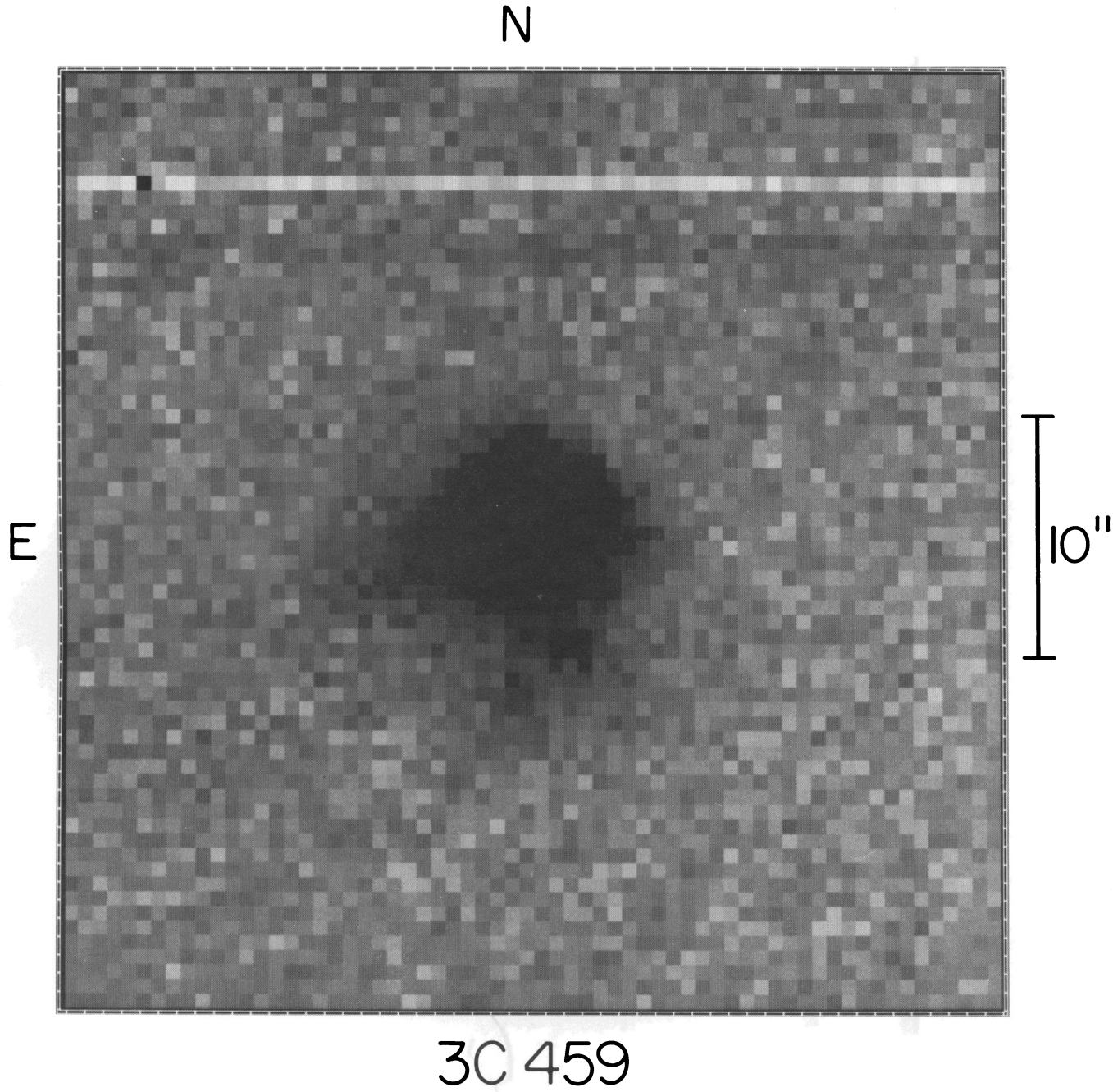

FIG. 20.—V-band image of 3C 459 showing east and south fans

HECKMAN *et al.* (*see* page 538)

© American Astronomical Society • Provided by the NASA Astrophysics Data System

1986ApJ...311..526H

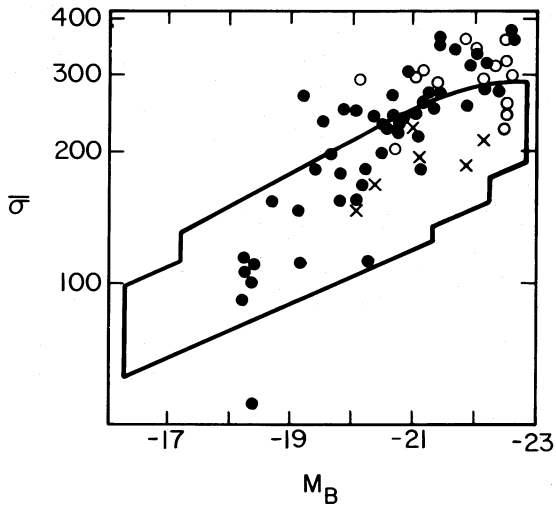

FIG. 21*a*

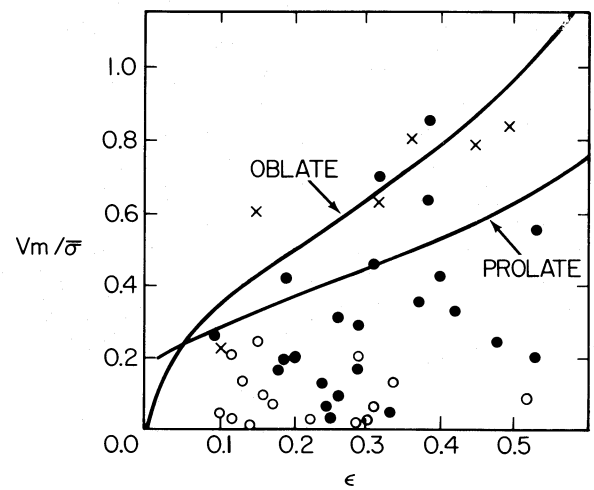

FIG. 21*b*

FIG. 21.—(*a*) Mean stellar velocity dispersion ($\bar{\sigma}$, in km s^{-1}) vs. absolute blue magnitude (M_B, for $H_0 = 75$ km s^{-1} Mpc^{-1}) for three samples of galaxies. Radio-quiet elliptical galaxies (*solid dots*) are from Veeraraghavan and White (1985). Radio galaxies with *normal* optical morphologies (*hollow dots*) and with *peculiar* optical morphologies (*crosses*) are taken from Heckman *et al.* (1985). Theoretical models of elliptical galaxies produced by the merger of two disk galaxies populate the area bounded by the solid line (Veeraraghavan and White 1985). (*b*) Ratio of the mean rotation speed of the stellar component to the stellar velocity dispersion ($V_m/\bar{\sigma}$) is plotted against galaxy ellipticity (ϵ) for the same three samples of galaxies as in (*a*). Solid line labeled "oblate" is the model relation for rotationally flattened oblate galaxies with isotropic velocity dispersions, while the line labeled "prolate" defines the median relation for like-structured prolate galaxies. See Heckman *et al.* (1985) for further details.

3. The capture of a relatively small disk or elliptical galaxy by a large elliptical has been investigated by Quinn (1984), and Hernquist and Quinn (1986), who find that shells or shell-like structures surrounding the elliptical are a natural consequence.

4. Encounters of two large elliptical galaxies (e.g., Villumsum 1982; Borne 1985; Borne and Hoessel 1985) are rather unspectacular morphologically. Broad fans can result from such an encounter, and *gaseous* tidal tails could be produced if gas disks were present prior to the encounter.

5. The morphology and dynamics of gas (and associated dust) which settles into an elliptical galaxy following a capture event has been discussed extensively in the recent literature (e.g., Merritt and de Zeeuw 1983). The presence of strong dust absorption may implicate a late Hubble type galaxy in the proceedings.

ii) *Recent Star Formation*

Since the seminal paper by Larson and Tinsley (1978), evidence has mounted that star formation can be induced by the collision/merger of gas-rich galaxies (e.g., Lonsdale, Persson, and Mathews 1984). Thus, the nature of the stellar population in radio galaxies is a potentially important clue to the nature of the participants and the interaction. As we have discussed in § III, many of the peculiar radio galaxies do exhibit evidence for recent star formation. Some (3C 305 and 3C 459) have spectra with strong stellar Balmer absorption lines; others (3C 120, 4C 29.30, 4C 12.50, 3C 293, 3C 305, 3C 321, 3C 327, 3C 445, and 3C 459) are strong far-infrared sources ($L_{60\mu} \approx 10^{10}$ to $\approx 10^{12}$ $L_\odot$). Finally, some (3C 285, 3C 293, 3C 305, PKS 1934−638, 3C 459) have extranuclear colors that are at least 0.1 mag bluer than a normal elliptical galaxy at the same redshift. These pieces of evidence are summarized in column (3) of Table 3.

iii) *Dynamical Peculiarities*

We (Heckman *et al.* 1985) have recently noted that of a sample of 21 radio galaxies with measured stellar kinematics, the most *dynamically* peculiar galaxies were the optically *morphologically* peculiar galaxies NGC 3801, 3C 293, 3C 305, NGC 5128 (Cen A), and NGC 1316 (Fornax A). Compared to typical luminous elliptical galaxies, these radio galaxies are rapidly rotating and have low central velocity dispersions (see Figs. 21*a*, 21*b*). These dynamical properties are consistent with simulations of the formation of elliptical galaxies by mergers of disk galaxies (see Veeraraghavan and White 1985). Determination of the stellar kinematics of more of the radio galaxies with peculiar optical morphologies in our sample is clearly important.

iv) *Local Galaxy Density*

Dressler (1980) and Postman and Geller (1984) have found an excellent correlation between local galaxy density and Hubble type: a decrease in the fractional spiral population with increasing local galaxy density. This means that the clustering environment of the radio galaxy should provide an additional important clue to the nature of the interacting galaxies. We have tabulated the local galaxy density parameters ρ_{01} and ρ_{11} (see HCB) in column (6) of Table 4. Radio galaxies with peculiar optical morphologies located in sparse local environments (e.g., 3C 33, 3C 120, 4C 29.30, 4C 12.50, 3C 293, 3C 305, 3C 327, OX 169) are therefore stronger candidates for disk-disk mergers than those in regions of high local density (e.g., PKS 0349−278, NGC 6047).

v) *Marriages or One-Night Stands?*

Since it takes two to Tango, it is natural to examine closely the galaxies described in § III above for evidence of the partner galaxy to attempt to discriminate between mergers and temporary encounters. In several cases, luminous bridges join the radio galaxy to a partner (PKS 0349−278 and 3C 293). These systems may be galaxy mergers in a fairly early evolutionary state (e.g., Toomre 1977) or simply galaxies having a temporary, "grazing" encounter.

© American Astronomical Society • Provided by the NASA Astrophysics Data System

1986ApJ...311..526H

TABLE 4

MISCELLANEOUS PROPERTIES

Name (1)	M_V^{gal} (2)	log P_{408} (3)	Radio Class (4)	Emission (5)	ρ_{11} (6)	ρ_{01} (7)
3C 17*	−22.3[a]	27.2	FR II	SE	2.0	0.7
3C 33*	−22.4	26.4	FR II	SE	0.0	0.0
PKS 0137+012	−23.3[a]	26.6	FR II	SE	0.7	0.2
3C 62*	?	?	FR II	?	?	?
3C 63*	−22.3	26.8	FR II	SE	2.2	1.5
PKS 0349−278*	−20.5	26.0	FR II	SE	8.7	3.6
3C 120	−21.3[b]	25.1	FC	SE	0.4	0.2
PKS 0736+017	−22.2[a]	26.4	FC	SE	5.0	3.9
4C 29.30	−21.6	25.1	FR I	SE	0.3	0.2
3C 218*	−23.0[c]	26.9	FR I	WE	8.8	2.1
3C 227*	−21.2[a]	26.5	FR II	SE	1.8	0.9
NGC 3801	−21.3	23.8	SC/FR I	WE	4.0	1.4
3C 285	−21.7	25.8	FR II	WE	2.3	1.6
4C 12.50*	−22.7	26.3	SC/?	SE	0.2	0.1
3C 293	−22.0	25.6	SC/FR II	WE	0.5	0.1
PKS 1358−113	−21.8	24.7	FR II?	WE	1.9	0.9
3C 300*	∼−23	27.2	FR II	SE	1.7	0.9
3C 305	−22.5	25.7	SC/FR II	SE	0.3	0.3
3C 310	−21.7	26.2	FR I	WE	12.0	2.2
3C 317*	−22.7[c]	25.7	FR I	WE	6.2	2.5
3C 321	−22.3[c]	26.3	FR II	SE	15.6	1.1
3C 327*	−22.7	26.8	FR II	SE	0.3	0.3
NGC 6047	−21.7	24.6	FR I	ABS	5.1	3.1
3C 346*	−22.5[c]	26.7	SC/FR I	WE	17.9	2.1
3C 348*	−22.8	27.9	FR I	WE	2.1	0.2
3C 353*	−20.7	26.3	FR II	WE	2.3	1.1
PKS 1934−638	−21.8[c]	26.5	SC/?	SE	6.1	0.5
3C 403*	−22.5	26.0	FR II	SE	0.0	0.0
3C 424*	−20.5	26.5	FR I	WE	8.4	5.8
PKS 2058−282*	−22.2	25.6	FR I	ABS	2.2	0.9
PKS 2104−256S*	−22.4	25.5	FR I	ABS	10.9	6.1
PKS 2104−256N*	−23.1[c]	25.5	FR I	ABS	21.5	3.2
3C 433	−23.1[c]	26.9	FR I	SE	13.9	1.8
PKS 2135−147*	−23.0[a]	27.0	FR II	SE	4.9	1.8
OX 169	−22.6[a]	25.5	FC	SE	0.4	0.3
3C 436	−22.4	27.1	FR II	SE	0.7	0.4
3C 444*	−22.9	27.2	FR II	?	13.6	2.1
3C 445*	−20.2[a]	26.0	FR II	SE	3.0	1.2
PKS 2247+140	−23.0[a]	26.7	SC/?	SE	1.7	1.1
PKS 2300−189	−21.4[a,c]	25.8	FR I	SE	3.5	0.6
3C 459*	−22.6[a]	27.2	SC/FR II	SE	0.0	0.0
MC3 2328+167	−22.0[a]	25.9	SC/?	SE	4.0	1.9
PKS 2355−082	−23.1[a]	25.4	FC	SE	0.0	0.0

Col. (1).—Name (asterisk denotes member of "complete" sample).

Col. (2).—Absolute V magnitude of radio galaxy for $H_0 = 75$ km s^{-1} Mpc^{-1} and $q_0 = 0$. We have used the V magnitudes from Table 2, the K corrections for E/S0 galaxies from Pence 1976, and the extinction corrections from Burstein and Heiles 1982. The value of M_V^{gal} with an "b" superscript is for 3C 120 for which we have *assumed* that the host galaxy and AGN are equally bright at V (i.e., the quoted value is for the *galaxy alone*). Values of M_V^{gal} with a "a" superscript are also for the host galaxy alone, but here the contribution of the AGN or QSO has been subtracted by modeling the images (see Smith *et al.* 1986). Values with a "c" superscript are total values for double or multiple systems in which it was difficult to disentangle the contributions of the various components.

Col. (3).—Log of the monochromatic radio power (W Hz^{-1}) at a frequency of 408 MHz in the galaxy frame.

Col. (4).—Radio class (see text):

FR I: Fanaroff/Riley class I source.

FR II: Fanaroff-Riley class II source.

SC: Steep radio spectrum, compact ($\sim 10^2$–10^4 pc) radio source. Classified as FR I or II if enough information is present in radio maps.

FC: Flat radio spectrum, compact ($\lesssim 10^2$ pc) radio source.

Col. (5).—Characterization of the nuclear emission-line spectrum:

SE: Strong emission lines (equivalent width of [O III] λ5007 $\geq$ 10 Å).

WE: Weak emission lines present.

Abs.: Stellar absorption lines only.

Col. (6).—A measure of the local ($r \leq 133$ kpc) galaxy density with companion galaxies weighted by size and proximity (see Heckman, Carty, and Bothun 1985).

Col. (7).—Measure of local galaxy density with companions weighted only by size (see Heckman, Carty, and Bothun 1985).

© American Astronomical Society • Provided by the NASA Astrophysics Data System

1986ApJ...311..526H

Several other of our galaxies apparently have a smaller, more compact companion located well within the envelope of the radio galaxy (4C 29.30, 3C 227, 4C 12.50, 3C 321, PKS 1934−638, and PKS 2300−189). Again, these systems may be either grazing encounters or mergers. This latter is especially plausible in 4C 29.30 in which the outer "shells" are reminiscent of Quinn's (1984) simulations of the capture and disruption of a disk galaxy by a massive elliptical (the small, blue secondary nucleus in 4C 29.30 being the last undigested piece of the former disk galaxy, presumably its nucleus).

There are also several radio galaxies in our sample that have one or more close neighbors (projected separation less than 100 kpc), but these neighbors are not joined to the radio galaxy by luminous material, nor are they themselves morphologically peculiar (3C 285, NGC 6047, 3C 445). Interpretation of these objects as the product of either a merger or a grazing encounter is ambiguous.

For the remaining objects (3C 33, 3C 120, 3C 305, 3C 327, OX 169, PKS 2247+140, and 3C 459), there is no evidence for a near neighbor which could have produced the observed morphological peculiarities. Provided that such peculiarities do indeed have a tidal origin, these galaxies seem likely to be mergers that have nearly reached completion. Of course, many of these objects are at considerable distances from us, and an inconspicuous (i.e., low surface brightness or compact, tidally stripped) partner may be unnoticed amidst the debris (e.g., 3C 459), disguised as what appears to be a star, or hidden by the glare from the quasar (OX 169 and PKS 2247+140).

vi) *Classification Summary*

Using the various clues discussed above, we have suggested the nature of the galaxies participating in the merger/collision (col. [6], Table 3). The presence of tails, dust, gas, young stars, and large-scale dynamical peculiarities in the stellar component, and the location of the radio galaxy in a sparsely populated region are taken as evidence implicating one or more gas-rich, disk galaxies. Since the above features are common in our sample, most of the galaxies in Table 3 are classified as elliptical-disk or disk-disk interactions. This is likely to be a selection effect, since elliptical-elliptical interactions are relatively dull morphologically (several excellent candidates for such interactions—3C 310, 3C 346, 3C 433, and PKS 2104−256N—are found among the radio galaxies with "normal" optical morphologies in Tables 2 and 4).

Discrimination between elliptical-disk and disk-disk interactions is difficult. In our sample 3C 305 is the least ambiguous candidate for a powerful radio source being produced by a merger of two disk galaxies (it has a single main body, two long tails, is in a very sparsely populated region, has young stars, gas, and dust, and is dynamical peculiar compared to bona fide luminous elliptical galaxies).

c) *Fractions of Morphologically Peculiar Galaxies*

i) *Redshift Dependence*

In estimating the fraction of radio galaxies that have peculiar optical morphologies and especially in comparing this estimate to that deduced for radio-quiet elliptical galaxies, it is important to emphasize that such peculiarities become increasingly difficult to detect as the galaxy redshift increases (due to cosmological $[1+z]^4$ dimming, atmosphere blurring, etc.). The estimates we make below for the radio galaxies will therefore be lower limits. This effect can in fact be clearly seen in our data. Of the 27 galaxies in Table 2 with $z < 0.15$, 15 ($\sim 56\%$) are classified as peculiar in optical morphology. The fraction drops to only four of 16 (25%) for the galaxies with $z = 0.15$–0.30. Part of the drop may also be due to the strong [O III] $\lambda\lambda$5007, 4959 lines moving out of the V passband for $z \gtrsim 0.2$ (since the morphological peculiarities are sometimes produced by emission-line gas).

ii) *Very Powerful Radio Galaxies*

For our sample of 43 radio galaxies observed (Table 2), about half (19) have peculiar optical morphologies at levels of surface brightness higher than $\mu_V = 25$ mag arcsec^{-2}. Since the sample as a whole was not selected according to any well-defined criteria, we prefer to make our estimate of the incidence of optical morphological peculiarities based on the 23 members of our radio selected complete sample. Of these, seven ($\sim 30\%$) are peculiar at levels $\mu_V \leq 25$ mag arcsec^{-2} (six of 14 or 43% at $z < 0.15$). More recent observations of another 12 such galaxies uphold these fractions.

We emphasize strongly that all 23 members of our complete sample (and the great majority of the other galaxies in Table 2) are very powerful radio sources (defined as log $P_{408} \geq 25.5$ W Hz^{-1} for $H_0 = 75$ km s^{-1} and $q_0 = 0$). It is this factor that—we believe—allows us to reconcile the above result with the conventional wisdom that radio galaxies are usually normal elliptical galaxies. This belief has been implicitly based on observations of nearby (easily studied) radio galaxies, which are almost invariably of much lower radio power (log $P_{408} \approx$ 23.5–25.5) than our sample. We attempt to quantify this below.

iii) *Lower Power Radio Galaxies*

There are some famous examples of optically morphologically peculiar galaxies with radio power log $P_{408} \approx 23.5$–25.5 W Hz^{-1} (NGC 1316 = Fornax A, Schweizer 1980; NGC 5128 = Centaurus A, Malin, Quinn, and Graham 1983). Several other examples have been described in § III above (3C 120, 4C 29.30, NGC 3801, and NGC 6047). Moreover, $\sim 10\%$–15% of the Markarian Seyfert galaxies have radio powers in this range (Meurs 1982), and few (if any) of these are believed to be normal elliptical galaxies (e.g., Adams 1977).

Despite these counterexamples, we believe that the fraction of lower power radio sources produced by morphologically peculiar galaxies is significantly lower than the fraction for very powerful radio sources.[4] During the observing run discussed in HCB, 17 lower power radio galaxies were observed. Only one of these (the distorted dumbbell system NGC 4782/4783 = 3C 278) had a peculiar optical morphology at a level of surface brightness higher than our detection threshold of $\mu_V \approx$ 24 mag arcsec^{-2}.

iv) *Radio-quiet Elliptical Galaxies*

We have equated the existence of the optical morphological peculiarities discussed in § III with the statement that the radio galaxies in question are not "normal elliptical galaxies." Is this necessarily so, given the recent discoveries of faints shells, fans, ripples, etc., associated with many ellipticals?

Malin and Carter (1983) have concluded that $\sim 10\%$ of all bright (nearby) ellipticals do indeed have such peculiar structures at large galaxy radii. However, these features typically

[4] We emphasize that we are restricting our attention here to radio sources which on *radio* morphological grounds are powered by jets, bubbles, plasmoids, etc., ejected from a compact active nucleus. Many sources with diffuse radio morphologies and log $P_{408} \lesssim 24$ W Hz^{-1} are known to be associated with galaxies having peculiar *optical* morphologies. These latter sources are hypothesized to be powered by energetic processes associated with a burst of star formation (e.g., Condon *et al.* 1982; Windhorst 1984).

© American Astronomical Society • Provided by the NASA Astrophysics Data System

1986ApJ...311..526H

have surface brightnesses of $\mu_V \sim 25.5$–$26.0V$ mag arcsec^{-2} and thicknesses of ~ 1–2 kpc ($\sim 1''$ at $z \approx 0.07$). At the redshifts of our very powerful radio sources, cosmological dimming and the dilution of the unresolved features by the sky background would lower their surface brightnesses to the range $\mu_V \approx 26$ ($z = 0.03$) to 28.0 ($z = 0.3$). The optical morphological peculiarities we observe for the very powerful radio galaxies in our sample are generally at much higher levels of surface brightness (see col. [4], Table 3). Thus, while $\sim 10\%$ of radio-quiet ellipticals may exhibit faint shells, etc., only a much smaller percentage could exhibit the kinds of peculiarities seen in our radio galaxies.

d) Differences between Very Powerful and Lower Power Radio Galaxies

We have concluded above that a significant fraction ($\sim 30\% \pm 15\%$) of very powerful radio galaxies have peculiar optical morphologies, compared to less than 10% of lower power radio galaxies (log $P_{408} = 23.5$–25.5). This result is especially intriguing because several other systematic differences between these two radio classes are known or suspected:

1. Very powerful radio sources are usually associated with galaxies having strong optical emission-lines, while lower power radio galaxies usually have weak or no emission (e.g., Hine and Longair 1979). See column (5) in Table 4.

2. Lilly, McLean, and Longair (1984) suggest that very powerful radio sources are rarely associated with giant elliptical galaxies with extended outer envelopes (cD galaxies), in contrast to lower power sources. We have begun a program of surface photometry of a large sample of radio galaxies which can further evaluate this idea.

3. Very powerful radio sources differ strongly in *radio* morphology from lower power sources (Fanaroff and Riley 1974 [FR]; Bridle 1984). Lower power sources usually exhibit two-sided jets with perpendicular magnetic fields and are often "edge-darkened" in overall radio morphology, having the brightest radio emission located closest in to the galaxy (FR class I). In contrast, very powerful sources usually have apparently one-sided jets with parallel magnetic fields and are more often "edge-brightened," with the brightest radio emission occurring in "hotspots" at the outer edges of the radio source (FR class II, the classic "Cygnus A" morphology). See also Miley (1980).

4. The radio luminosity function of elliptical and lenticular galaxies may exhibit a break (change in slope), steepening above $P_{408} \sim$ few $\times 10^{25}$ W Hz^{-1} (Auriemma *et al.* 1977).

5. Cosmological evolution of radio sources appears to be strongly luminosity dependent (see Schmidt 1972; Laing, Riley, and Longair 1984).

The crucial point is that very powerful radio sources differ *qualitatively* in many important respects from the far more common lower power sources. It is not yet clear how all these various differences between very powerful and lower power radio sources are interrelated, or how they might be related to the morphological distortions we have found to be common in the parent galaxies of very powerful sources. We will discuss this in § V.

e) Comparison of Peculiar and Normal Radio Galaxies

A detailed attempt to interrelate the properties of the radio galaxies, their clustering environment, their radio sources, and their nuclear spectra is beyond the scope of the present paper (some of us are engaged in a long-term project to address this general issue). Here we present some preliminary results having special relevance to the galaxy morphological peculiarities under consideration. These results are based on the comparison of the radio galaxies with peculiar optical morphologies (those objects discussed in § III and listed in Table 3) to the radio galaxies with normal optical morphologies (the other objects in Tables 2 and 4).

i) *Radio Properties*

We have noted above that a greater fraction of very powerful radio galaxies have peculiar optical morphologies, compared to lower power radio galaxies. Since we also pointed out that the *radio source* morphology tends to change from FR I to FR II at high levels of radio power, it is of interest to ascertain whether there is any correlation between an FR II *radio* morphology and a peculiar *galaxy* morphology, for the very powerful radio galaxies alone. Restricting our attention then to the very powerful radio galaxies in Table 4, we find that 10 of the 20 with an FR II radio morphology are optically peculiar galaxies, compared to only one of the 11 with an FR I radio morphology (a difference which is significant at the $\sim 98\%$ confidence level).

While many (nine of 19, or 47%) of the radio galaxies with peculiar optical morphologies are associated with compact radio sources (radio classes FC or SC; see Table 4), there is no evidence that the peculiar galaxies as a whole are characterized by abnormally small radio sizes. Indeed, eight of the radio sources are very large (~ 250–700 kpc): 3C 33, PKS 0349−278, 3C 321, 3C 327, and 3C 445 are straight FR II sources, 3C 227 and 3C 285 are moderately bent (by $\sim 15°$) FR II sources, and PKS 2300−189 is a strongly curved FR I source. The amount of bending seen in this small sample of FR II sources is consistent with the distribution of bending angles in large samples of FR II radio sources (Hintzen, Ulvestad, and Owen 1983; Barthel 1984).

The presence of large, straight sources associated with radio galaxies having peculiar optical morphologies is intriguing, since it suggests that the radio ejection axis can remain fixed over long times despite dynamical disorder in the parent galaxy.

ii) *Optical Emission Lines*

It is tempting to link the origin of the optical emission-line gas seen in many powerful radio galaxies to the collision or merger of one or more gas-rich galaxies. We have therefore used our own or published spectroscopic data to classify the nuclear spectra of 35 very powerful radio galaxies in Table 4 as to the strength of the optical emission lines (see also Spinrad *et al.* 1985; Hine and Longair 1979). In column (5) of Table 4, "SE" means that the equivalent width of the [O III] $\lambda 5007$ line is greater than 10 Å (galaxy rest frame), while "WE" and "ABS" denote weaker emission lines or stellar absorption lines only.

Breaking this sample down according to the optical morphology of the parent galaxy then shows that 13 of the 15 optically peculiar galaxies have strong emission lines compared to only ten of the 20 normal galaxies. The present sample is rather small, but the difference in these two fractions is statistically significant at the 98% confidence level using a χ^2 contingency table test.

iii) *Galaxy Absolute Magnitude*

If the morphologically peculiar radio galaxies are in fact galaxy collisions or mergers there would be no reason *a priori*

© American Astronomical Society • Provided by the NASA Astrophysics Data System

1986ApJ...311..526H

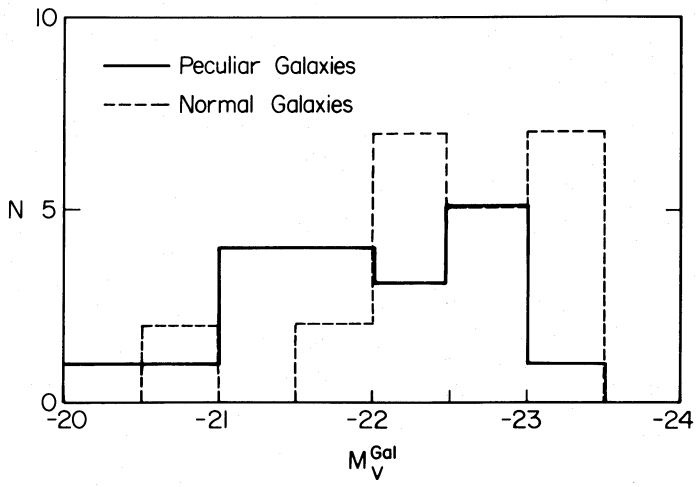

FIG. 22.—Histograms of the absolute V magnitudes of the radio galaxies (M_V^{gal}), computed as described in the text and the notes to Table 4. Radio galaxies with peculiar (normal) optical morphologies are indicated by the solid (dashed) histogram. The peculiar galaxies are less luminous on average in the optical.

for them to be as luminous optically as the morphologically normal (giant elliptical) radio galaxies in our sample. In fact, we find (see Fig. 22) that the average absolute magnitudes (excluding nonstellar nuclear light) are -21.86 ± 0.17 for the radio galaxies with peculiar optical morphologies versus -22.42 ± 0.16 for the radio galaxies with normal optical morphologies (see col. [4] of Table 4 and the associated notes). This difference is significant at the 98% confidence level (two-tailed Wilcoxon rank test).

The interpretation of this result is uncertain given the possibility of both significant dust extinction and recent star formation in the peculiar galaxies. Near-infrared photometry of our sample would be very useful in this sense (see Lilly and Longair 1984). Understanding this result may be crucial to attempts to use radio galaxies as probes of galaxy evolution at early epochs.

iv) *Star Formation: Blue Colors and Far-Infrared Emission*

Eight of the 15 radio galaxies at $z < 0.15$ with peculiar optical morphologies in our sample have been detected as strong far-infrared sources ($\gtrsim 10^{10}\ L_\odot$) by *IRAS* (see § III and Table 3). In contrast, only two of the 12 morphologically normal radio galaxies at $z < 0.15$ were detected, despite having similar apparent magnitudes as the peculiar galaxies. This difference is significant at the 95% confidence level (χ^2 test).

Similarly, $B-V$ colors have been measured for 19 of the radio galaxies in Table 2 (Sandage 1972 and the present paper). Thirteen of these galaxies are known *not* to have strong nonstellar nuclear sources (i.e., they are definitely not broad-line radio galaxies or BL Lacs), and so their colors should not be significantly contaminated by the active nucleus. Of these, all six of the galaxies with normal optical morphologies have colors consistent with those of an elliptical galaxy at the appropriate redshift. In contrast, five of the seven galaxies with peculiar optical morphologies are *at least* 0.1 mag bluer than a normal elliptical (see § III). The sample is small, but the difference is significant at the 99% confidence level (χ^2 test).

Together, the two above results suggest that the radio galaxies with peculiar optical morphologies are significantly more likely to have recent or on-going star formation, as is also the case for radio-quiet peculiar galaxies (e.g., Larson and Tinsley 1978; Lonsdale, Persson, and Mathews 1984).

v) *Local Galaxy Density*

In order to quantify the local galaxy density, we have measured the parameters ρ_{01} and ρ_{11} as defined by HCB (see our Table 4). These parameters measure the galaxy surface density within a projected separation of 133 kpc from the radio galaxy, with ρ_{01} weighting the companion galaxies only according to their relative size and ρ_{11} weighting them according to both relative size and proximity to the radio galaxy (see HCB for details). The distributions of ρ_{01} and ρ_{11} are compared for very powerful radio galaxies with peculiar optical morphologies to those for very powerful radio galaxies with normal optical morphologies in Figure 23. The mean values of ρ_{01} and ρ_{11} are both larger by factors ~ 2 for the optically morphologically normal sample, with statistical significances of 97% and 95% confidence levels for ρ_{01} and ρ_{11}, respectively (using a two-tailed Wilcoxon rank test). It will be important to enlarge significantly the sample of very powerful radio galaxies with deep imaging data to verify this potentially important result.

f) The Role of Local Galaxy Density

Just above, we have concluded that the very powerful radio galaxies with peculiar optical morphologies probably inhabit regions of lower average galaxy density than the very powerful radio galaxies with normal optical morphologies. Previous studies (e.g., Longair and Seldner 1979; Stocke and Perrenod

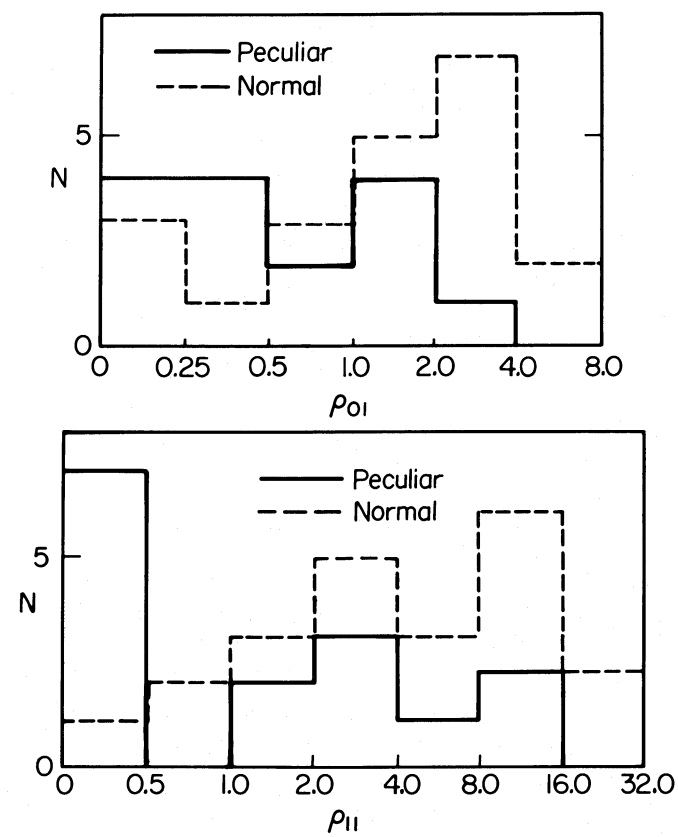

FIG. 23.—Histograms of the local galaxy density parameters ρ_{01} and ρ_{11} (see text and Heckman, Carty, and Bothun 1985). The histograms for very powerful radio galaxies in our sample having normal (peculiar) *optical* morphologies are indicated by dashed (solid) lines. Galaxies with peculiar optical morphologies are found in regions of significantly lower average density.

© American Astronomical Society • Provided by the NASA Astrophysics Data System

1986ApJ...311..526H

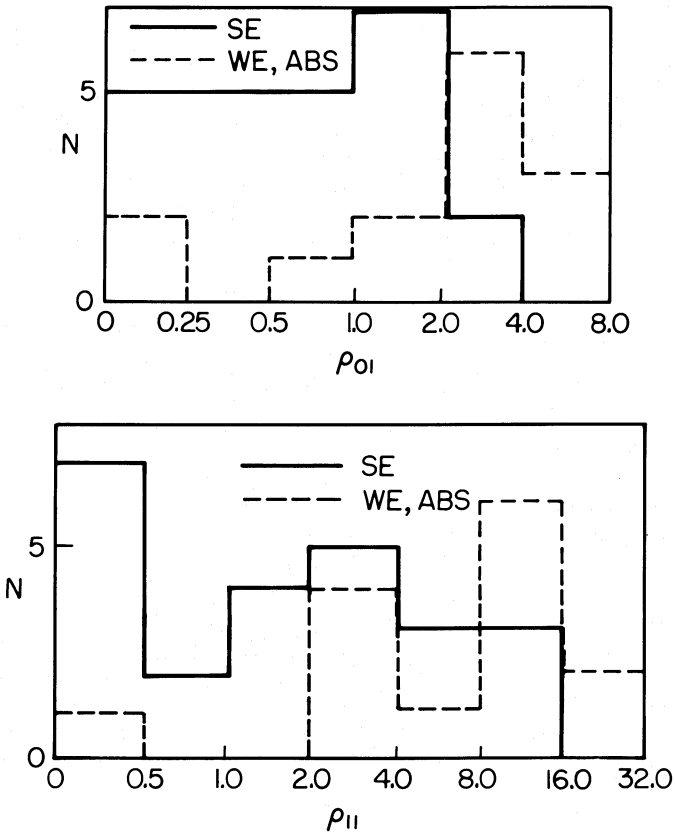

FIG. 24.—Histograms of the local galaxy density parameters ρ_{01} and ρ_{11} for the very powerful radio galaxies in our sample and in HCB with strong optical emission lines (*solid line*) and with weak or no optical emission lines (*dashed line*). Galaxies with strong emission lines are found in regions of lower average density.

1981; Wilkinson, Hine, and Sargent 1981) have linked a number of the other properties of radio galaxies with their clustering environment, so we can use our new data (and that in HCB) to conduct a similar investigation.

i) *Presence of Strong Optical Emission Lines*

We find that very powerful radio galaxies with strong optical emission lines are found on average in regions of lower galaxy density than are similarly powerful radio galaxies with weak or no emission lines (Fig. 24). The difference in the two distributions of density is significant at the 99% confidence level (Wilcoxon rank test) for both ρ_{01} and ρ_{11}.

The anticorrelation between strong emission lines and regions of high galaxy density has been noted before in the context of radio galaxies (Stocke and Perrenod 1981; Longair and Seldner 1979; Wilkinson, Hine, and Sargent 1981) and of other classes of galaxies (e.g., Gisler 1978; Dressler, Thompson, and Schectman 1985).

ii) *Radio Class*

We confirm the results of Stocke and Perrenod (1981) and Longair and Seldner (1978): the very powerful FR II radio sources inhabit less dense regions on average than the very powerful FR I sources. The differences between the two respective distributions in Figure 25 are significant at the ~99% confidence level.

V. SUMMARY AND CONCLUSIONS

a) Principal Conclusions

1. We have found that about one-fourth to one-third of very powerful (log $P_{408} \geq 25.5$ W Hz^{-1}) radio galaxies are strongly peculiar in optical morphology. These peculiarities occur at levels of surface brightness higher than $\mu_V \approx 25$ mag arcsec^{-2}, and take the form of tails, fans, bridges, dust features, shells, etc. The peculiar features are often continuum emitting (starlight?) but sometimes line emitting (ionized gas) and usually bear no obvious morphological relationship to the radio source.

2. While an explosive origin for these peculiar structures cannot always be ruled out (see Williams and Christiansen 1985), we believe that a more natural interpretation is that they arise from the collision or merger of pairs of galaxies, at least one member of which is a disk system. This is suggested by their morphological resemblance to both known interacting galaxies and to theoretical simulations of such interactions. Other evidence also favors the involvement of disk galaxies: many of the radio galaxies with peculiar optical morphologies exhibit evidence for recent or on-going star formation; they are usually found in regions of low or moderate galaxy density, and some are also *dynamically* peculiar relative to bona fide elliptical galaxies (see Heckman *et al.* 1985).

3. The fraction of radio-quiet ellipticals exhibiting morphological peculiarities at levels of surface brightness as high as our radio galaxies is $\ll 10\%$ (the Malin-Carter shells are much fainter).

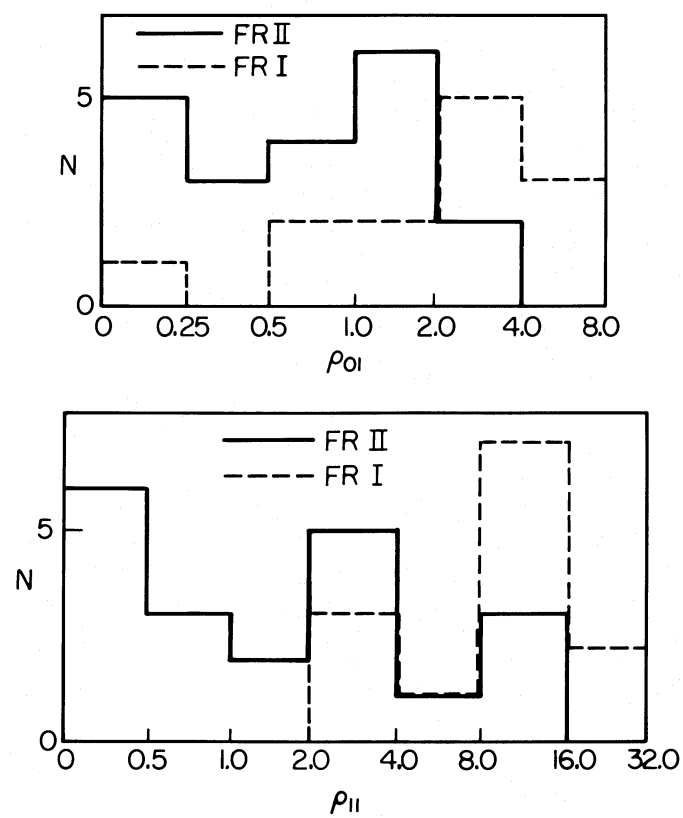

FIG. 25.—Local galaxy density parameters ρ_{01} and ρ_{11} for the very powerful radio galaxies in our present sample and in HCB having Fanaroff-Riley class I radio morphologies (*dashed lines*) and class II radio morphologies (*solid lines*), the FR class II sources ("edge-brightened" sources) are found in regions of lower average density.

© American Astronomical Society • Provided by the NASA Astrophysics Data System

1986ApJ...311..526H

4. It appears that lower power radio galaxies (log P_{408} = 23.5–25.5 W Hz^{-1}) are much less likely than the very powerful galaxies to be peculiar in optical morphology. We note that several important differences in the radio and optical properties of very powerful and lower power radio galaxies are known.

5. Considering only the very powerful radio galaxies, we find that the galaxies with peculiar *optical* morphologies have stronger optical emission lines, are $\sim$0.5 mag less optically luminous on average, and inhabit regions of lower average local galaxy density than the radio galaxies with normal optical morphologies.

6. The *radio sources* produced by the galaxies with peculiar optical morphologies do not appear to be systematically small or distorted. However, a greater fraction of the very powerful Fanaroff-Riley class II sources (edge-brightened outer hot spots) are associated with parent galaxies that are morphologically peculiar than are equally powerful Fanaroff-Riley class I radio sources ("edge-darkened" radio morphology).

7. We find—in agreement with previous studies—that very powerful radio galaxies in regions of high galaxy density are less likely to have either strong optical emission lines or a Fanaroff-Riley class II radio morphology than are similarly powerful radio galaxies in regions of low galaxy density.

b) Two Classes of Radio Galaxies: A Unifying Hypothesis

The results above suggest that a complex web of interrelationships exists among the following parameters: radio power, strength of optical emission lines, *radio source* morphological (Fanaroff-Riley) class, *optical* morphology of the parent galaxy, and local galaxy density. The present base of data is too small to allow a detailed statistical investigation that would determine which are the primary, most physically inportant relationships. Nevertheless, this web can be visualized most simply if we posit the existence of two idealized classes of radio galaxies:

1. The Class A radio galaxies produce FR II ("edge-brightened") radio sources, inhabit regions of low to moderate galaxy density, exhibit strong optical emission lines, and often have peculiar optical morphologies apparently indicative of collisions or mergers involving at least one disk galaxy. We interpret these objects as being fueled by the captured interstellar medium of a gas-rich galaxy. This captured cool, dense gas may provide the raw material for the optical emission-line clouds. At the present epoch, mergers involving disk galaxies will occur primarily (but not exclusively) in regions of rather low galaxy density (low velocity dispersions and high spiral galaxy fractions), such as poor groups or the field (e.g., Quinn 1984). *If* the radio jets can successfully exit from the galaxy's interstellar medium, they can then efficiently travel outward before depositing their energy in bright radio hot spots (classical FR II morphology). If *not*, the jets are disrupted inside the galaxy, and a compact ($\sim$0.1–10 kpc) double radio source results (see van Breugel, Miley, and Heckman 1984).

2. The Class B radio galaxies produce radio sources with an FR I ("edge-darkened") morphology, inhabit regions of high galaxy density, exhibit only weak or no optical emission lines, and are luminous elliptical (or cD) galaxies. We interpret these objects as being fueled by the accretion of either their own atmospheres or of an intracluster or intragroup gaseous medium (e.g., Sanders 1981; Canizares, Steward, and Fabian 1983; Forman, Jones, and Tucker 1985; Valentijn and Bijleveld 1983). The preference of class B radio galaxies for regions of high local galaxy density may then primarily reflect the high density of the hot (X-ray emitting) gas at such locations. Such gas can have relatively short cooling times, allowing it to be accreted (e.g., Binney and Cowie 1981), and/or it may provide enough external "back pressure" to inhibit or thwart wind-driven mass loss from a giant elliptical embedded in it (Stocke and Perrenod 1981). Radio jets propagating through this environment may tend to be inefficient (strongly radiating), leading to an FR I radio morphology. Alternatively, the class B radio sources may be powered magnetohydrodynamically by the stored rotational energy of the central engine, rather than by accretion (Phinney 1983). This power source would account for the lack of strong optical emission (Phinney 1983) and for the normal morphology of the parent galaxy (no accretion necessary). The preference of class B radio galaxies for regions of high galaxy density has no obvious interpretation in this case, but may be related to the processes (at early epochs) that produced the massive, spinning black hole in the radio galaxy nucleus.

The above must be an overly idealized description of a complex situation, if only because not all radio galaxies can be easily classifed (mixed breeds exist). Also radio galaxies are at least a two-parameter family, since the power output of the central engine (the first parameter?) is clearly important but is not explicitly included in the above scheme. For example, the trend toward strong optical emission lines and an FR II morphology as the radio power increases is presumably due—at least in part—to a concomitant increase in the photoionizing continuum luminosity and changes in the radio jet properties (jet thrust, internal energy density, etc.). However, we would argue that the environment is apparently also playing an important role, and is probably the second parameter.

c) Implications

The results and discussion presented above have a number of interesting implications and raise several important questions:

1. In a physical and/or evolutionary sense, are the class A radio galaxies (as defined above) related more directly to class B radio galaxies or to Seyfert galaxies? The class A galaxies probably share at least as many important characteristics with the Seyferts as with the class B galaxies, namely strong optical emission lines, high fraction of morphologically peculiar galaxies (see Adams 1977), location in regions of lower galaxy density than the class B radio galaxies, possible involvement of disk galaxies. While Seyfert galaxies are not usually very powerful radio sources (Meurs 1982), most do exhibit evidence for twin-sided ejection of radio plasma (e.g., Ulvested and Wilson 1984*a*, *b*). Moreover, given the difference in the average galaxy density of the regions in which the class A and class B radio galaxies are found, class A and B radio galaxies *cannot* be related to one another in an evolutionary sense. A corollary of the above would be that radio-loud QSOs are also more directly related to Seyfert galaxies and to radio-quiet QSOs than to class B radio galaxies. As we have noted earlier, many low redshift QSO host galaxies appear distorted, and appear similar to the morphologically peculiar radio galaxies we have discussed (e.g., Hutchings, Crampton, and Campbell 1984; Stockton 1984). Su and Simkin (1980) have also argued for a close physical relationship between Seyfert galaxies and radio galaxies with strong optical emission lines (our class A), although on different grounds from us.

© American Astronomical Society • Provided by the NASA Astrophysics Data System

1986ApJ...311..526H

2. Why are active elliptical galaxies able to produce very powerful radio sources, while active disk galaxies (e.g., Seyfert galaxies) apparently are not? This question has proved to be one of the most puzzling of all regarding active galaxies. Our results make the question even more puzzling, since they suggest that active galaxies which appear to be on-going or recently completed mergers between disk galaxies (e.g., 3C 305) *can* sometimes produce very powerful radio sources. This suggests that the ability to produce a very powerful radio source is not always determined by the nature of the central engine, but sometimes by the environment of the central engine. But in what way does the central region of a disk-disk merger resemble more strongly the central region of an elliptical than of a disk galaxy?

3. How can a morphologically peculiar galaxy produce a very large ($\gtrsim 300$ kpc), straight radio source? The correlation between gas rotation and radio ejection axes seen in large radio sources (Simkin 1979; Kotanyi and Ekers 1979; Heckman *et al.* 1985) implies that a relationship between gas dynamics on scales $\lesssim$ few kpc from the nucleus and the radio ejection axis exists. Thus, the gas dynamics in this interior region must be orderly, even when severe disorder apparently exists on larger scales.

4. The study of the stellar population of radio galaxies at high redshift may tell us more about the cosmological evolution of the galaxy merger rate (e.g., Roos 1985) than about the *passive* evolution of elliptical galaxies. This conjecture is supported not only by our results on relatively low-redshift galaxies, but by recent investigations of high-redshift radio galaxies (Spinrad and Djorgovski 1984*a*, *b*; Lilly and Longair 1984; Eisenhardt and Lebofsky 1985). In particular, could the era of very powerful radio sources at $z \approx 2$ correspond to the epoch at which many(?) elliptical galaxies were produced by mergers of gas-rich systems (disk galaxies)?

The authors wish to thank the staffs of the Kitt Peak National Observatory, Cerro Tololo Inter-American Observatory, Lick Observatory, and the National Radio Astronomy Observatory for their help in obtaining and reducing the data discussed in this paper. T. H. thanks the National Science Foundation (AST 82-16553 and AST 85-15896) and the Alfred P. Sloan Foundation for financial assistance. He would also like to gratefully acknowledge the hospitality and financial support provided by the Department of Physics and Astronomy at Johns Hopkins University (Colin Norman in particular). The research of W. v. B. is supported by NSF grant AST 84-16177 and that of B. B. by AST 82-08041. The authors thank C. Norman, H. Spinard, M. Fall, L. Hernquist, and P. Quinn for useful conversations, S. Simkin for providing inspiration, and M. Aaronson for taking a deep image of 3C 305 and E. Olszewski and N. Suntzeff likewise for PKS 0349−278.

REFERENCES

Adams, T. F. 1977, *Ap. J. Suppl.*, **33**, 19.
Arp, H. C. 1975, *Pub. A.S.P.*, **87**, 545.
Auriemma, C., Perola, G. C., Ekers, R., Fanti, R., Lari, C., Jaffe, W. J., and Ulrich, M. H. 1977, *Astr. Ap.*, **57**, 41.
Baade, W., and Minkowski, R. 1954, *Ap. J.*, **119**, 206.
Baan, W. A., and Haschick, A. D. 1981, *Ap. J.* (*Letters*), **243**, L143.
———. 1984, *Ap. J.*, **289**, 574.
Baldwin, J. A., Carswell, R. F., Wampler, E. J., Smith, H. E., Burbidge, E. M., and Boksenberg, A. 1980, *Ap. J.*, **236**, 388.
Balick, B., and Heckman, T. M. 1982, *Ann. Rev. Astr. Ap.*, **20**, 431.
Balick, B., Heckman, T. M., and Crane, P. C. 1982, *Ap. J.*, **254**, 483.
Barthel, P. 1984, Ph.D. thesis, Leiden University.
Binney, J., and Cowie, L. 1981, *Ap. J.*, **247**, 464.
Borne, K. 1985, preprint.
Borne, K., and Hoessel, J. 1985, preprint.
Boroson, T. A., and Oke, J. B. 1984, *Ap. J.*, **281**, 535.
Boroson, T. A., Persson, S. E., and Oke, J. B. 1985, *Ap. J.*, **293**, 120.
Bridle, A. H. 1984, *A.J.*, **89**, 7.
Bridle, A. H., and Perley, R. A. 1984, *Ann. Rev. Astr. Ap.*, **22**, 319.
Burbidge, G. R., and Crowne, A. H. 1979, *Ap. J. Suppl.*, **40**, 583.
Burstein, D., and Heiles, C. 1982, *A.J.*, **87**, 1165.
Canizares, C. R., Steward, G. C., and Fabian, A. C. 1983, *Ap. J.*, **272**, 449.
Condon, J. J., Condon, M., Gisler, G., and Puschell, J. 1982, *Ap. J.*, **252**, 102.
Dahari, O. 1984, *A.J.*, **89**, 966.
Danziger, I. J., Fosbury, R. A. E., Goss, W. M., Bland, J., and Boksenberg, A. 1984, *M.N.R.A.S.*, **208**, 589.
Davies, R. L., Efstathiou, G., Fall, S. M., Illingworth, G., and Schecter, P. L. 1983, *Ap. J.*, **266**, 41.
Dixon, R. S. 1970, *Ap. J. Suppl.*, **20**, 1.
Dressler, A. 1980, *Ap. J.*, **236**, 351.
Dressler, A., Thompson, I. B., and Schectman, S. A. 1985, *Ap. J.*, **288**, 481.
Eisenhardt, P. R. M., and Lebofsky, M. J. 1985, preprint.
Fanaroff, B. L., and Riley, J. M. 1974, *M.N.R.A.S.*, **167**, 31p.
Forman, W., Jones, C., and Tucker, W. 1985, *Ap. J.*, **293**, 102.
Gehren, T., Fried, J., Wehinger, P. A., and Wyckoff, S. 1984, *Ap. J.*, **278**, 11.
Gilmore, G., and Shaw, M. A. 1986, *Nature*, in press.
Gisler, G. R. 1978, *M.N.R.A.S.*, **183**, 633.
Heckman, T. M., and Balick, B. 1979, *Astr. Ap.* **76**, L7.
Heckman, T. M., Balick, B., van Breugel, W. J. M., and Miley, G. K. 1983, *A.J.*, **88**, 583.
Heckman, T. M., Carty, T. J., and Bothun, G. D. 1985, *Ap. J.*, **288**, 122.
Heckman, T. M., Illingworth, G. D., Miley, G. K., and van Breugel, W. J. M. 1985, *Ap. J.*, **299**, 41.
Heckman, T. M., Miley, G. K., Balick, B., van Breugel, W. J. M., and Butcher, H. R. 1982, *Ap. J.*, **262**, 529.
Heckman, T. M., van Breugel, W. J. M., and Miley, G. K. 1984, *Ap. J.*, **286**, 509.
Hernquist, L., and Quinn, P. 1986, preprint.
Hewitt, A. H., and Burbidge, G. R. 1980, *Ap. J. Suppl.*, **43**, 57.
Hine, R. G., and Longair, M. S. 1979, *M.N.R.A.S.*, **188**, 111.
Hintzen, P., Ulvestad, J., and Owen, F. 1983, *A.J.*, **88**, 709.
Hunstead, R. W., Murdoch, H. S., Condon, J. J., and Phillips, M. M. 1984, *M.N.R.A.S.*, **207**, 55.
Hutchings, J. B., Crampton, D., and Campbell, B. 1984, *Ap. J.*, **280**, 41.
Keel, W. C., Kennicutt, R. C., Jr., Hummel, E., and van der Hulst, J. M. 1985, *A.J.*, **90**, 708.
Kotanyi, C. G., and Ekers, R. D. 1979, *Astr. Ap.*, **73**, L1.
Kühr, H., Nauber, U., Pauliny-Toth, I. I. K., and Witzel, A. 1979, *A Catalog of Radio Sources* (Bonn: Max-Planck-Institut für Radioastronomie).
Laing, R. A., Riley, J. M., and Longair, M. S. 1983, *M.N.R.A.S.*, **204**, 151.
Larson, R. B., and Tinsley, B. M. 1978, *Ap. J.*, **219**, 46.
Lauer, T. R. 1985, *M.N.R.A.S.*, **216**, 429.
Lilly, S. J., and Longair, M. S. 1984, *M.N.R.A.S.*, **211**, 833.
Lilly, S. J., McLean, I. S., and Longair, M. S. 1984, *M.N.R.A.S.*, **209**, 401.
Longair, M. S., and Seldner, M. 1979, *M.N.R.A.S.*, **189**, 433.
Lonsdale, C. J., Persson, S. E., and Mathews, K. 1984, *Ap. J.*, **287**, 95.
Malin, D. F., and Carter, D. 1983, *Ap. J.*, **274**, 534.
Malin, D. F., Quinn, P. J., and Graham, J. R. 1983, *Ap. J.* (*Letters*), **271**, L5.
Merritt, D., and de Zeeuw, T. 1983, *Ap. J.* (*Letters*), **267**, L19.
Meurs, E. 1982, Ph.D. thesis, Leiden University.
Miley, G. K. 1980, *Ann. Rev. Astr. Ap.*, **18**, 165.
Miller, J. S. 1981, *Pub. A.S.P.*, **93**, 681.
Pence, W. 1976, *Ap. J.*, **203**, 39.
Penston, M. V., and Fosbury, R. A. E. 1979, *M.N.R.A.S.*, **183**, 479.
Phinney, E. S. 1983, Ph.D. thesis, Cambridge University.
Postman, M., and Geller, M. J. 1984, *Ap. J.*, **281**, 95.
Quinn, P. J. 1984, *Ap. J.*, **279**, 596.
Roos, N. 1985, *Ap. J.*, **209**, 486.
Sandage, A. R. 1972, *Ap. J.*, **178**, 25.
———. 1966, *Ap. J.*, **145**, 1.
Sanders, R. H. 1981, *Ap. J.*, **244**, 820.
Saslaw, W. C., Tyson, J., and Crane, P. 1978, *Ap. J.*, **222**, 435.
Schmidt, M. S. 1972, *Ap. J.*, **176**, 289.
Schweizer, F. 1980, *Ap. J.*, **237**, 303.
Simkin, S. M. 1979, *Ap. J.*, **234**, 56.
Simkin, S. M., and Michel, D. 1985, preprint.
Smith, E. P., Heckman, T. M., Bothun, G. D., Romanishin, W. R., and Balick, B. 1986, *Ap. J.*, **306**, 64.
Soifer, B. T., *et al.* 1984, *Ap. J.* (*Letters*), **283**, L1.
Spinrad, H., and Djorgoviski, S. 1984*a*, *Ap. J.* (*Letters*), **280**, L9.
———. 1984*b*, *Ap. J.* (*Letters*), **285**, L49.
Spinrad, H., Djorgovski, S., Marr, J., and Aguilar, L. 1985, preprint.
Stocke, J. T., and Perrenod, S. C. 1981, *Ap. J.*, **245**, 375.
Stockton, A. 1984, private communication.
Su, H. J., and Simkin, S. M. 1980, *Ap. J.* (*Letters*), **238**, L1.

© American Astronomical Society • Provided by the NASA Astrophysics Data System

1986ApJ...311..526H

Thompson, L. A. 1984, *Ap. J. (Letters)*, **279**, L47.
Toomre, A. 1977, in *The Evolution of Galaxies and Stellar Populations*, ed. B. M. Tinsley and R. B. Larson (New Haven: Yale University Observatory), p. 401.
Toomre, A., and Toomre, J. 1972, *Ap. J.*, **178**, 623.
Ulvestad, J. S. 1985, *Ap. J.*, **288**, 514.
Ulvestad, J. S., and Wilson, A. S. 1984*a*, *Ap. J.*, **278**, 544.
———. 1984*b*, *Ap. J.*, **285**, 439.
Valentijn, E. A., and Bijleveld, W. 1983, *Astr. Ap.*, **125**, 223.
van Breugel, W. J. M., Filippenko, A. V., Heckman, T. M., and Miley, G. K. 1985*b*, *Ap. J.*, **293**, 83.
van Breugel, W. J. M., Heckman, T. M., Miley, G. K., and Filippenko, A. V. 1986, *Ap. J.*, submitted.
van Breugel, W. J. M., Heckman, T. M., Butcher, H. R., and Miley, G. K. 1984, *Ap. J.*, **277**, 82.
van Breugel, W. J. M., Miley, G. K., and Heckman, T. M. 1984, *A.J.*, **89**, 5.
van Breugel, W. J. M., Miley, G. K., Heckman, T. M., Butcher, H. R., and Bridle, A. H. 1985*a*, *Ap. J.*, **290**, 496.
Veeraraghavan, S., and White, S. D. M. 1985, *Ap. J.*, **296**, 336.
Villumsen, J. V. 1982, *M.N.R.A.S.*, **199**, 493.
Wilkinson, A., Hine, R. G., and Sargent, W. L. W. 1981, *M.N.R.A.S.*, **196**, 669.
Williams, R. E., and Christiansen, W. A. 1985, *Ap. J.*, **291**, 80.
Windhorst, R. 1984, Ph.D. thesis, Leiden University.
Yee, H. K. C., and Green, R. F. 1984, *Ap. J.*, **280**, 79.

BRUCE BALICK: Department of Astronomy, University of Washington, Seattle, WA 98195

STEFI A. BAUM: National Radio Astronomy Observatory, Edgemont Rd., Charlottesville, VA 22901

GREG BOTHUN: Department of Astronomy, University of Michigan, Ann Arbor, MI 48109

WIL VAN BREUGEL: Radio Astronomy Laboratory, Campbell Hall, University of California, Berkeley, CA 94720

TIMOTHY M. HECKMAN and ERIC P. SMITH: Astronomy Program, University of Maryland, College Park, MD 20742

GARTH D. ILLINGWORTH and GEORGE K. MILEY: Space Telescope Science Institute, Homewood Campus, Baltimore, MD 21218

© American Astronomical Society • Provided by the NASA Astrophysics Data System